2018

Investigating the impacts of human decision-making and climate change on hydrologic response in an agricultural watershed

David Dziubanski
Iowa State University

Investigating the impacts of human decision-making and climate change on hydrologic response in an agricultural watershed

by

David Joseph Dziubanski

A dissertation submitted to the graduate faculty

in partial fulfillment of the requirements for the degree of

DOCTOR OF PHILOSOPHY

Major: Civil Engineering and Geology (Environmental Engineering)

Program of Study Committee:
Kristie J. Franz, Major Professor
William W. Simpkins
Matthew J. Helmers
Chris R. Rehmann
Roy R. Gu

The student author, whose presentation of the scholarship herein was approved by the program of study committee, is solely responsible for the content of this dissertation. The Graduate College will ensure this dissertation is globally accessible and will not permit alterations after a degree is conferred.

Iowa State University

Ames, Iowa

2018

DEDICATION

I would like to dedicate this work to my mom and dad. Without your upbringing, I would probably never have the scientific curiosity that I have today.

TABLE OF CONTENTS

LIST OF FIGURES

LIST OF TABLES

Page

ACKNOWLEDGEMENTS

I would like to sincerely thank numerous people who guided me through this project and helped me achieve my goal. I would like to thank my advisor, Kristie Franz, for providing me with the opportunity to perform some excellent research. Kristie guided me through many steps of this project and helped me gain the skills that will be useful to me as I move on in my scientific career.

I would like to thank my committee members, Bill Simpkins, Chris Rehmann, Matt Helmers, and Roy Gu for their excellent feedback and ideas, and for teaching me a thing or two about hydrology. Your courses were excellent.

Special thanks to my family for their encouragement and support through the many years of my education. I would not be at the point where I currently am without their guidance. Lastly, I would like to thank Ms. Amanda Black for the many fun times together as Ph.D. students.

ABSTRACT

The hydrologic system has increasingly been experiencing change due to a combination of human and natural factors. Human decision making within the landscape impacts the characteristics of various hydrologic processes, namely runoff, through changes in land use. Equally important, shifting climate is changing precipitation patterns, particularly precipitation intensity, which is changing the quantity of surface water flows. Quantifying the relative impacts of these two dominant components is necessary for fully understanding hydrologic variability and uncertainty, and for future flood and drought planning. The main objective of this study was to analyze the impacts of human decision-making and changing climate on streamflow for the U.S. Midwest Corn Belt under future climate scenarios through use of a social-hydrologic modeling system.

The first part of this study focused on building and conducting a sensitivity analysis of a socio-hydrological model that combines an agent-based model (ABM) of human decision-making with a semi-distributed hydrologic model. The hydrologic model uses the curve number (CN) method to relate land cover to hydrologic response. Agents (based on two types) make decisions that affect land use within the watershed. A city agent aims to reduce flooding in a downstream urban area by paying farmer agents a subsidy for allocating land towards conservation practices that reduce runoff. Farmer agents decide how much land to convert to conservation based on factors related to profits, past land use and conservation-mindedness (willingness to convert land to conservation). In order to accurately represent a conservation practice within the hydrologic model, CNs were derived using precipitation and runoff data for 14 small watersheds in Iowa which were planted with varying amounts of native prairie vegetation (NPV) located in different watershed positions. The social-hydrologic model was

implemented for a watershed representative of the mixed agricultural/small urban area land use found in Iowa, USA (Squaw Creek watershed). Scenarios of crop yield trend, crop prices, and conservation subsidies along with varied farmer parameters were simulated to illustrate the effects of human system variables on peak discharges. High corn prices lead to a decrease in conservation land from historical levels; consequently, mean peak discharge increases by 6%, creating greater potential for downstream flooding within the watershed. Overall, results indicated that changes in mean peak discharge are mostly driven by changes in crop prices as opposed to yields or conservation subsidies.

In the second part of this study, the watershed was simulated into the future under two different climate scenarios. The agent-based model was upgraded to include a social network and a "pothole module" to capture the effect of neighbor influence and on-farm flooding on decision-making. Under the RCP 4.5 (greenhouse gas concentrations peak around 2040) and RCP 8.5 (greenhouse gas concentrations continuously rise through 2100) scenarios, conservation land increases by approximately 20-60% and 40-60%, respectively. This results in a 5% and 6% decrease in mean 95th percentile discharge relative to scenarios where conservation land is treated as constant at the historical mean. If farmers are allowed to modify their behavior through time, a 10% and 16% decrease in mean 95th percentile discharge is seen under the RCP 4.5 and 8.5 scenarios. However, overall changes to peak discharge are dominated by future changes in precipitation, with climate scenarios depicting mean 95th percentile discharge to increase by 46% if conservation land is kept constant at the historical mean.

CHAPTER 1

GENERAL INTRODUCTION

The hydrologic system has been undergoing changes due to combined impacts from the human and climate systems. Human activities modify the hydrologic system through decision-making that affects physical and chemical aspects of the landscape (Vorosmarty and Sahagian, 2000). Some examples of human activities that modify the hydrologic system include land use alterations, river channel modification, urban expansion, and changes in agricultural crops (Carpenter et al., 2011; Montanari et al., 2013; Sivapalan et al., 2012; Turner and Rabalais, 2003) However, changes in the hydrologic system are not exclusively caused by human modification. Changing precipitation patterns as a result of shifting climate are causing changes in runoff volume across many regions of the world (Huntington, 2006). Several recent studies have indicated climate to be the dominant driver in changing river discharge in certain regions of the U.S (Frans et al., 2013; Tomer and Schilling, 2009).

Despite their impacts to the landscape, humans remain poorly represented in hydrologic modeling studies (Sivapalan et al., 2012). Land cover and land use are commonly treated as fixed in time in many hydrologic models through the use of static parameters. The field of integrated water resources management (IWRM) attempts to explore the interactions between humans and water through use of "scenario-based" approaches (Savenije and Van der Zaag, 2008), but significant limitations exist with this approach (Elshafei et al., 2014; Sivapalan et al., 2012). Human and environmental systems are highly coupled with feedbacks from one system creating stress on the other system, which in turn affects the behavior of the first system. Therefore, representing the evolution of the coupled system through pre-determined scenarios will not reproduce the real-world variability that may arise as a result of complex feedbacks.

Over the last several years, the field of socio-hydrology has emerged in which an increasing need is being place on explicitly representing connections between the human and hydrologic systems (Di Baldassarre et al., 2013; Montanari, 2015; Sivapalan et al., 2012; Sivapalan and Blöschl, 2015). In the hydrologic literature, two approaches have been used to simulate the two systems in unison: a classic top-down approach and a bottom-up approach using agent-based modeling (ABM). In the first approach, all aspects of the human system are represented through a set of parametrized differential equations (Di Baldassarre et al., 2013; Elshafei et al., 2014; Viglione et al., 2014). For example, Elshafei et al. (2014) characterizes the population dynamics, economics, and sensitivity of the human population to hydrologic change through differential equations to simulate the coupled dynamics of the human and hydrologic systems in an agricultural watershed. In contrast, the ABM approach consists of a set of algorithms that encapsulate the behaviors of agents and their interactions within a defined system, where agents can represent individuals, groups, companies, or countries (Axelrod and Tesfatsion, 2006; Borrill and Tesfatsion, 2011; Parunak et al., 1998). These agents are typically autonomous, have certain goals, and act on inputs from the environment with the intention of meeting their goals (Jennings, 2000). The agents can also have learning capabilities, with the ability to optimize their decision-making based on the current state of their environment.

ABM has been used to study the influence of human decision making on hydrologic topics such as water balance and stream hydrology (Bithell and Brasington, 2009), irrigation and water usage (Barreteau et al., 2004; Becu et al., 2003; Berger et al., 2006; van Oel et al., 2010; Schlüter and Pahl-wostl, 2007), water quality (Ng et al., 2011), and groundwater resources (Noel and Cai, 2017; Reeves and Zellner, 2010). Becu et al. (2003) coupled an ABM (CATCHSCAPE) with a water balance model, CATCHCROP, to study the effects of upstream irrigation

management on downstream agricultural viability within the Mae Uam Catchment in Northern Thailand. Farmer decision-making within CATCHSCAPE is based on constraints of cash, labor force, and water availability. Becu et al. (2003) simulated four scenarios and found a predominant trend of poor farmer agents having an increasingly negative cash position through time in contrast to rich farmer agents, hypothesized to be due to the spatial distribution of water within the watershed. Ng et al. (2011) more recently developed an ABM of the Salt Creek watershed in Central Illinois to explore the impacts of various economic factors on farmer behavior and stream nitrate loads. In that study, the SWAT model was coupled with a stochastic model of individual farmer agents in which each farmer forms perceptions of crop price, production costs, and weather variables using Bayesian inferencing. The main objective of each farmer was to maximize profit over the planning horizon based on his/her perceptions of future conditions. A sensitivity analysis of the model revealed that stream nitrate load was lowest when the population of farmer agents was highly adaptive and prices of Miscanthus were favorable compared to corn prices.

A dominating topic in the hydrologic sciences that can be studied through use of coupled ABMs is the issue of hydrologic trends and uncertainties in intensively managed landscapes. Many recent studies have focused on quantifying the impacts of the human and climate systems on trends in streamflow through use of modeling and statistical methods such as linear regression, water balance approaches, trend analysis, and Budyko analysis (Ahn and Merwade, 2014; Bao et al., 2012; Guo and Shen, 2015; Li et al., 2009; Steffens and Franz, 2012; Tomer and Schilling, 2009; Wang and Hejazi, 2011; Zhang et al., 2012). These studies have attempted to determine what percentage of the recent changes in streamflow can be attributed to human-induced changes in the landscape. However, the extent to which humans are altering streamflow

is still unclear, with certain studies indicating a stronger climate signal (e.g (Li et al., 2009; Tomer and Schilling, 2009). Given the wide range of results from these studies, social-hydrologic models that couple these two systems may allow for a more complete analysis of how changes in precipitation coupled with human decision-making on the landscape affect streamflow.

1.1 Research Objectives

The *overarching* goal of this research is to improve understanding and consideration of the causes of hydrologic variability and uncertainty through use of advanced modeling approaches that incorporate dynamic, coupled human-environment interaction. Leveraging off of extensive development of agent-based modeling (ABM) techniques in recent years (Berger and Troost, 2014; Ng et al., 2011; Schreinemachers and Berger, 2011), this project combines an ABM of on-farm decision making with an existing hydrologic model to provide comprehensive representation of all primary system processes within highly-managed agricultural watersheds.

I hypothesize that a fully coupled social-hydrologic model will reveal hydrologic system sensitivities to human influences under climate change. Such a model will produce more robust information applicable to water management decision making and planning than present models that treat humans as unresponsive to their environment. It will allow for the quantification of the relative influence of internal perturbations (e.g. land use management) to external perturbations (e.g. climate variability) on hydrologic outcomes such as flooding.

The combination of an agent-based model with a hydrologic modeling in this work aims to improve current understanding of hydrologic system dynamics through analysis of two key objectives:

1. *To elicit new understanding of the hydrologic system under dynamic interaction between the social and natural system using an ABM approach, specifically focusing on the importance of extrinsic factors (i.e. global crop prices, crop yields, subsidy rates) versus intrinsic factors (i.e human behavior and response) for determining hydrologic outcomes.*
2. *To quantify the individual and combined impacts of human-decision making and changing climate on future hydrologic outcomes under two climate scenarios: Representative Concentration Pathways 4.5 and 8.5.*

This dissertation is organized as follows. Chapter 2 describes a study conducted to parameterize the hydrologic model within the coupled socio-hydrologic modeling system. Chapter 3 gives a thorough overview of the socio-hydrologic model that was developed and a sensitivity analysis that was conducted. Chapter 4 describes as application of the model to future climate scenarios. Finally, chapter 5 provides a summary of findings and gives a brief philosophy of the usefulness of the type of modeling conducted to the hydrological sciences field.

1.2 References

Ahn, K.H. and V. Merwade, 2014. Quantifying the Relative Impact of Climate and Human Activities on Streamflow. Journal of Hydrology 515:257–266.

Axelrod, R. and L. Tesfatsion, 2006. A Guide for Newcomers to Agent-Based Modeling in the Social Sciences. Handbook of Computational Economics 2:1647–1659.

Di Baldassarre, G., A. Viglione, G. Carr, L. Kuil, J.L. Salinas, and G. Blöschl, 2013. Socio-Hydrology: Conceptualising Human-Flood Interactions. Hydrology and Earth System Sciences 17:3295–3303.

Bao, Z., J. Zhang, G. Wang, G. Fu, R. He, X. Yan, J. Jin, Y. Liu, and A. Zhang, 2012. Attribution for Decreasing Streamflow of the Haihe River Basin, Northern China: Climate Variability or Human Activities? Journal of Hydrology 460-461:117–129.

Barreteau, O., F. Bousquet, C. Millier, and J. Weber, 2004. Suitability of Multi-Agent Simulations to Study Irrigated System Viability: Application to Case Studies in the Senegal River Valley. Agricultural Systems 80:255–275.

Becu, N., P. Perez, a Walker, O. Barreteau, and C.L. Page, 2003. Agent Based Simulation of a Small Catchment Water Management in Northern Thailand. Ecological Modelling 170:319–331.

Berger, T., R. Birner, N. Mccarthy, J. DíAz, and H. Wittmer, 2006. Capturing the Complexity of Water Uses and Water Users within a Multi-Agent Framework. Water Resources Management 21:129–148.

Berger, T. and C. Troost, 2014. Agent-Based Modelling of Climate Adaptation and Mitigation Options in Agriculture. Journal of Agricultural Economics 65:323–348.

Bithell, M. and J. Brasington, 2009. Coupling Agent-Based Models of Subsistence Farming with Individual-Based Forest Models and Dynamic Models of Water Distribution. Environmental Modelling & Software 24:173–190.

Borrill, P. and L. Tesfatsion, 2011. Agent-Based Modeling: The Right Mathematics for the Social Sciences? The Elgar Companion to Recent Economic Methodology. New York, New York, pp. 228–258.

Carpenter, S.R., J. Cole, M.L. Pace, R. Batt, W.A. Brock, and T. Cline, 2011. Early Warnings of Regime Shifts. Science 332:1076–1079.

Elshafei, Y., M. Sivapalan, M. Tonts, and M.R. Hipsey, 2014. A Prototype Framework for Models of Socio-Hydrology: Identification of Key Feedback Loops and Parameterisation Approach. Hydrology and Earth System Sciences 18:2141–2166.

Frans, C., E. Istanbulluoglu, V. Mishra, F. Munoz-Arriola, and D.P. Lettenmaier, 2013. Are Climatic or Land Cover Changes the Dominant Cause of Runoff Trends in the Upper Mississippi River Basin? Geophysical Research Letters 40:1104–1110.

Guo, Y. and Y. Shen, 2015. Quantifying Water and Energy Budgets and the Impacts of Climatic and Human Factors in the Haihe River Basin, China: 2. Trends and Implications to Water Resources. Journal of Hydrology 527:251–261.

Huntington, T.G., 2006. Evidence for Intensification of the Global Water Cycle: Review and Synthesis. Journal of Hydrology 319:83–95.

Jennings, N.R., 2000. On Agent-Based Software Engineering. Artificial Intelligence 117:277–296.

Li, Z., W.Z. Liu, X.C. Zhang, and F.L. Zheng, 2009. Impacts of Land Use Change and Climate Variability on Hydrology in an Agricultural Catchment on the Loess Plateau of China. Journal of Hydrology 377:35–42.

Montanari, A., 2015. Debates-Perspectives on Socio-Hydrology: Introduction. Water Resources Research 51:4768–4769.

Montanari, a., G. Young, H.H.G. Savenije, D. Hughes, T. Wagener, L.L. Ren, D. Koutsoyiannis, C. Cudennec, E. Toth, S. Grimaldi, G. Blöschl, M. Sivapalan, K. Beven, H. Gupta, M. Hipsey, B. Schaefli, B. Arheimer, E. Boegh, S.J. Schymanski, G. Di Baldassarre, B. Yu, P. Hubert, Y. Huang, a. Schumann, D. a. Post, V. Srinivasan, C. Harman, S. Thompson, M. Rogger, a. Viglione, H. McMillan, G. Characklis, Z. Pang, and V. Belyaev, 2013. "Panta Rhei—Everything Flows": Change in Hydrology and society—The IAHS Scientific Decade 2013–2022. Hydrological Sciences Journal 58:1256–1275.

Ng, T.L., J.W. Eheart, X. Cai, and J.B. Braden, 2011. An Agent-Based Model of Farmer Decision-Making and Water Quality Impacts at the Watershed Scale under Markets for Carbon Allowances and a Second-Generation Biofuel Crop. Water Resources Research 47. doi:10.1029/2011WR010399.

Noel, P.H. and X. Cai, 2017. On the Role of Individuals in Models of Coupled Human and Natural Systems : Lessons from a Case Study in the Republican River Basin. Environmental Modelling & Software 92:1–16.

Van Oel, P.R., M.S. Krol, A.Y. Hoekstra, and R.R. Taddei, 2010. Feedback Mechanisms between Water Availability and Water Use in a Semi-Arid River Basin: A Spatially Explicit Multi-Agent Simulation Approach. Environmental Modelling & Software. Elsevier Ltd, pp. 433–443.

Parunak, H.V.D., R. Savit, and R.L. Riolo, 1998. Multi-Agent Systems and Agent-Based Simulation. Proceedings of the First International Workshop of Multi-Agent Systems and Agent-Based Simulation:10–25.

Reeves, H.W. and M.L. Zellner, 2010. Linking MODFLOW with an Agent-Based Land-Use Model to Support Decision Making. Ground Water 48:649–60.

Savenije, H.H.G. and P. Van der Zaag, 2008. Integrated Water Resources Management: Concepts and Issues. Physics and Chemistry of the Earth 33:290–297.

Schlüter, M. and C. Pahl-wostl, 2007. Mechanisms of Resilience in Common-Pool Resource Management Systems : An Agent-Based Model of Water Use in a River Basin. Ecology and Society 12. http://www.ecologyandsociety.org/vol12/iss2/art4/.

Schreinemachers, P. and T. Berger, 2011. An Agent-Based Simulation Model of Human–environment Interactions in Agricultural Systems. Environmental Modelling & Software 26:845–859.

Sivapalan, M. and G. Blöschl, 2015. Time Scale Interactions and the Coevolution of Humans and Water. Water Resources Research 51:6988–7022.

Sivapalan, M., H.H.G. Savenije, and G. Blöschl, 2012. Socio-Hydrology: A New Science of People and Water. Hydrological Processes 26:1270–1276.

Steffens, K.J. and K.J. Franz, 2012. Late 20th-Century Trends in Iowa Watersheds: An Investigation of Observed and Modelled Hydrologic Storages and Fluxes in Heavily Managed Landscapes. International Journal of Climatology 32:1373–1391.

Tomer, M.D. and K.E. Schilling, 2009. A Simple Approach to Distinguish Land-Use and Climate-Change Effects on Watershed Hydrology. Journal of Hydrology 376:24–33.

Turner, R.E. and N.N. Rabalais, 2003. Linking Landscape and Water Quality in the Mississippi River Basin for 200 Years. Bioscience 53:563–572.

Viglione, A., G. Di Baldassarre, L. Brandimarte, L. Kuil, G. Carr, J.L. Salinas, A. Scolobig, and G. Blo¨schl, 2014. Insights from Socio-Hydrology Modelling on Dealing with Flood Risk - Roles of Collective Memory, Risk-Taking Attitude and Trust. Journal of Hydrology 518:71–82.

Vorosmarty, C. and D. Sahagian, 2000. Anthropogenic Disturbance of the Terrestrial Water Cycle. BioScience 50:753–765.

Wang, D. and M. Hejazi, 2011. Quantifying the Relative Contribution of the Climate and Direct Human Impacts on Mean Annual Streamflow in the Contiguous United States. Water Resources Research 47. doi:10.1029/2010WR010283.

Zhang, A., C. Zhang, G. Fu, B. Wang, Z. Bao, and H. Zheng, 2012. Assessments of Impacts of Climate Change and Human Activities on Runoff with SWAT for the Huifa River Basin, Northeast China. Water Resources Management 26:2199–2217.

CHAPTER 2

EFFECTS OF SPATIAL DISTRIBUTION OF PRAIRIE VEGETATION IN AN AGRICULTURAL LANDSCAPE ON CURVE NUMBER VALUES

A paper published in *Journal of the American Water Resources Association*[1]

David J. Dziubanski[2,3], Kristie J. Franz[2], and Matthew J. Helmers[4]

Abstract

The Curve Number (CN) method is used to calculate runoff in many hydrologic models, including the Soil and Water Assessment Tool (SWAT). The CN method does not account for the spatial distribution of land cover types, an important factor controlling runoff patterns. The objective of this study was to empirically derive CN values that reflect the strategic placement of native prairie vegetation (NPV) within row crop agricultural landscapes. CNs were derived using precipitation and runoff data from a seven year period for 14 small watersheds in Iowa. The watersheds were planted with varying amounts of NPV located in different watershed positions. The Least Squares and Asymptotic Least Squares methods were used to derive CNs using an initial abstraction coefficient (λ) of 0.2 and 0.05. The CNs were verified using leave-one-out cross-validation and adjustment for Antecedent Moisture Conditions (AMC) was tested. The Asymptotic method produced CN values for watersheds with NPV treatment that were 8.9% and 14.7% lower than watersheds with 100% row crop at λ = 0.2 and λ = 0.05 respectively. The

[1] Dziubanski, D.J., K.J. Franz, and M.J. Helmers, 2017. Effects of Spatial Distribution of Prairie Vegetation in an Agricultural Landscape on Curve Number Values. JAWRA Journal of the American Water Resources Association 53:365–381.

[2] Graduate Research Assistant (Dziubanski) and Associate Professor (Franz), Department of Geological and Atmospheric Sciences, Iowa State University.

[3] Primary researcher and corresponding author.

[4] Professor, Department of Agricultural and Biosystems Engineering, Iowa State University.

derived CNs produced Nash-Sutcliffe Efficiency (NSE) values ranging from 0.4-0.7 during validation. Our analyses show that the CNs verified best for the Asymptotic Least Squares method, when using λ of 0.05 and adjusting for AMC. Further, comparison of derived CNs against an area weighted CN indicated that the placement of vegetation does impact the CN value.

2.1 Introduction

The simplicity of the Curve Number (CN) method, which summarizes an area's runoff potential into a single number, makes it a consistently popular choice for hydrologic modelers. This method has been widely used in a number of models, including the Agricultural Non-Point Source Pollution (AGNPS) model (Young et al., 1989), Environmental Policy Integrated Climate (EPIC) model (Williams, 1990, 1995), Soil and Water Assessment Tool (SWAT) (Arnold et al., 1998; Arnold and Fohrer, 2005), and Agricultural Policy/Environmental eXtender (APEX) model (Williams et al., 2000), among others. The CN method was empirically developed in the 1950s by the USDA Soil Conservation Service (SCS) using data collected from numerous small experimental watersheds (Hawkins et al., 2009; USDA-SCS, 1964). As developed, the technique is limited in application to a single rainfall event lasting 24 hours or less; however, it has been applied to continuous simulation models, most notably SWAT, by adjusting the CNs for "Antecedent Moisture Conditions" (AMC) over time (Arnold and Fohrer, 2005).

In hydrologic modeling applications, the CN is often applied at the watershed-scale in a spatially lumped manner. A weighted average CN can be computed to represent the relative composition of heterogeneous land cover conditions within a watershed. However, the weighted CN does not account for the physical distribution of those land cover types. This distribution can be accounted for by discretizing the modeling domain into subunits, which forms the basis of

semi-distributed modeling (Beven, 2012). In the SWAT model, watersheds are divided into subwatersheds with each subwatershed further divided into Hydrologic Response Units (HRUs) (Arnold et al., 2010). HRUs are typically delineated based on regions of similar soil type, topography, and land use; however, the specific location of the HRUs within the subwatershed is not accounted for. Similar to the SWAT model, The APEX model subdivides an area into homogenous land units (HLU) at the farm plot scale, which can be based on topography, soil, and similar land use. As the modeling domain gets further discretized into finer scale grids or smaller, more homogenous watersheds, the model approaches a fully distributed application. The AGNPS model is one example of a model using the fully distributed approach.

An advantage of a fine level of discretization is the ability to more accurately assess the impact of small scale processes (Arnold et al., 2010). Arnold et al. (2010) studied the effects of various levels of discretization within the SWAT model by comparing four landscape delineations (lumped, HRUs, catena – delineation method based on topography (Volk et al., 2007) , and grid) and assessed the overall model accuracy of simulated discharge for the Brushy Creek Watershed near Riesel, Texas. They found that all four methods simulated discharge at the outlet with similar accuracy (Nash-Sutcliffe efficiency of approximately 0.65); however, with the finer scale model (catena and grid), they were able to simulate the impacts of spatial land cover changes and best management practices (BMPs) across hillslopes more realistically than with the other two methods. At the same time, each level of discretization adds complexity to the model application with computational costs, difficulty finding high resolution forcing data, and calibration and parameters identification problems increasing at finer and finer resolutions (Beven, 2012).

Recently there has been a focus on realistically modeling small scale best management practices (BMPs) within the semi-distributed SWAT model without further discretization beyond HRUs (Arabi et al., 2008; Artita et al., 2013; Bosch et al., 2013; Bracmort et al., 2006; Kalcic et al., 2015; Santhi et al., 2006; Chu et al., 2005; Vaché et al., 2003). The studies looked at conservation practices that included no-till, cover crops, grassed waterways, buffer strips, contour farming, and wetlands, among others. Most commonly, the BMPs were introduced into the SWAT model by modifying the CN, Manning's roughness coefficient, and parameters associated with the universal soil loss equation (USLE) (Arabi et al., 2008). Arabi *et al.* (2008) developed a relationship between the CN and various field practices based on a table of recommended CNs provided by Neitsch *et al.* (2005) and decreased the CNs by 2-6 units depending on the conservation practice. Using the methodology of Arabi *et al.* (2008), Bosch *et al.* (2013) tested the effectiveness of filter-strips, cover crops and no-till for 6 watersheds in the Lake Erie Basin using SWAT and found the method to produce up to an 11% reduction in sediment and nutrient yields, with larger reductions for strategically placed BMPs. More recently, defining HRUs at the farm field scale has been tested (Kalcic et al., 2015; Teshager et al., 2016b) with conservation practices represented with modified parameters based on Arabi *et al.* (2008). While these studies have made progress, the CN adjustments were somewhat subjective and not based on empirically derived values for the specific land use practice. Further, these studies relied on the HRU concept that aggregates local response to the watershed-scale without fully considering the effects of spatial placement of land cover types within the watershed.

One possible means of overcoming the limitations associated with not accounting for spatial land cover placement within the model, while retaining the advantages of a simple

lumped or semi-lumped modeling approach, is to use parameters empirically-derived from field data collected from sites that contain the type of land practice that is being modeled. This approach may be particularly useful when modeling the impacts of BMPs. The objective of this study is to empirically derive CN values that reflect the strategic spatial placement of native prairie vegetation (NPV) within hillslope-scale watersheds for use in lumped and semi-lumped models (e.g. SWAT). Our study focuses on 14 watersheds with various combinations of row crop and NPV. As benchmarks, we include 3 watersheds containing 100% row crop and 2 watersheds containing 100% NPV. Curve number values were derived for each hillslope using a least squares fitting method and Asymptotic least squares fitting method (Hawkins et al., 2009). Verification of CN values was performed using leave-one-out cross-validation. Finally, given recent discussions in the literature, we also explored the impacts of different initial abstractions and AMC conditions on the CN verification.

2.2 Methods

2.2.1 Site description and data

The study sites consisted of three clusters of agricultural hillslope-scale watersheds located in the Neal Smith National Wildlife Refuge in Jasper County, Iowa (Figure 2.1). These sites were part of a three year study to assess the effects of varying location and amount of NPV in agricultural landscapes (Helmers et al., 2012; Hernandez-Santana et al., 2013). The study area is characterized by steep rolling hills formed from Wisconsin-age loess. Row crop (corn and soybean) agriculture is the dominant land use. Mean annual precipitation over the last 30 years for the region is 850 mm. The growing season months of May and June typically receive the heaviest rainfalls. The study sites are fully rainfed, with no irrigated agriculture.

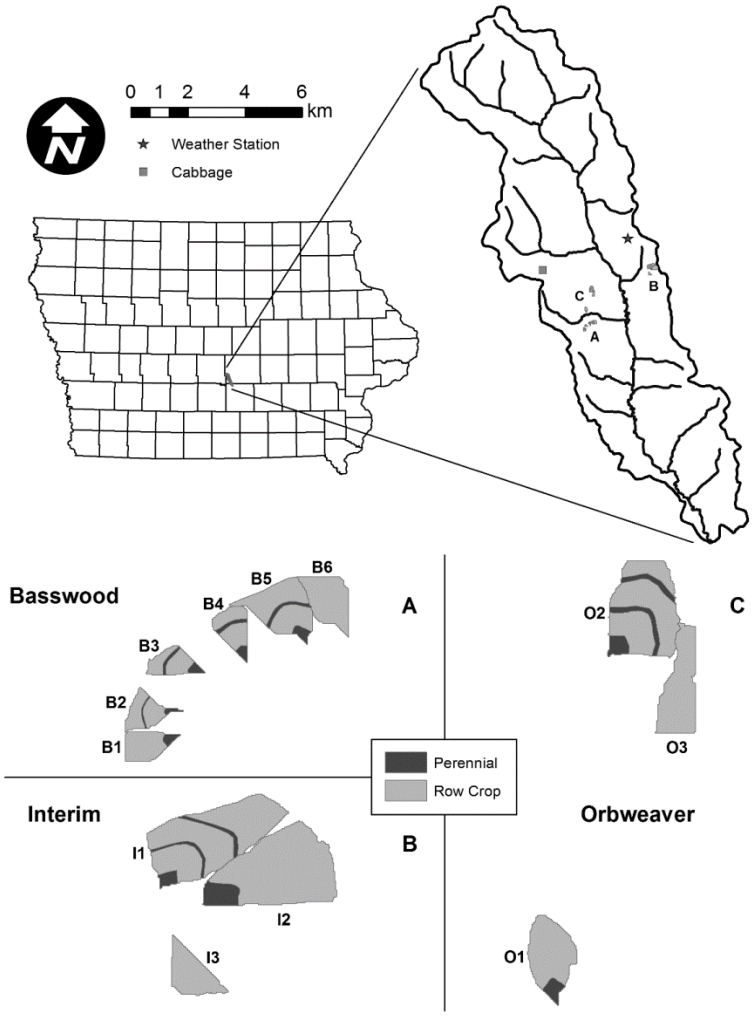

Figure 2.1. Location of study sites within Walnut Creek watershed, Iowa (USA), and experimental design of native prairie strips for A) Basswood, B) Interim, and C) Orbweaver.

A total of 14 watersheds (Basswood (B1-B6), Interim (I1-I3), Orbweaver (O1-O3), Cabbage (C1-C2)) were used in this study (Figure 2.1A,B,C). Soil samples were taken at the summit, side, and toe of each study site (B1-B6, I1-I3, O1-O3) at depth ranges of 0-5 cm, 5-15 cm, and 15-30 cm (Helmers et al., 2012; Zhou et al., 2010). The soil samples were characterized by a high percentage of silt (60-70%) and a sizable percentage of clay (25-30%), indicating a predominantly silt loam or silty clay loam soil type across the watersheds. A higher sand

percentage (30-35%) was found at the toe of two sites (O1, B6), indicating a loam soil, while approximately equal percentages of sand, silt, and clay where found at the toe of B5, indicating a clay loam soil. At sites C1 and C2, the predominant soil type fell in the silt loam or silt categories (70-98% silt) based on samples collected at the summit and drainageways (Schilling et al., 2007). The Natural Resources Conservation Service (NRCS) classifies the soils at these sites as soil group C of the CN method soil types (USDA-NRCS, 2015).

Table 2.1. Study site descriptions.

Site	Size(ha)	Slope (%)	Maximum slope length (m)	Location and percentage of prairie filter strips (PFS)	Width of PFS at footslope (m)[1]	Width of PFS at upslope (m)[2]
Orbweaver 1	1.18	10.3	187	10% at footslope (10FootNPV)	57.3	--
Orbweaver 2	2.40	6.7	220	6.7% at footslope, 6.7% at sideslope, 6.7% at upslope (20StNPV)	52.0	9.8
Orbweaver 3	1.24	6.6	230	100% row crop (100RC)	--	--
Interim 1	3.00	7.7	288	3.3% at footslope, 3.3% at sideslope, 3.3% at upslope (10StNPV)	51.0	6.0
Interim 2	3.19	6.1	284	10% at footslope (10FootNPV)	78.2	--
Interim 3	0.73	9.3	137	100% row crop (100RC)	--	--
Basswood 1	0.53	7.5	120	10% at footslope (10FootNPV)	38.2	--
Basswood 2	0.48	6.6	113	5% at footslope and 5% at upslope (10StNPV)	40.5	3.1
Basswood 3	0.47	6.4	110	10% at footslope and 10% at upslope (20StNPV)	37.6	6.0
Basswood 4	0.55	8.2	118	10% at footslope and 10% at upslope (20StNPV)	38.1	7.5
Basswood 5	1.24	8.9	144	5% at footslope and 5% at upslope (10StNPV)	46.4	7.0
Basswood 6	0.84	10.5	140	100% row crop (100RC)	--	--
Cabbage 1	1.8	3.5	N/A	100% NPV (100NPV)	--	--
Cabbage 2	3.3	3.5	N/A	100% NPV (100NPV)	--	--

(1) Width of PFS along primary flow pathway.

(2) Average width of prairie filter strip if more than one strip at upslope

In 2007, each site received various treatments of NPV strategically placed at different positions of the hillslope: 10% NPV (10FootNPV) in a single filter strip at the footslope (B1, I2, O1), 10% NPV (10StNPV) divided between various contour filter strips at the footslope and backslope positions (B2, B5, I1), 20% NPV (20StNPV) distributed between the footslope and filter strips further upslope (B3, B4, O2) (Table 2.1). Three watersheds (B6, I3, O3) received 100% row crop (100RC) treatment. Two hillslopes (C1-C2) received 100% NPV treatment (100NPV) prior to 2007. Due to limited runoff data availability for C1 and C2, data from these

sites were combined (C1-2). A 2-year no-till corn-soybean rotation was implemented in areas of the watershed not planted with NPV (Hernandez-Santana et al., 2013). For more information on site description and prairie implementation, refer to Hernandez-Santana et al. (2013).

Runoff data were collected at fiberglass H flumes installed at the bottom of each hillslope, beginning in 2005 and 2006 (Hernandez-Santana et al., 2013). Flow (L/T) within each flume was measured at a 5 min interval and summed for each precipitation event to compute total event runoff. Data from 1 May to 30 September for the 2008-2014 period were used in this study. Hourly precipitation data from a National Weather Service Hydrometeorological Automated Data System (HADS) station located approximately 1.3 – 3.6 km from the study sites (Station NSWI4) were used as observed precipitation for each study site.

2.2.2 SCS Curve Number Method

The Curve Number Method was first introduced in the National Engineering Handbook, Section 4 (NEH4) by the USDA Soil Conservation Service (USDA-SCS, 1964) as a way to determine the depth of runoff resulting from a given precipitation event over a watershed based on land cover and soil conditions (Hawkins et al., 2009; USDA-NRCS, 2004). The conceptual model begins by separating rainfall into three components:

$$P = P_e + I_a + F_a \tag{2.1}$$

where P is the depth of precipitation, P_e is the depth of runoff, I_a is the initial abstraction before runoff occurs, and F_a is the additional depth of retention after runoff begins. F_a is less than or equal to a potential maximum retention S, and the maximum amount of potential P_e is the total P minus the I_a. Therefore, from continuity, the following ratios of the actual to the potential quantities are assumed equal:

$$\frac{F_a}{S} = \frac{P_e}{P - I_a} \tag{2.2}$$

Combining (2.2) with (2.1) and solving for the depth of runoff (millimeters) gives the SCS rainfall-runoff relationship:

$$P_e = \frac{(P - I_a)^2}{P - I_a + S} \qquad for\ P > I_a \tag{2.3}$$

The relationships for I_a (millimeters) and S(millimeters) were empirically found to be:

$$I_a = \lambda S \tag{2.4}$$

$$S = \frac{25400}{CN} - 254 \tag{2.5}$$

where λ is the initial abstraction coefficient, and CN is the curve number value as a function of land cover, soil type, and antecedent soil moisture conditions.

Although a value of 0.2 for λ was adopted by the SCS (Hawkins et al., 2009; Ponce and Hawkins, 1996), Ponce and Hawkins (1996) suggested that the value of λ may vary regionally based on the local geologic and climatic setting. A recent study examining rainfall runoff data from 307 study sites across 23 US states found λ to be closer to 0.05 (Woodward et al., 2003). This value for λ is supported by other studies (Baltas et al., 2007; Shi et al., 2009). Shi et al. (2009) found λ to equal a value of 0.048 for an experimental watershed in the three gorges area of China, while Baltas et al. (2007) found λ to equal a value of 0.014 for an experimental watershed in Greece. Given these recent studies and the uncertainty of the proper value for λ, values of λ = 0.2 and λ = 0.05 are tested in this study.

To account for the effect of AMC on the amount of runoff produced, the CN can be adjusted to three basic moisture conditions based on the 5-day prior rainfall and time of year: AMC I (dry), AMC II (average), and AMC III (wet). However, adjusting the CN solely based on

prior moisture conditions has been found to be inaccurate in most cases (Hawkins et al., 2009). Hawkins and Cate (1998) analyzed runoff data against 5-day prior rainfall for 25 agricultural watersheds and found a correlation between the two variables for only 11 of the watersheds. Van Mullem (1992) used infiltrometer data to determine the effects of prior soil moisture on calculated CN values. The results did reveal an average CN increase of 9%-40% between the dry conditions and wet conditions, but the overall relationship between CN and prior soil moisture was very weak. A study by Hawkins and VerWeire (2005) further affirm the Van Mullem (1992) results. In contrast, Montgomery and Clopper (1983) found a strong correlation between 15-day antecedent precipitation and potential maximum retention S. More recently, Jacobs et al. (2003) were able to extract a soil moisture signal in CN values using remotely sensed soil moisture.

Due to the general consensus that variations in CN are related to multiple factors including location, soil type, vegetation, storm intensity, etc., the Antecedent Runoff Condition (ARC) concept (Hawkins et al., 2009; Hjelmfelt, 1991; Hjelmfelt et al., 1982; Van Mullem et al., 2002) is suggested as a better alternative to using AMC. ARC III (wet) corresponds to the 90^{th} percentile runoff value, whereas ARC I corresponds to the 10^{th} percentile runoff value at a given rainfall amount (Hjelmfelt, 1983; Hjelmfelt et al., 1982).This generalization acknowledges that CN is a random variable that falls within a given range depending upon a number of possibly varying conditions.

2.2.3 Rainfall-runoff data preparation

For each precipitation event in the 2008-2014 record, the corresponding runoff was identified from the observed time series at each site. Due to the 60 minute reporting interval of the HADS station, runoff analysis began in the hour before precipitation was recorded. Following the precipitation event, the point at which runoff ended was identified and the total

depth of runoff for each event was computed for each site. In some cases, a steady but negligible flow of runoff continued well past the completion of the event. Therefore, if outflow changed minimally over the course of a one hour period, it was assumed that event-based surface runoff was complete. For each precipitation event, the 5-day AMC were also determined.

Between 382-441 precipitation events were analyzed for each study site depending on periods of missing precipitation or runoff data. If erroneous values were extracted for a given hillslope (i.e site runoff greater than total precipitation), then rainfall-runoff data for that event were not included in the analysis. Approximately 35-40 events had total precipitation greater than 25.4 mm (1 inch).

Prior to deriving the CN values, the precipitation (P) and runoff (Q) data were reordered using a technique called "frequency matching". Because the original use of the SCS rainfall-runoff equation was to determine a given return period runoff (i.e. 100-year flood) from the same return period rainfall (i.e., 100 year storm), several studies recommend reordering the data such that the N year return period rainfall is matched with the N year return period runoff (Hjelmfelt, 1980, 1983, 1991; Van Mullem *et al.*, 2002; Hawkins *et al.*, 1993, 2009). This frequency matching method, which was introduced by Schaake *et al.* (1967), entails sorting the P and Q datasets separately and then rematching both data sets on a rank-order basis, essentially relating the rainfall frequency curve to the runoff frequency curve. This creates new P:Q data pairs, also called "ordered data", in which the pairs have equal return periods. In the studies mentioned above, the reordering technique has been found to be the most reliable technique and was able to give accurate CN values based on a fairly small sample size (minimum sample size approximately 30).

2.2.4 Deriving the CN

The CN was computed for each P:Q pair by solving for S within equation 2.3 using the following relationship (Hawkins, 1973):

$$S = 5\left[P + 2Q - (4Q^2 + 5PQ)^{\frac{1}{2}}\right] \quad (2.6)$$

Traditionally, the CN for a watershed has been determined by taking the median of the CNs associated with all annual maximum P,Q events; this is known as the NEH4 method (Hawkins et al., 2009; Ponce and Hawkins, 1996; USDA-NRCS, 2004; USDA-SCS, 1964). However, the limitation of this method is the long period of record that is required to collect a sufficient number of maximum annual P,Q events to accurately define the CN. To overcome this, studies now typically use many rainfall-runoff events per year to determine CNs. However, using smaller events introduces unwanted rainfall depth effects. For example, Sneller (1985) was the first to show a high bias in CN values for low rainfall events. A possible reason for this is due to data censoring in which any rainfall event that produce no runoff, i.e. $P < I_a$, is purposefully eliminated by the analyzer (Hawkins et al., 2009). Hjelmfelt (1991) suggests that these P,Q data pairs should be included in CN derivation to avoid a high bias in the CN. High bias may also become manifest through error in the CN method or data. Specifically, any CNs that are realized at small rainfalls will inevitably have high values. To overcome the limitations in the NEH4 method, Hawkins et al. (2009) recommends using one of two techniques for deriving CN values: the Least Squares method (LSM) or the Asymptotic method. A number of recent studies have successfully used these methods to derive watershed CNs (D'Asaro et al., 2014; D'Asaro and Grillone, 2012; Stewart et al., 2012; Tedela et al., 2012) and both were tested in this study.

2.2.4.1 Least Squares Method

The objective of the Least Squares Method is to minimize the sum of squares between the calculated runoff (Q_{calc}) and observed runoff (Q_{obs}) using the following objective function (Hawkins et al., 2009):

$$F = \sum (Q_{calc} - Q_{obs})^2 \quad (2.7)$$

where Q_{calc} is equal to P_e in equation 2.3. In order to avoid over biasing affects for small CN values, it is typical to fit the CN equation (2.3) to P,Q data for events greater than 25.4 mm. Therefore, only frequency-matched P,Q data points for P > 25.4 mm were used with the LSM to derive a CN for each study site. CNs were derived using $\lambda = 0.2$ (LSM-0.2) and $\lambda = 0.05$ (LSM-0.05) and compared. Events that produced zero runoff were included in this method.

2.2.4.2 Asymptotic fitting method

The Asymptotic fitting method is based on findings by Hawkins (1993), who identified several relationships between CN values and rainfall depth when using ordered data. The calculated CN values tended to approach a constant value at higher rainfalls, but displayed increasing or decreasing trends at lower rainfalls. Three defining relationships were identified between the CN and total P: standard, violent, and complacent (Hawkins, 1993; Hawkins et al., 2009).

Standard behavior is described as having an initially declining CN with increasing storm size. CN approaches a near constant value, called CN_∞, at higher rainfalls. Approximately 70% of watersheds display this relationship (Van Mullem et al., 2002). Complacent behavior is characterized by a declining CN with no approach to a stable asymptotic value at high rainfalls. The CN method is not a suitable choice for estimating runoff from a watershed displaying complacent behavior because it is likely that only a small percentage of the watershed is

contributing to runoff in these cases (Hawkins, 1993). Data displaying complacent behavior more appropriately fits a linear relationship $Q = cP$, with c equal to the fractional area contributing to runoff (Hawkins, 1993; Hawkins et al., 2009). D'Asaro and Grillone (2012) modified the above linear relationship for data that does not indicate complete complacent behavior. This modified relationship was further successfully verified by D'Asaro and Grillone (2015) for the Upper Debidue Creek Watershed in South Carolina. In the present study, asymptotic fitting was performed using only standard or violent behavior. Violent behavior is characterized by complacent behavior at small rainfall values, with an abrupt rise to a higher stable CN value for larger rainfall events (indicating a larger runoff response). This abrupt rise typically occurs in the range of 25.4 mm (1 in) to 76.2 mm (3 in) of rainfall (Hawkins et al., 2010). Violent behavior is characteristic of headwater basins with high infiltration soils and steep topography.

Given the three described behaviors, asymptotic least squares fitting was used to determine the steady-state CN at higher rainfall values (CN_∞). Hawkins et al. (2009) recommends using:

$$CN(P) = CN_\infty + (100 - CN_\infty)e^{-kP} \qquad Standard\ Behavior \tag{2.8}$$

for the standard case, and:

$$CN(P) = CN_\infty\left(1 - e^{-k(P - P_{min})}\right) \qquad Violent\ Behavior \tag{2.9}$$

for the violent case, where k (mm^{-1}) in both equations is a fitting coefficient and P_{min} (mm or inch) is a threshold rainfall value identified by the user. In this study, the asymptotic method was used to derive a CN for each study site using the frequency-matched P,Q data. As with the LSM, CNs were derived using $\lambda = 0.2$ (ASM-0.2) and $\lambda = 0.05$ (ASM-0.05).

2.2.5 CN Verification

Derived CN values were verified for each study site using leave-one-out cross-validation (Efron, 1982). This procedure entailed deriving the CN using the LSM and Asymptotic method with $\lambda = 0.2$ and $\lambda = 0.05$ for 6 of the 7 years. For the 7th year, runoff was computed for all rainfall events with P > 25.4 mm. The runoff was computed with and without the original NEH4 AMC adjustment to determine any significant performance differences. The verification was conducted for all 7 years (2008-2014) and the calculated runoff was evaluated against observed runoff using the Nash–Sutcliffe efficiency measure (NSE):

$$NSE = 1 - \left(\sum_{t=1}^{N}(Q_{calc} - Q_{obs})^2 \Big/ \sum_{t=1}^{N}(Q_{obs} - \overline{Q_{obs}})^2\right) \quad (2.10)$$

where Q_{calc} is the calculated runoff using the estimated CN, and Q_{obs} is the observed runoff for that particular event. NSE is one minus the mean square error divided by the variance of the observations and indicates how well the simulation accounts for variance in the observations. Values for the NSE range from $-\infty$ to 1, where 1 is an optimal score. NSE > 0.30 was considered to be satisfactory performance, and NSE > 0.60 was considered to be good performance (Motovilov et al., 1999).

2.3 Results

2.3.1 CN Values

Example results from the LSM-0.2 and ASM-0.2 methods are shown for the Basswood sites (Figure 2.2) and final curve numbers are given in Table 2.2. For the LSM-0.2 method, the Basswood sites generally had the highest CN values, ranging from 66.2 to 84.6 (Figure 2.2a, Table 2.2). The Orbweaver sites had the lowest CN values and range across sites, from 72.5 (10FootNPV) to 74.5 (100RC) (Table 2.2). A CN = 66.2 was produced for the Basswood 1 site;

this value is lower than the two 100NPV sites (Cabbage 1-2) which had an average value of 70.4. All other sites with some row crop had higher CNs than the 100NPV sites. The ASM-0.05 method produced similar results, and in general higher CNs. The ASM-0.05 method produced the lowest CN for the 100NPV sites, Cabbage 1-2, as would be expected. However, Basswood 1 was only about 2% higher than Cabbage 1-2.

Table 2.2. CN values derived using the least squares method and asymptotic least squares method with a λ of 0.2. Percent change from all row crop was calculated for each method using the site with 100% row crop (100RC) from the corresponding cluster.

Site	Treatment	CN - Least Squares	% Change from all row crop	CN - Asymptotic	% Change from all row crop
Orbweaver 1	10FootNPV	72.5	2.7	74.4	-1.3
Orbweaver 2	20StNPV	73.0	2.1	71.1	3.2
Orbweaver 3	100RC	74.5		73.4	
Interim 1	10StNPV	72.3	11.9	72.1	13.8
Interim 2	10FootNPV	75.3	7.7	74.8	10.2
Interim 3	100RC	81.4		82.8	
Basswood 1	10FootNPV	66.2	23.4	68.6	24.6
Basswood 2	10StNPV	80.0	4.4	81.4	7.6
Basswood 3	20StNPV	78.7	6.1	77.7	12.3
Basswood 4	20StNPV	84.6	-1.1	87.1	0.8
Basswood 5	10StNPV	80.8	3.4	80.1	9.2
Basswood 6	100RC	83.7		87.8	
Cabbage 1-2	100NPV	70.4		67.4	

CN values for watersheds with NPV treatment were, on average, 10.4% lower than CN values for 100RC treatment when comparing across paired watersheds (i.e., comparing CN values between Basswood sites); however, results did vary among the different sites. With the exception of Basswood 1, the Interim sites 1 and 2 displayed the most significant reduction in the CN compared to the 100RC treatment (Interim 3) (Table 2.2). Orbweaver sites 1 and 2 and Basswood sites 2, 4-5 had less than a 10% decrease in the CN compared to the 100RC treatment watersheds for both the LSM-0.2 and ASM-0.2 methods.

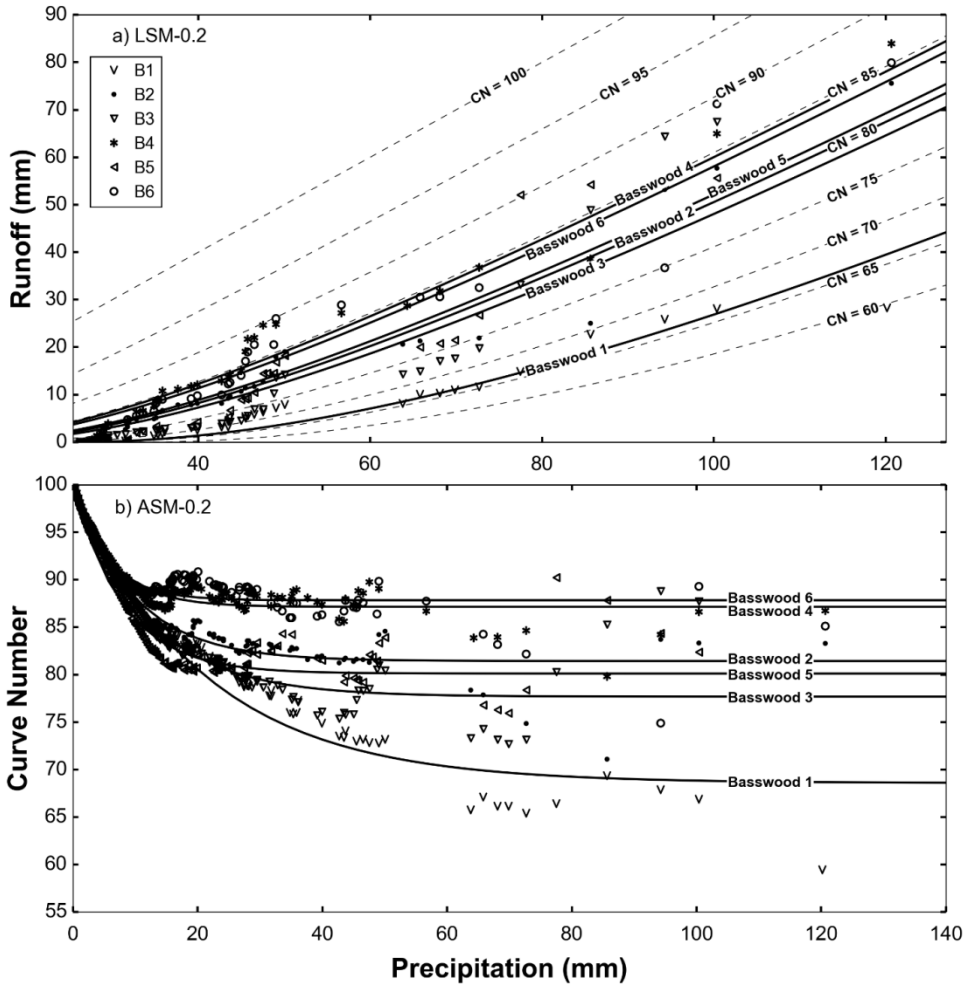

Figure 2.2. Curve number derivation for the Basswood hillslopes (B1-B6) using the a) least squares method and b) asymptotic least squares method for a λ of 0.2. Runoff versus precipitation is plotted for the least squares method (a) and curve number versus precipitation is plotted for the asymptotic least squares method (b).

Using λ = 0.05 (Table 2.3) resulted in curve numbers that were approximately 12.0% lower than those produced with λ = 0.2 (Table 2.2), with the Asymptotic method again producing higher values than the Least Squares Method. The spread between CNs across paired watersheds was greater when using λ = 0.05. This resulted in greater differences between the sites with 100RC and those with some NPV, with the largest differences again occurring for Basswood 1 (39.2%) and Interim 1 (19.8%) for LSM-0.05 (Table 2.3). A greater spread between

100RC and NPV sites at λ = 0.05 can be expected due to the exponential term in the SCS CN relationship (equation 2.3).

Table 2.3. CN values derived using the least squares method and asymptotic least squares method with a λ of 0.05. Percent change from all row crop was calculated for each method using the site with 100% row crop (100RC) from the corresponding cluster.

Site	Treatment	CN - Least Squares	% Change from all row crop	CN - Asymptotic	% Change from all row crop
Orbweaver 1	10FootNPV	61.2	5.0	65.9	0.5
Orbweaver 2	20StNPV	62.4	3.1	54.5	19.4
Orbweaver 3	100RC	64.3		66.2	
Interim 1	10StNPV	61.5	19.8	60.2	21.2
Interim 2	10FootNPV	66.0	12.7	66.1	11.8
Interim 3	100RC	75.0		74.4	
Basswood 1	10FootNPV	52.6	39.2	61.4	29.4
Basswood 2	10StNPV	73.0	7.0	71.1	15.0
Basswood 3	20StNPV	71.0	9.7	65.7	22.8
Basswood 4	20StNPV	79.6	-1.7	82.1	0.6
Basswood 5	10StNPV	74.1	5.5	73.7	11.3
Basswood 6	100RC	78.3		82.6	
Cabbage 1-2	100NPV	57.1		59.6	

CN values for 100NPV treatment were found to be lower than CN values for most sites with mixed NPV and row crop. In addition, sites with some NPV treatment were generally found to have lower CNs than the sites with 100RC. These results are consistent with those seen in Hernandez-Santana et al. (2013) who found an average 37% reduction in runoff volume from 100RC for sites with NPV treatment. In their study, 100NPV treatment consistently had the lowest runoff volumes. One exception was Basswood 1, which had CN values similar to 100NPV treatment. Further, the decline in the CN was not always consistent with the increase in percent NPV. For example, Basswood 2 with 10% NPV had a lower CN than Basswood 4 with 20% NPV for all methods tested (Tables 2.2 and 2.3). The Asymptotic method (ASM-0.2 and ASM-0.05) actually showed an increase in CN value for Orbweaver 1 (10FootNPV) compared to

Orbweaver 3 (100RC), indicating that results for the Orbweaver sites are more inconclusive compared to the Interim and Basswood sites.

Table 2.4. Weighted-average CN values calculated using the CN values derived from the least squares and asymptotic methods with a λ of 0.2. Curve numbers were calculated using the site with 100% row crop (100RC) from the corresponding cluster and CN values for 100% native prairie vegetation (100NPV) derived from Cabbage 1-2.

Site	Treatment	Weighted CN Least Squares	% Change from NPV treatment	Weighted CN Asymptotic	% Change from NPV treatment
Orbweaver 1	10FootNPV	74.1	2.1	72.8	-2.1
Orbweaver 2	20StNPV	73.7	1.0	72.2	1.5
Interim 1	10StNPV	80.3	10.5	81.3	11.9
Interim 2	10FootNPV	80.3	6.4	81.3	8.3
Basswood 1	10FootNPV	82.3	21.8	85.8	22.3
Basswood 2	10StNPV	82.3	2.9	85.8	5.2
Basswood 3	20StNPV	81.0	2.8	83.7	7.5
Basswood 4	20StNPV	81.0	-4.3	83.7	-4.0
Basswood 5	10StNPV	82.3	1.9	85.8	6.8

To evaluate the impact of spatial placement of NPV in the watershed on CN values, area weighted CNs were derived for each basin with NPV treatment using the standard CN weighting method and the values derived for 100% NPV or RC (Table 2.4). For example, Orbweaver 1 has 10% NPV and 90% row crop. Weighting the LSM-0.2 CN value from Cabbage 1-2 at 10% and the CN value from Orbweaver 3 at 90% produces a weighted CN value for Orbweaver 1 of 74.1 (Table 2.4). With the exception of Basswood 4, the weighted CNs were higher than the empirically derived CNs for the basins. Further, sites with equal percentage NPV (e.g. Basswood 1, 2 and 5) all had the same weighted CN, even though the runoff potential is less for the basin where the NPV is concentrated in the footslope as indicated by the lower CN for Basswood 1. It should be noted that the impact of NPV placement on the CN value is not consistent across the study sites, thus there is uncertainty in the observed CN.

2.3.2 Verification

The CNs were verified first by applying the CN method without adjusting the value for AMC conditions. As discussed in section "*SCS Curve Number Method"*, there is uncertainty regarding the use of antecedent precipitation to change the CN value. We tested the effects of using the method with the values found in Tables 2.2 and 2.3 without adjustment. For sites Basswood 1, Interim 1 and 2, performance was poor without consideration of AMC for LSM-0.2 (Figure 2.3a). There were only five sites that met a minimal acceptance criterion of NSE > 0.30. The NSE values for the sites vary by method used to derive the CN (Figure 2.3).

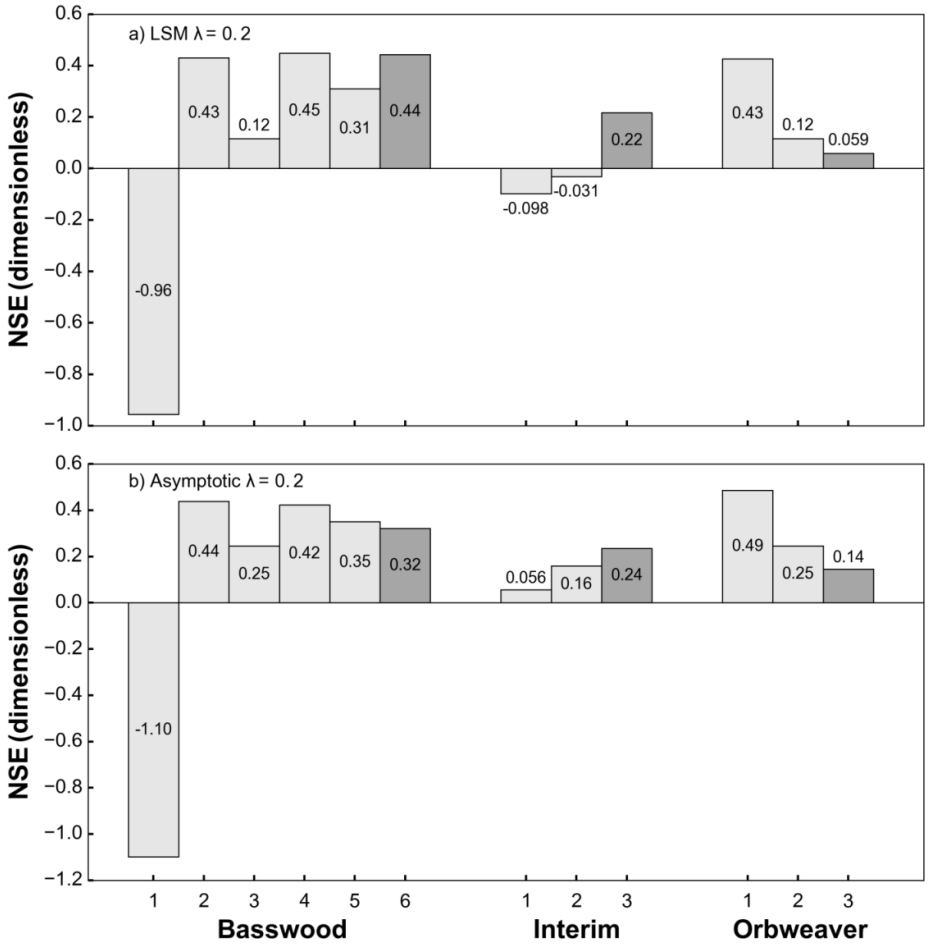

Figure 2.3. Nash Sutcliffe Efficiency scores verifying the CN values derived using the a) least squares method and b) asymptotic least squares method for a λ of 0.2 with no AMC adjustment. Dark gray bars indicate sites with 100% row crop (100RC) treatment.

Including an adjustment for AMC, as per original CN guidelines, improved the CN application considerably overall (Figure 2.4). For the LSM-0.2 method, 10 sites met the minimally acceptable level for NSE, and two showed good performance with values > 0.60 (Figure 2.4a). Values were still lower than 0.30 for Basswood 1 and 6. NSE values were better for most sites for the Asymptotic method (Figure 2.4b), with eleven of the sites having minimally acceptable performance. A notable improvement occurred for the 100RC sites (Basswood 6, Interim 3, and Orbweaver 3). Basswood 1 displayed poor performance, regardless of the method used to derive the CN.

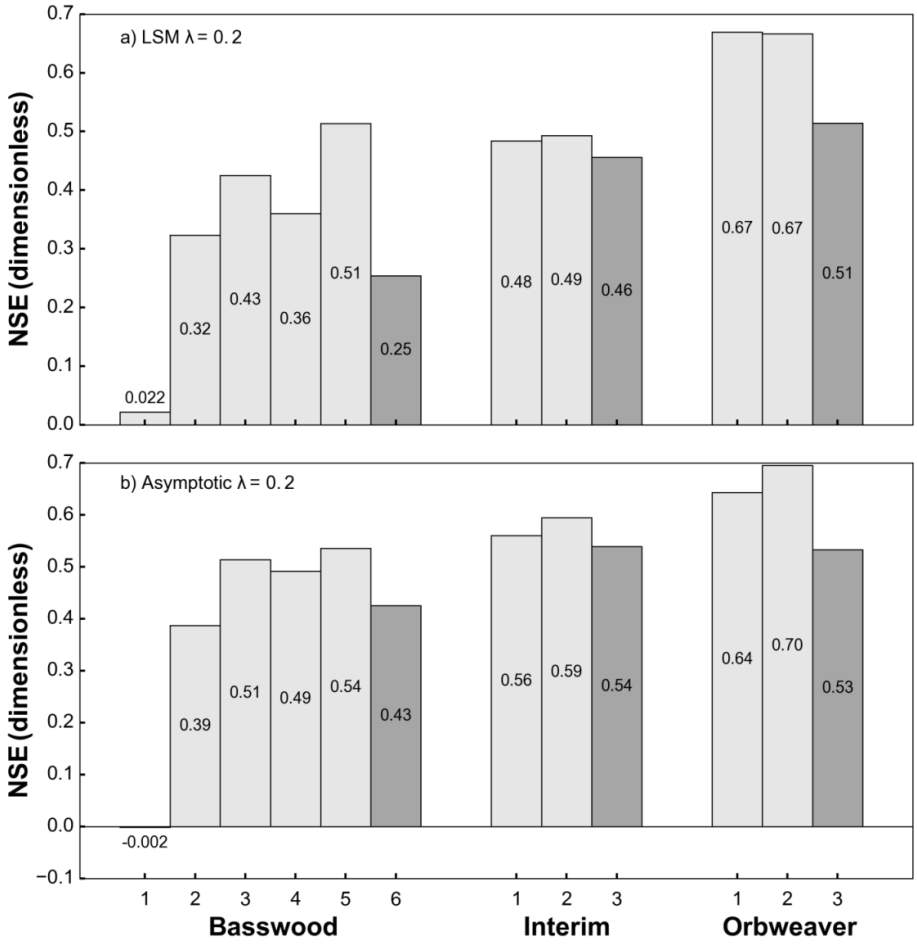

Figure 2.4. Nash Sutcliffe Efficiency scores verifying the CN values derived using the a) least squares method and b) asymptotic least squares method for a λ of 0.2 with AMC adjustment. Dark gray bars indicate sites with 100% row crop (100RC) treatment.

Finally, CNs derived using λ = 0.05 were verified (Figure 2.5). For the majority of cases (the exception being Basswood 3 and Orbweaver 2 for the LSM method), the NSE values were improved when using the smaller λ value. The Asymptotic method again produced the better results, with five sites above or near NSE values of 0.60, compared to two for the LSM.

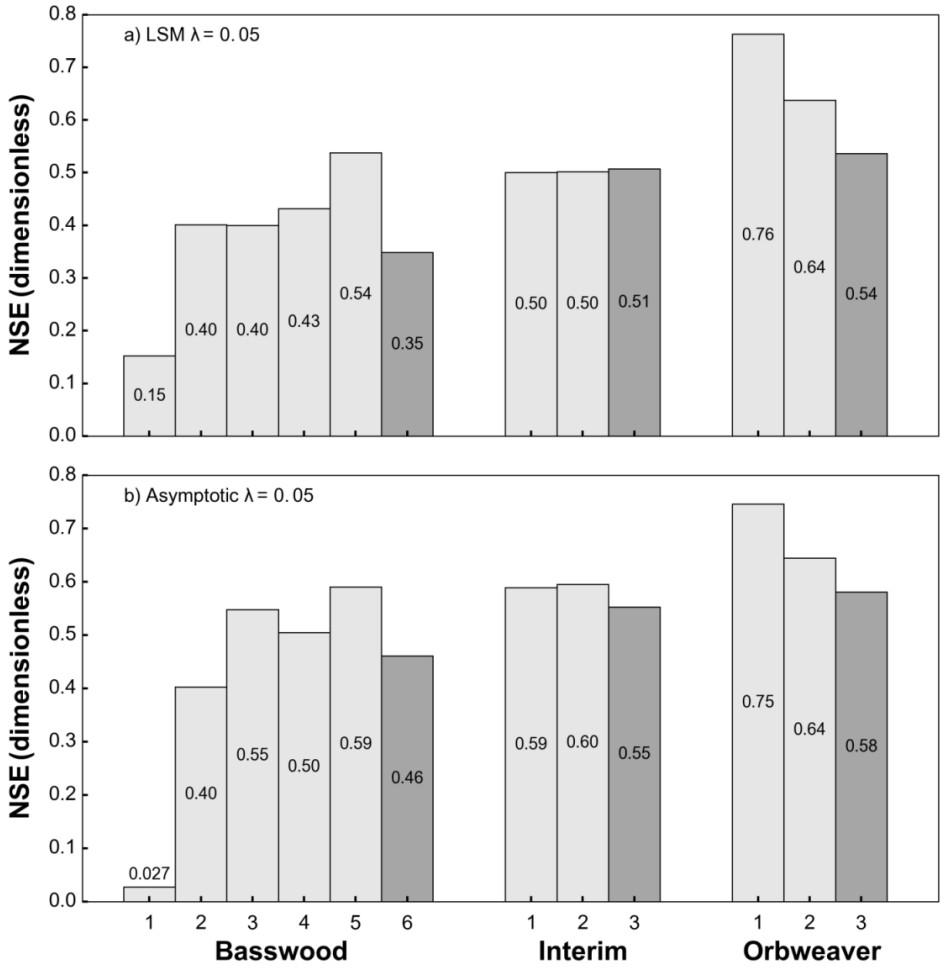

Figure 2.5. Nash Sutcliffe Efficiency scores verifying the CN values derived using the a) least squares method and b) asymptotic least squares method for a λ of 0.05 with AMC adjustment. Dark gray bars indicate sites with 100% row crop (100RC) treatment.

Derived CN values for Orbweaver proved to consistently perform best for estimating runoff from rainfall data. The Orbweaver sites had the highest NSE values (0.58 – 0.75 for ASM-0.05), closely followed by the Interim sites (0.55 – 0.6 ASM-0.05). The Basswood sites

were overall lower (0.02 – 0.59 ASM-0.05). Basswood 1 only had significant verification improvement using CNs derived from LSM-0.05, however the NSE was still unacceptable at 0.15.

Overall, the best verification results were found for the asymptotic method with $\lambda = 0.05$ when AMC corrections were performed. However, the CNs derived with ASM-0.2 with AMC corrections also had good results. The derived CN values for all sites, with the exception of B1, were shown to be effective for estimating runoff from rainfall data.

2.4 Discussion

2.4.1 CN derivation and verification

Based on our results, NPV placed within row crops reduced the CN (and runoff) in all cases. However, we show there is considerable variation in the degree to which the CN is affected by the NPV. Hernandez-Santana et al. (2013) found that the 10FootNPV treatment produced the lowest cumulative runoff volume for the years of 2008-2010. In their study, runoff data from the three 10FootNPV plots are combined into a single average runoff value to determine cumulative runoff. In this study, we evaluated each watershed separately and found only weak evidence that the 10FootNPV is the most effective treatment for runoff reduction based on the CNs produced. While we did find that Basswood 1 with 10% NPV at the footslope consistently showed the lowest CN values across all study plots, the CN values for Basswood 1 did not verify well for any method tested. Interim 2, which also had 10% NPV at the footslope, had CN values that were greater than two sites receiving different NPV treatments - Interim 1 (10StNPV) and Orbweaver 2 (20StNPV). Additionally, Orbweaver 1 (10FootNPV) did not have CN values significantly different from Orbweaver 2 (20StNPV), with the exception of ASM-0.05, where a significantly higher CN than Orbweaver 2 was found.

Verification results indicated that the most accurate estimations of runoff were produced when using the AMC corrections as originally published by the SCS (USDA-SCS, 1964) and a λ value of 0.05. Basswood 1 was the only site that verified significantly better using the LSM-0.05 method than the ASM-0.05 method. When applying the Asymptotic method for Basswood 1, the equation for standard behavior was used. Upon further examination, it appeared that Basswood 1 possibly displayed a complacent behavior rather than a standard behavior because the CN values display a broader decline for small precipitation events and continue to decline for higher precipitation values (Figure 2.2). This would indicate that only a small portion of the watershed actually contributes to runoff (Hawkins et al., 2009). A complacent behavior would make the Asymptotic CN fitting method invalid for the watershed and may explain the poor results for this site during verification. This conclusion is supported by data analyses conducted by Chen et al. (2015) for these sites using the 2008-2011 period. In their study, a scaling factor was used to analyze the similarity of the runoff magnitude of the hydrologic responses between each of the plots and hillslope Basswood 6. Chen et al. (2015) found a low scaling factor for Basswood 1 with a relatively narrow range of values for 72 events during the 2008-2011 period. This indicates that the magnitude of runoff produced by Basswood 1 was not similar to the runoff produced by Basswood 6 for these 72 events. Additionally, using 44 events in 2010 and 2011, Chen *et al.* (2015) performed a multivariate linear regression to determine any relationship between scaling factor and antecedent soil moisture and maximum hourly rain accumulation. They found relatively little correlation ($R^2 = 0.03$) between the scaling factor and the two variables for Basswood 1. At all other sites, R^2 values between 0.36 and 0.75 were found. The scaling factor was also found to be consistently low for Basswood 1 for all 44 events. The results from Chen et al. (2015) correspond to the suspected complacent relationship observed in our

study for Basswood 1, suggesting that the CN for this basin might be erroneous. Watersheds Basswood 2-5 showed a higher average scaling factor (Chen et al. (2015) and followed standard behavior in this study; we therefore have more confidence in those values.

Assuming a linear relationship between P and Q may be more appropriate for Basswood 1 (Hawkins et al., 2009); however, Basswood 1 does not display an obvious complacent behavior given that is does not fully fit either a linear relationship or the traditional CN relationship (equation 2.3). To test this, CNs were derived for Basswood 1 using the relationship by D'Asaro and Grillone (2012) for semi-complacent behavior. Using this method, the CNs for Basswood 1 increased significantly to 76.0 and 55.4 for LSM-0.2 and LSM-0.05, respectively. These values, particularly for $\lambda = 0.2$, are more in line with CN values derived for the other Basswood sites. The fraction of the watershed found to be contributing to runoff (C in the relationship) was found to be 0.57 and 0.89 for $\lambda = 0.2$ and $\lambda = 0.05$. This signifies that a large percentage of the site appears to have infinite storage. It is not clear why this site tends to displays a complacent behavior. Soil type, slope, size, and the width of the prairie filter strip for this site are very similar to the other Basswood sites (Table 2.1). D'Asaro and Grillone (2015) found a strong correlation between the fraction of the watershed contributing to runoff and high water table elevations at the Upper Debidue Creek Watershed. It is a possibility that such an effect may be occurring at this site; however, measurements would be necessary to definitively support this statement. The complacent behavior seen at Basswood 1 needs further investigation, as based on current measurements of physical site characteristics and observed data, it is not obvious why this site behaves differently than others.

Results from the CN verification indicated that runoff is modeled more accurately when antecedent precipitation was taken into account to adjust the CN for soil moisture conditions.

This finding contrasts with Hjelmfelt (1983) who stated that the AMC moisture classes based on 5-day antecedent precipitation are not applicable to Iowa or Missouri. Furthermore, the NRCS no longer endorses the AMC table because a review by the NRCS found that the AMC table was only applicable to certain small watersheds in Texas (Hawkins et al., 2009). There are many factors that can influence runoff in addition to soil moisture. These factors include storm duration, spatial variability of rainfall (intensity and amount), stage of plant growth, microtopography, among others (Beven, 2012; Dunne et al., 1991). Recent work has attempted to create more accurate soil moisture accounting algorithms to avoid problems with AMC adjustments such as large jumps in estimated runoff and to take into account other factors such as evapotranspiration, soils with low storage, and shallow soils (Kannan et al., 2008; Michel et al., 2005; Mishra et al., 2008; Sahu et al., 2007). Findings in this study do support the conversion of CN values based on AMC conditions for Iowa, as can be seen in the improved NSE results between Figures 2.3 and 2.4.

The use of a λ value of 0.05 led to marginal improvements for most study sites compared to the traditional value of 0.2. These results support the recent findings by a number of studies (Baltas et al., 2007; Shi et al., 2009; Woodward et al., 2003). As was previously mentioned, Woodward *et al.* (2003) used iterative least squares fitting to determine the optimal λ for rainfall-runoff data from 307 USDA-ARS watersheds; the optimal λ value was 0.05. Most recently, D'Asaro *et al.* (2014) derived λ values for 46 watersheds in Sicily and found that λ was equal to or exceeded 0.2 for only 5 of 46 watersheds. Most λ values in their study were less than 0.1, which led them to conclude that a λ of 0.05 is appropriate. The λ values derived in these studies correspond to the improved NSE values seen for λ of 0.05.

2.4.2 CN Uncertainty

CNs for Orbweaver had smaller differences across the various treatments compared to the Interim or Basswood sites. Using the 10FootNPV case as an example, published SCS values for straight row crop in good condition (85, soil group C) and grassland in good condition (74, soil group C), would produce a simple weighted average CN of 83.9, a difference of 1.1 from row crop. This is the approximate difference between Orbweaver 1 and 3. An average difference of 7.9 was found in CNs between Interim 2 and 3, and an average difference of 20.9 was found between Basswood 1 and 6. Given the possible issues discussed above, the differences for the 100RC and 10FootNPV site at Basswood are likely unreasonably large.

One factor that may be influencing the range and variability of CNs between sites is the watershed size. The Basswood sites were generally smallest (0.47 - 1.24 ha), followed by Orbweaver (1.18 - 2.40 ha) and Interim (0.73 - 3.19 ha). It is possible that the small size of the Basswood plots may be inducing a more rapid and peaky response compared to the Orbweaver or Interim plots. This may lead to more runoff and higher CNs relative to the other sites. In contrast, the larger plot sizes in the Interim cluster may produce longer travel times and more opportunity for infiltration, thereby reducing runoff. Simanton et al. (1996) derived CNs for 18 watersheds in Arizona, USA ranging from 0.00069 Ha to 785.3 Ha and found a strong relationship of decreasing CN with increasing basin size. While it is difficult to isolate this effect in the current study, Chen et al. (2015) found a weak relationship between the watershed size and magnitude of response for the Basswood sites. Their finding was, however, not consistent across all events.

The higher slope of Orbweaver 1 (10.3%) as opposed to Orbweaver 3 (6.6%) may explain, in part, why there was only a slight CN decrease in the CN for Orbweaver 1

(10FootNPV) compared to Orbweaver 3 (100RC). However, Orbweaver 2 has an almost identical slope (6.7%) to Orbweaver 3, and also produced CNs that were close to Orbweaver 3. Likewise, it may be assumed that the lower slopes of Interim 1 (7.7%) and Interim 2 (6.1%) may have aided in runoff reduction compared to Interim 3 (9.3%), but it is very difficult to prove this. Currently, SWAT does not take into account slope; however, the theoretical documentation suggests using a relationship developed by Williams (1995) to modify CNs prior to input into SWAT. This relationship assumes that CNs derived by the SCS are appropriate for 5% slopes. The equation used by SWAT increases the CN by 0.93 with each percent increase in slope at a CN of 50, and by 0.25 at a CN of 90. To test the impact on the CNs derived in this study, the CNs were adjusted down to the baseline 5% slope using the slope correction equation. The Williams (1995) relationship decreased the CNs by 0.8 – 2.8 when tested for the LSM-0.2 and ASM-0.2 methods, with an average decrease of 1.2. The cabbage sites were the only sites where CN increased by approximately 1 due to the slope being less than 5% (approximate 3.5% slope). Prior to slope correction, an average 6.7 and 8.9% decrease in CN was seen for sites with NPV treatment when compared to sites with 100RC for LSM-0.2 and ASM-0.2. Following slope correction, these percent decreases changed to 6.5% and 9.0% respectively, a relatively insignificant difference given all other sources of error in the CN method. Studies by Garg et al. (2003) and VerWeire et al. (2005) indicated a -1.3 and -1.73 CN reduction per percent increase in slope, which is in contrast to Williams (1995). A more recent study by Suresh et al. (2013) found that slope significantly affects the CN in forested landscapes; however, this effect is minimal for areas where agriculture is the dominant land use. Hawkins *et al.* (2009) notes that no significant verification has been performed on the equation presented by Williams (1995) and a reference slope of 5% is not found in NEH4. In light of the minimal effects seen above and the

statements by Hawkins et al. (2009), results presented were not slope corrected. It is also possible that slope length may be effecting CN values to some degree, but studies indicate that slope effects may be negligible considering the range of slope and slope lengths of these study plots (Chen et al., 2015).

A final consideration is the impact of width of the prairie filter strips on the runoff. The width of the filter strips at the footslope range from 37.6 m to 46.4 m for the Basswood sites, with even greater widths and ranges for the Interim and Orbweaver sites. Chen et al. (2015) did not find filter strip width to have a meaningful effect on runoff. However, Hernandez-Santana et al. (2013) found the filter strips width to be the main controlling variable for runoff reduction during an initial runoff analysis performed for these sites.

Small scale spatial variability in antecedent moisture and rainfall intensity may also be contributing to the variations in CNs seen across the sites. However, because results are based on numerous events that occurred across several years, it would be unusual if these effects were not averaged out over time. Further, the clustered watersheds are located within close spatial proximity to one another – typically less than 0.5 km distance. Therefore, it can be assumed that spatial variation of soil characteristics and moisture conditions, as well as temporal variation of rainfall intensity within a cluster, is small (Chen et al., 2015). This assumption is supported by the good correspondence in CN values among clustered watersheds. For instance, the Basswood cluster tends to have higher CN values, and the Interim and Orbweaver clusters tend to have lower overall CN values. The intercluster distance was on the order of 1-3 km, which could explain differences in CN values between clusters. It is difficult to pinpoint any one variable as being the dominating factor in influencing the CN. This study highlights the complexity of the

runoff processes, and thus uncertainty of CN values at the hillslope scale observed by others (Scherrer et al., 2007; Sivapalan, 2003).

Error may also be present in the measurement of runoff and precipitation. Several events indicated a runoff depth slightly greater than precipitation depth. One possible explanation may be that flow within the unsaturated zone (interflow) may be exiting the surface near the flume; thus, this flow would be irrelevant to the Curve Number method but was still recorded as surface runoff. At some flumes, a minimal flow would continue to be recorded for several hours after the conclusion of a precipitation event. Even though this flow was negligible compared to flow during the event, it is difficult to know when surface runoff has truly stopped. Error may also be present in precipitation measurements due to gage undercatch and the limited observation points across the study region.

2.4.3 Spatial Effects of NPV Treatment on CN

The CNs derived empirically for eight of the nine sites with NPV treatment were lower than CNs derived using a weighted average method. Unfortunately, only the Cabbage 1-2 sites, which were located approximately 2 km from the nearest cluster (Orbweaver) and up to 3 km from the furthest cluster (Interim), had 100NPV. There were no 100NPV watersheds included in any of the clustered watersheds. Due to physiographic factors mentioned previously, the response of 100NPV treatment at the location of Cabbage 1-2 may not be the same as a 100NPV watershed at the other locations. The values derived for 100NPV for LSM-0.2 and ASM-0.2 (70.4 and 67.4 respectively), were lower than published value for grassland with soil group C (74). Due to the limited data available, it was difficult to evaluate the appropriateness of the asymptotic least squares fitting method for Cabbage 1-2 because the watershed behavior (i.e. standard or complacent) could not be clearly distinguished.

Despite some uncertainties in the analyses, the results indicate that the specific placement of different land covers within a watershed does impact the CN value. Taking into consideration both methods of derivation and both λ values, the derived CNs for NPV treated watersheds were 7.8% lower than the CNs calculated using a weighted-average. The ASM-0.05 method, which verified best, produced CNs for NPV treated watersheds that were on average 11.7% lower compared to the weighted-average CN. This difference could be significant when trying to model the impact of strategic placement of the NPV on runoff at a larger scale. Therefore, models that rely on the CN method may be improved by developing an approach to adjust the CN according to the physical placement of the different vegetation within the landscape, or by adopting a spatially-explicit distributed modeling approach.

2.5 Conclusions

Curve number values were derived for 14 watersheds located in south central Iowa using seven years of observed precipitation and runoff data. Three watersheds contained 100% row crop, two watersheds contained 100% native prairie vegetation, while nine watersheds contained varying percentages of prairie (10-20%) interspersed among row crops. Two methods of deriving the CN were tested along with two different values for the initial abstraction coefficient and antecedent moisture conditions. Major findings are:

- Strategic placement of native prairie vegetation within an agricultural landscape decreases the curve number. Our study indicated that derived CN values for NPV treatments were, on average, 7.8% lower than weighted-average CN values for the same hillslope.
- Our analysis suggests that the reduction in runoff from 10footNPV compared to 100RC may not be as significant as previously reported. Basswood 1, which had the lowest

overall CN and is characterized by 10FootNPV, displayed complacent behavior when deriving the CN using the asymptotic least squares method and did not produce acceptable NSE values during verification. If one does not consider Basswood 1 due to the poor verification, then the reduction in the CN values due to 10footNPV is similar to or lower than the other treatments tested.

- The CNs derived with the Asymptotic Method verified better than those derived with the Least Square Method, indicating this may be the most robust approach for empirically deriving CNs. Neither method produced acceptable NSE results during verification for the basin that appeared to have complacent behavior (e.g. Basswood 1).
- The CNs verified best when using a λ of 0.05. This supports other studies that suggest actual initial abstractions may be lower than originally published by the SCS.
- Adjusting for antecedent moisture conditions significantly improved the CN verification and had a bigger impact on NSE values than either the λ value or the CN derivation method.

Overall, the findings of this study reveal that the spatial placement of vegetation within an agricultural landscape has an observable impact on runoff and should be considered when modeling using the CN method. In lieu of implementing a fully distributed model, empirically-deriving CNs for particular land use configurations is possible. Although application of the CN values within hydrologic models was out of scope for this paper, the CN values derived here are likely to aid explorations of the effects of prairie filter strips on runoff and streamflow using watershed-scale models, such as SWAT.

2.6 Acknowledgments

Funding for this project was provided by the Iowa State University College of Liberal Arts and Sciences. Data was collected using support from the Leopold Center for Sustainable Agriculture (SI2009), Iowa State University College of Agriculture and Life Sciences, USDA Forest Service Northern Research Station, Iowa Department of Agriculture and Land Stewardship Division of Soil Conservation, USDA North Central Region Sustainable Agriculture Research and Education program (H001226911), USDA–AFRI Managed Ecosystems program (IOW5249), and the Iowa Flood Center.

2.7 References

Arabi, M., J.R. Frankenberger, B.A. Engel, and J.G. Arnold, 2008. Representation of Agricultural Conservation Practices with SWAT. Hydrological Processes 3055:3042–3055.

Arnold, J.G., P.M. Allen, M. Volk, J.R. Williams, and D.D. Bosch, 2010. Assessment of Different Representations of Spatial Variability on SWAT Model Performance. Transactions of the ASABE 53:1433–1443.

Arnold, J.G. and N. Fohrer, 2005. SWAT2000 : Current Capabilities and Research. Hydrological Processes 572:563–572.

Arnold, J.G., R. Srinivasan, R.S. Muttiah, and J.R. Williams, 1998. Large Area Hydrologic Modeling and Assessment Part 1: Model Development. Journal of the American Water Resources Association 34:73–89.

Artita, K.S., P. Kaini, and J.W. Nicklow, 2013. Examining the Possibilities : Generating Alternative Watershed-Scale BMP Designs with Evolutionary Algorithms. Water Resources Management 27:3849–3863.

Baltas, E. a., N. a. Dervos, and M. a. Mimikou, 2007. Technical Note: Determination of the SCS Initial Abstraction Ratio in an Experimental Watershed in Greece. Hydrology and Earth System Sciences 11:1825–1829.

Beven, K.J., 2012. Down to Basics: Runoff Processes and the Modelling Process. Rainfall-Runoff Modelling: The Primer: Second Edition. John Wiley & Sons, West Sussex, UK, pp. 1–22.

Bosch, N.S., J.D. Allan, J.P. Selegean, and D. Scavia, 2013. Scenario-Testing of Agricultural Best Management Practices in Lake Erie Watersheds. Journal of Great Lakes Research 39:429–436.

Bracmort, K.S., M. Arabi, J.R. Frankenberger, B.A. Engel, and J.G. Arnold, 2006. Modeling Long-Term Water Quality Impacts of Structural BMPs. Transactions of the ASABE 49:367–374.

Chen, B., W.F. Krajewski, X. Zhou, and M.J. Helmers, 2015. Organized Variability of Surface Runoff Responses across Neighboring Hillslopes in Iowa. Journal of Hydrology 523:1–13.

Chu, T.W., A. Shirmohammadi, H. Montas, L. Abott, and A. Sadeghi, 2005. Watershed Level BMP Evaluation with SWAT Model. 2005 ASAE Annual International Meeting. St. Joseph, MI.

D'Asaro, F. and G. Grillone, 2012. Empirical Investigation of Curve Number Method Parameters in the Mediterranean Area. Journal of Hydrologic Engineering 17:1141–1152.

D'Asaro, F. and G. Grillone, 2015a. Discussion. JAWRA Journal of the American Water Resources Association 51:573–578.

D'Asaro, F. and G. Grillone, 2015b. Discussion. JAWRA Journal of the American Water Resources Association 51:573–578.

D'Asaro, F., G. Grillone, and R.H. Hawkins, 2014. Curve Number: Empirical Evaluation and Comparison with Curve Number Handbook Tables in Sicily. Journal of Hydrologic Engineering 19:04014035.

Dunne, T., W. Zhang, and B.F. Aubry, 1991. Effects of Rainfall, Vegetation, and Microtopography on Infiltration and Runoff. Water Resources Research 27:2271–2285.

Efron, B., 1982. The Jackknife, the Bootstrap and Other Resampling Plans. doi:10.1137/1.9781611970319.

Garg, V., I. Chaubey, and B.E. Haggard, 2003. Impact of Calibration Watershed of Runoff Model Accuracy. Transactions of the ASAE 46:1347–1353.

Hawkins, R.H., 1973. Improved Prediction of Storm Runoff in Mountain Watersheds. Journal of Irrigation and Drainage Engineering 99:519–523.

Hawkins, R.H., 1993. Asymptotic Determination of Runoff Curve Numbers from Data. Journal of Irrigation and Drainage Engineering 119:334–345.

Hawkins, R.H. and Cate, 1998. Secondary Effects in Curve Number Rainfall-Runoff. Water Resources Engineering 98. Memphis, TN.

Hawkins, R.H. and K.E. VerWeire, 2005. Effects of Prior Rainfall and Storm Variables on Curve Number Rainfall-Runoff. ASCE Symposium on Watershed Management. Williamsburg, VA.

Hawkins, R.H., T. Ward, D.E. Woodward, and J. Van Mullem, 2009. Curve Number Hydrology: State of the Practice. American Society of Civil Engineers, Reston, VA.

Hawkins, R.H., T.J. Ward, D.E. Woodward, and J.A. Van Mullem, 2010. Continuing Evolution of Rainfall-Runoff and the Curve Number Precedent. 4th Federal Interagency Hydrologic Modeling Conf., Advisory Committee on Water Information (ACWI). Washington, DC.

Helmers, M.J., X. Zhou, H. Asbjornsen, R. Kolka, M.D. Tomer, and R.M. Cruse, 2012. Sediment Removal by Prairie Filter Strips in Row-Cropped Ephemeral Watersheds. Journal of Environment Quality 41:1531.

Hernandez-Santana, V., X. Zhou, M.J. Helmers, H. Asbjornsen, R. Kolka, and M. Tomer, 2013. Native Prairie Filter Strips Reduce Runoff from Hillslopes under Annual Row-Crop Systems in Iowa, USA. Journal of Hydrology 477:94–103.

Hjelmfelt, A.T., 1980. Empirical Investigation of Curve-Number Technique. Journal of the Hydraulics Division 106:1471–1476.

Hjelmfelt, A.T., 1983. Curve Numbers: A Personal Interpretation. Specialty Conference on Advances in Irrigation and Drainage: Surviving External Pressures. American Society of Civil Engineers, Jackson, WY, pp. 208–215.

Hjelmfelt, A.T., 1991. Investigation of Curve Number Procedure. Journal of Hydraulic Engineering 117:725–737.

Hjelmfelt, A.T., L.A. Kramer, and R.E. Burwell, 1982. Curve Numbers as Random Variables. Rainfall-Runoff Relationship. Water Resources Publications, Littleton, CO, pp. 365–370.

Jacobs, J.M., D. a. Myers, and B.M. Whitfield, 2003. Improved Rainfall/Runoff Estimates Using Remotely Sensed Soil Moisture. Journal of the American Water Resources Association 39:313–324.

Kalcic, M.M., J. Frankenberger, and I. Chaubey, 2015. Spatial Optimization of Size Conservation Practices Using SWAT in Tile-Drained Agricultural Watersheds. Journal of the American Water Resources Association 51:956–972.

Kannan, N., C. Santhi, J.R. Williams, and J.G. Arnold, 2008. Development of a Continuous Soil Moisture Accounting Procedure for Curve Number Methodology and Its Behaviour with Different Evapotranspiration Methods. Hydrological Processes 22:2114–2121.

Michel, C., V. Andréassian, and C. Perrin, 2005. Soil Conservation Service Curve Number Method: How to Mend a Wrong Soil Moisture Accounting Procedure? Water Resources Research 41:W02011.

Mishra, S.K., R.P. Pandey, M.K. Jain, and V.P. Singh, 2008. A Rain Duration and Modified AMC-Dependent SCS-CN Procedure for Long Duration Rainfall-Runoff Events. Water Resources Management 22:861–876.

Montgomery, R.J. and P.E. Clopper, 1983. A Data-Based Evaluation of the Curve Number Method. Advances in Irrigation and Drainage: Surviving External Pressures. American Society of Civil Engineers, Jackson, WY, pp. 290–297.

Motovilov, Y., L. Gottschalk, K. Engeland, and A. Rodhe, 1999. Validation of a Distributed Hydrological Model against Spatial Observations. Agricultural and Forest Meteorology 98–99:257–277.

Van Mullem, J.A., 1992. Soil Moisture and Runoff—Another Look. ASCE Water Forum 92, Irrigation and Drainage Session. Baltimore, MD.

Van Mullem, J.A., R.H. Hawkins, A.T. Hjelmfelt, and Q.D. Quan, 2002. Runoff Curve Number Method: Beyond the Handbook. Proc., 2nd Federal Interagency Hydrologic Modeling Conf., Advisory Committee on Water Information. Washington, DC.

Neitsch, S.L., J.G. Arnold, J.R. Kiniry, and J.R. Williams, 2005. Soil Water and Assessment Tool Theoretical Documentation. Temple, Texas.

Ponce, V.M. and R.H. Hawkins, 1996. Runoff Curve Number: Has It Reached Maturity? Journal of Hydrologic Engineering 1:11–19.

Sahu, R.K., S.K. Mishra, T.I. Eldho, and M.K. Jain, 2007. An Advanced Soil Moisture Accounting Procedure for SCS Curve Number Method. Hydrological Processes 21:2872–2881.

Santhi, C., R. Srinivasan, J.G. Arnold, and J.R. Williams, 2006. A Modeling Approach to Evaluate the Impacts of Water Quality Management Plans Implemented in a Watershed in Texas. Environmental Modelling & Software 21:1141–1157.

Schaake, J., J. Geyer, and J. Knapp, 1967. Experimental Examination of the Rational Method. Journal of Hydraulics Division 93:353–370.

Scherrer, S., F. Naef, A.O. Faeh, I. Cordery, and C. Engineers, 2007. Formation of Runoff at the Hillslope Scale during Intense Precipitation. Hydrol. Earth Syst. Sci. 11:907–922.

Schilling, K.E., M.D. Tomer, Y.-K. Zhang, T. Weisbrod, P. Jacobson, and C.A. Cambardella, 2007. Hydrogeologic Controls on Nitrate Transport in a Small Agricultural Catchment, Iowa. Journal of Geophysical Research 112:G03007.

Shi, Z.-H., L.-D. Chen, N.-F. Fang, D.-F. Qin, and C.-F. Cai, 2009. Research on the SCS-CN Initial Abstraction Ratio Using Rainfall-Runoff Event Analysis in the Three Gorges Area, China. CATENA 77:1–7.

Simanton, J.R., R.H. Hawkins, M. Mohseni-Saravi, and K.G. Renard, 1996. Runoff Curve Number Variation with Drainage Area, Walnut Gulch, Arizona. Transactions of the ASAE 39:1391–1394.

Sivapalan, M., 2003. Process Complexity at Hillslope Scale , Process Simplicity at the Watershed Scale : Is There a Connection? Hydrological Processes 1041:1037–1041.

Sneller, J.A., 1985. Computation of Runoff Curve Number from Landsat Data. Beltsville, MD.

Stewart, D., E. Canfield, and R. Hawkins, 2012. Curve Number Determination Methods and Uncertainty in Hydrologic Soil Groups from Semiarid Watershed Data. Journal of Hydrologic Engineering 17:1180–1187.

Suresh, D., U. Chandra, A. Ekube, D. Aberra, and M. Tegene, 2013. Estimation and Comparision of Curve Numbers Based on Dynamic Land Use Land Cover Change , Observed Rainfall-Runoff Data and Land Slope. Journal of Hydrology 492:89–101.

Tedela, N.H., S.C. McCutcheon, T.C. Rasmussen, R.H. Hawkins, W.T. Swank, J.L. Campbell, M.B. Adams, C.R. Jackson, and E.W. Tollner, 2012. Runoff Curve Numbers for 10 Small Forested Watersheds in the Mountains of the Eastern United States. Journal of Hydrologic Engineering 17:1188–1198.

Teshager, A.D., P.W. Gassman, S. Secchi, J.T. Schoof, and M. Girmaye, 2016. Modeling Agricultural Watersheds with the Soil and Water Assessment Tool (SWAT): Calibration and Validation with a Novel Procedure for Spatially Explicit HRUs. Environmental Management 57:894–911.

USDA-Natural Resources Conservation Service (USDA-NRCS), 2004. National Engineering Handbook, Part 630. Washington, DC.

USDA-Natural Resources Conservation Service (USDA-NRCS), 2015. Field Office Technical Guide. http://www.nrcs.usda.gov/wps/portal/nrcs/main/national/technical/fotg/. Accessed 9 Apr 2016.

USDA-SCS, 1964. National Engineering Handbook, Section 4. Washington, DC.

Vaché, K.B., J.M. Eilers, and M. V Santelmann, 2003. Water Quality Modeling of Alternative Agricultural Scenarios in the U.S. Corn Belt. Journal of the American Water Resources Association 38:773–787.

VerWeire, K.E., R.H. Hawkins, Q.Q. D., and C.C. Scheer, 2005. Relationship of Hydrologic Soils Groups to Curve Numbers: Results of a Study. American Society of Civil Engineers Watershed Management Conference. Williamsburg Virginia.

Volk, M., J.G. Arnold, D.D. Bosch, P.M. Allen, and C.H. Green, 2007. Watershed Configuration and Simulation of Landscape Processes with the SWAT Model. MODSIM 2007 International Congress on Modelling and Simulation:2383–2389.

Williams, J.R., 1990. The Erosion-Productivity Impact Calculator (EPIC) Model : A Case History. Philosphical Transactions of the Royal Society, London (Part B: Biological Science) 329:421–428.

Williams, J.R., 1995. The EPIC Model. Computer Models of Watershed Hydrology. Water Resources Publications, Highlands Ranch, CO, pp. 909–1000.

Williams, J.R., J.G. Arnold, and R. Srinivasan, 2000. The Apex Model. Blackland Research and Extension Center, Texas Agricultural Experiment Station.

Woodward, D.E., R.H. Hawkins, R. Jiang, A.T. Hjelmfelt Jr, J.A. Van Mullem, and Q.D. Quan, 2003. Runoff Curve Number Method: Examination of the Initial Abstraction Ratio. World Water and Environmental Resources Congress., pp. 1–10.

Young, R.., C.A. Onstand, D.D. Bosch, and W.P. Anderson, 1989. AGNPS: A Nonpoint-Source Pollution Model for Evaluating Agricultural Watersheds. Journal of Soil and Water Conservation 44:168–173.

Zhou, X., M.J. Helmers, H. Asbjornsen, R. Kolka, and M.D. Tomer, 2010. Perennial Filter Strips Reduce Nitrate Levels in Soil and Shallow Groundwater after Grassland-to-Cropland Conversion. Journal of Environment Quality 39:2006.

CHAPTER 3

INVESTIGATING THE IMPACTS OF HUMAN-DECISION MAKING ON HYDROLOGIC RESPONSE IN AN AGRICULTURAL WATERSHED

A paper to be submitted to *Hydrologic and Earth System Sciences*

David J. Dziubanski[5,6], Kristie J. Franz[5], and William J. Gutowski[7]

Abstract

Humans are factored into hydrologic models in a variety of ways, most often with humans imposing changes to the natural system through prescribed actions. Many hydrological modeling studies fail to include a representation of the human system and the adaptive behavior of humans to changing hydrologic conditions. By treating both human and hydrologic systems as dynamic and co-evolving, we build a socio-hydrological model that combines an agent-based model (ABM) with a semi-distributed hydrologic model. This model uses the curve number method to relate land cover to hydrologic response. Agents (based on two types) make decisions that affect land use within the watershed. A city agent aims to reduce flooding in a downstream urban area by paying farmer agents a subsidy for allocating land towards conservation practices that reduce runoff. Farmer agents decide how much land to convert to conservation based on factors related to profits, past land use and conservation-mindedness (willingness to convert land to conservation). The model is implemented for a watershed representative of the mixed

[5] Graduate Research Assistant (Dziubanski) and Associate Professor (Franz), Department of Geological and Atmospheric Sciences, Iowa State University.
[6] Primary researcher and corresponding author.
[7] Professor, Department of Geological and Atmospheric Sciences, Iowa State University.

agricultural/small urban area land use found in Iowa, USA. In this preliminary study, we simulate scenarios of crop yield trend, crop prices, and conservation subsidies along with varied farmer parameters that illustrate the effects of human system variables on peak discharges. High corn prices lead to a decrease in conservation land from historical levels; consequently, mean peak discharge increases by 6%, creating greater potential for downstream flooding within the watershed. However, when corn prices are low and the watershed is characterized by a conservation-minded farmer population, mean peak discharge is reduced, but by a smaller amount of 3%. Overall, changes in mean peak discharge are mostly driven by changes in crop prices as opposed to yields or conservation subsidies.

3.1 Introduction

Humans change the water cycle through actions that affect physical and chemical aspects of the landscape, and these changes occur from global to local scales and over varying time periods (Vorosmarty and Sahagian, 2000). Despite their significant impacts to the landscape, humans remain the most poorly represented variable in hydrologic models (Sivapalan et al., 2012). Land cover and land use are commonly treated as fixed in time in many hydrologic models through the use of static parameters. When made dynamic, landscape change is often limited to predefined scenarios that are developed without consideration of how economics, local culture, or climate may combine to influence land use decisions. For example, the field of integrated water resources management (IWRM), which attempts to explore the interactions between humans and water, typically uses “scenario-based” approaches (Savenije and Van der Zaag, 2008). While scenario-based studies allow quantification of the impacts of a management decision on the hydrologic system, there are significant limitations (Elshafei et al., 2014; Sivapalan et al., 2012). Human and environmental systems are highly coupled with

feedbacks from one system creating stress on the other system, which in turn affects the behavior of the first system. Therefore, representing management decisions as pre-determined will not reproduce the real-world variability that may arise as a result of complex feedbacks between the human system and the physical system.

Arguments have emerged for socio-hydrological modeling in which humans and the environment are treated as co-evolving (Di Baldassarre et al., 2013; Montanari, 2015; Sivapalan et al., 2012; Sivapalan and Blöschl, 2015). In this way, models can account for disturbances to natural systems by humans and simultaneously assess physical processes and economic and social issues. In the hydrologic literature, two approaches have been used to simulate coupled human and natural systems: a classic top-down approach and a bottom-up approach using agent-based modeling (ABM). In the first approach, all aspects of the human system are represented through a set of parametrized differential equations (Di Baldassarre et al., 2013; Elshafei et al., 2014; Viglione et al., 2014). For example, Elshafei et al., (2014) characterizes the population dynamics, economics, and sensitivity of the human population to hydrologic change through differential equations to simulate the coupled dynamics of the human and hydrologic systems in an agricultural watershed. In contrast, the ABM approach consists of a set of algorithms that encapsulate the behaviors of agents and their interactions within a defined system, where agents can represent individuals, groups, companies, or countries (Axelrod and Tesfatsion, 2006; Borrill and Tesfatsion, 2011; Parunak et al., 1998). System agents can range from passive members with no cognitive function to individual and group decision-makers with sophisticated learning and communication capabilities. ABM has been used to study the influence of human decision making on hydrologic topics such as water balance and stream hydrology (Bithell and Brasington, 2009), irrigation and water usage (Barreteau et al., 2004;

Becu et al., 2003; Berger et al., 2006; van Oel et al., 2010; Schlüter and Pahl-wostl, 2007), water quality (Ng et al., 2011), and groundwater resources (Noel and Cai, 2017; Reeves and Zellner, 2010).

A dominating topic in the hydrologic sciences that can be studied through use of coupled ABMs is the issue of hydrologic trends and uncertainties in intensively managed landscapes. Many recent studies have focused on quantifying the impacts of the human and climate systems on trends in streamflow through use of modeling and statistical methods such as linear regression, water balance approaches, trend analysis, and Budyko analysis (Ahn and Merwade, 2014; Bao et al., 2012; Guo and Shen, 2015; Steffens and Franz, 2012; Tomer and Schilling, 2009; Wang and Hejazi, 2011; Zhang et al., 2012). These studies have attempted to determine what percentage of the recent changes in streamflow can be attributed to human-induced changes in the landscape. However, the extent to which humans are altering streamflow is still unclear. Ahn and Merwade (2014) analyzed the relative impact of the human and climate systems on streamflow in four different states (Indiana, New York, Arizona, Georgia). Their results indicated that the effect of the human system on streamflow varies between the states analyzed and the technique used to derive the impacts. For instance, 85% of streamflow stations in Georgia indicated a significant human impact on streamflow in contrast to only 55% in New York State. Other studies have concluded that climate may be the leading factor controlling hydrologic changes (Li et al., 2009) in watersheds. Yet another study by Tomer and Schilling (2009) for the Midwest suggested that change in land use was the primary driver of streamflow change in the 1960s and 1970s, but since then, climate has been the primary driver. Given the wide range of results from these studies, social-hydrologic models that couple these two

systems may allow for a more complete analysis of how changes in precipitation coupled with human decision-making on the landscape affect streamflow.

In this study, we develop a coupled social-hydrologic model that represents changes in conservation land over time within an agricultural watershed as a function of dynamic human and natural factors, and through a sensitivity analysis, we attempt to quantify the role of human factors intrinsic and extrinsic to the system on hydrologic variability and uncertainty. Using simulations of a historical 47 year period, we explore hydrologic and agent outcomes for a typical agricultural watershed in Iowa under the following scenarios: time trend of yield at historical levels and 50% below historical levels, corn prices 25% above and below historical values, and conservation subsidy rates 25% above and below historical cash rent values. The following model methodology is described using the ODD (Overview, Design Concepts, and Details) protocol developed by Grimm et al., (2006).

3.2 Model Methodology

3.2.1 Model Purpose

The purpose of the model is to understand the impact of land use decisions by upstream farmers on flooding response in a downstream urban area under perturbations to extrinsic economic and natural factors (e.g. crop prices, land rental values, climate), as well as intrinsic factors (e.g. internal farmer behavior, local government incentives). System behavior under changes in extrinsic and intrinsic factors is analyzed using a scenario-based ensemble approach.

3.2.2 State Variables and Scales

The modeling system couples an agent-based model of human decision making with a rainfall-runoff model to simulate social and natural processes within highly-managed

agricultural watersheds (Figure 3.1). The agent-based model consists of two primary agents: a farmer agent and a city agent.

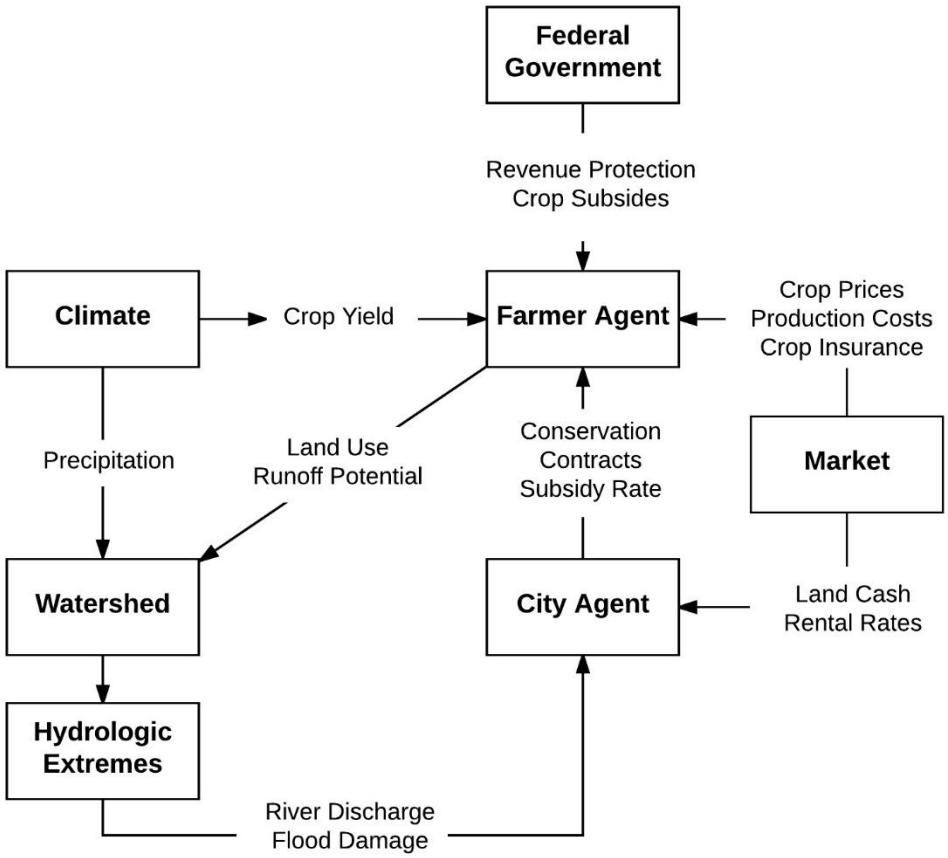

Figure 3.1. Flow of information within the coupled modeling system.

The primary modeling domain consists of the watershed and the subbasins located within the watershed. The hydrologic model is run at the subbasin level, and the model user must define the subbasins based on external analyses of hydrologic flows and conditions. Each subbasin is populated by one or more farmer agents as specified by the user. A farmer agent modifies the land use of their subbasin in proportion to the subbasin area assigned to that agent. The most downstream subbasin in the watershed is populated by an urban center, which is represented by a city agent.

3.2.2.1 Hydrologic state variables

The primary state variable in the hydrology module is the Curve Number (CN). The CN is a parameter that describes the condition of the landscape based on the land use, condition of vegetation, soil type, and prior soil moisture (Hawkins et al., 2009). The CN is used to determine the amount of runoff occurring from the landscape based on a given precipitation amount. Each subbasin is assigned a CN based on a weighted average of the percent of land cover type in the watershed and its associated CN. A full description of the CN method can be found in Hawkins et al. (2009).

3.2.2.2 Farmer agent state variables

The primary state variable for a farmer agent is the conservation parameter ($Cons_{max}$), which characterizes the degree to which a farmer agent is "production-minded" versus "conservation-minded". This concept is based on McGuire et al. (2013) who identified that US cornbelt farmer agents tend to fall along a spectrum from purely productivist to purely conservationist. $Cons_{max}$ is randomly assigned to each farmer agent upon initialization and provides variation in farmer agent behavior based on how an individual agent may prefer to balance producing high crop yields versus protecting the environment. $Cons_{max}$ represents the maximum fraction of land a farmer is willing to put into conservation. The minimum value is 0.0, in which case a farmer is purely production-minded and is unwilling to convert any production land into conservation. We set the maximum value at 10% ($Cons_{max}$ = 0.10) based on the conservation practice used in this study (Section 3.2.9). Therefore, a farmer is purely conservation-minded at a parameter value of 0.1 and is willing to convert up to 10% of his/her production land into conservation.

Farmer agents are further characterized by their decision-making preferences, which describe the relative importance that farmer agents place on different decision variables when adjusting their land use. The farmer agent decision characteristics are described in section 3.2.9.

Each farmer agent is also assigned state variables characterizing the percent of different soil types associated with the farmer's land. Corn crop productivity and crop production costs (including the land rental value) vary for each soil type. Thus, the soil types associated with a farmer agent's land impact his/her revenue.

3.2.2.3 City Agent State Variables

The city agent is characterized by a conservation goal that defines the amount of acres of conservation land desired. The purpose of the conservation land is to reduce flooding in the city, and the conservation goal changes from year-to-year depending on prior hydrologic events. The damage that the city agent incurs from a flood event is defined by a flood damage function. A parameter, P_{new}, in the agent model defines how responsive the city agent is to prior hydrologic outcomes and determines by how much the city agent will change the conservation goal after experiencing a flood event (Section 3.2.10).

3.2.3 Model Overview and Scheduling

The hydrologic model proceeds in hourly time steps to capture flood discharge events, while the agent-based model proceeds in sub-annual time steps to capture yearly on-farm decision making. The agent-based model proceeds as follows. In January, the city agent determines how much land to allocate into conservation based on the previous year's flood damage (Figure 3.2). The farmer agent then calculates his/her preferred land division between production and conservation based on their conservation-mindedness, newly acquired information about the global market (crop prices, crop production costs, and crop insurance),

crop subsidies provided by the city agent, as well as recent farm performance (profits and yields) (Figure 3.1).

In February, the city agent contacts farmer agents in random order to establish new conservation contracts if an unmet conservation goal remains or to renew any expiring contracts (Figure 3.2). If the farmer agent wants to add additional conservation acreage, a new contract is established. Each new contract is established for a 10 year period. However, if the farmer agent wants fewer conservation hectares, expiring contracts are renewed for a smaller number of hectares or are ended. The farmer is obligated to fulfill any contracts that have not yet expired (i.e. contracts less than 10 years old). Any new acreage that has been established in conservation in addition to currently active contracts is subtracted from the city agent's conservation goal that was established in January. The city agent contacts as many farmer agents as needed until the conservation goal is reached. If there are not enough farmer agents willing to enter into conservation contracts and the conservation goal is not reached, the goal rolls into the next year. Because the farmer agents' land use decisions change on a yearly basis, it may be possible for the city agent to establish further contracts in the next year and fulfill the conservation goal.

Prior to May, the farmer agent establishes any newly contracted conservation land on the historically poorest yielding land. No further decision making occurs during May through August, however, during this time, a maximum discharge event occurs. The associated flood damage cost is calculated in September and used by the city agent the following January to calculate whether any further conservation land should be added. If no flooding occurred, the conservation goal remains unchanged. In October, the farmer agent harvests his/her crop, and calculates yields and profits for that year.

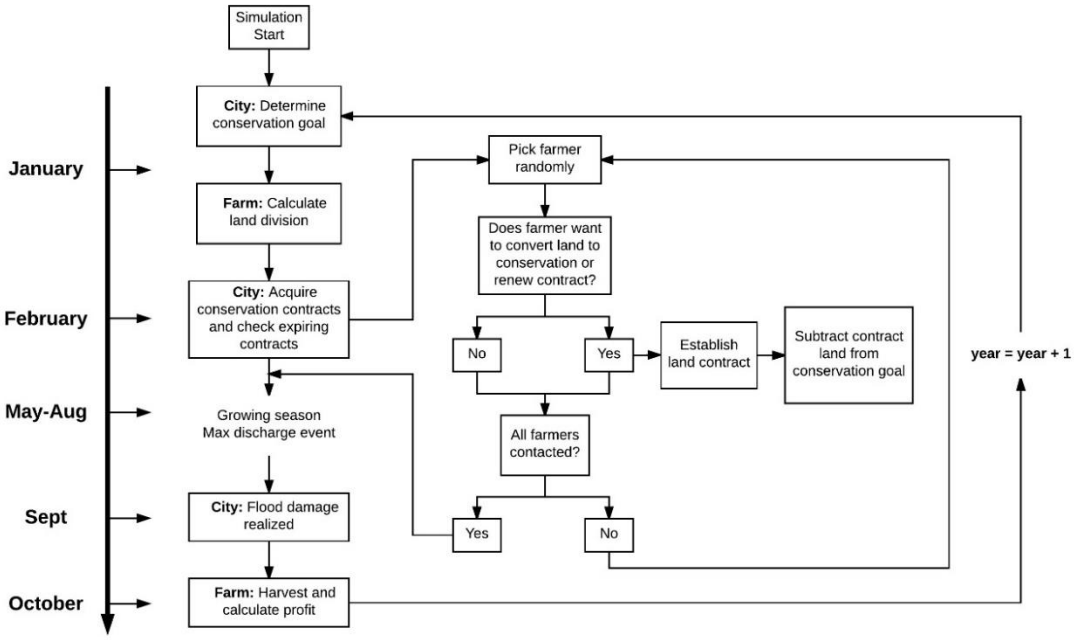

Figure 3.2. Timeline of agent decisions and actions within the coupled modeling system.

3.2.4 Design Concepts

Emergence: Patterns in total conservation land and flood magnitude arise over time, depending on a number of variables. Agent decision-making parameters and behavioral characteristics (e.g. conservation-mindedness) ultimately influence the total acreage in conservation land, which in turn affects the magnitude of floods through changes in runoff productivity of the landscape.

Adaptation: Agents incrementally adjust their decision goals based on changes in environmental and economic factors. If the city agent incurs a large cost from flooding in a given year, the city agent adjusts his/her "conservation goal" upward in order to minimize future flood damage from events of similar magnitude. The farmer agents, on the other hand, focus on their land allocation. For example, the farmer agents adapt to a decrease in marginal profit from crop production by increasing their acreage in conservation land.

Objectives: The objective of the city agent is to reduce flood damage in the city. The city agent attempts to meet this objective through an incentive program in which farmer agents are paid to convert production land to a conservation practice that will reduce runoff. The objective of the farmer agent is to balance a maximization of profits with conservation and risk-aversion attitude. The farmer agents incrementally adjust their land use on an annual basis by taking into account profit variables, risk-aversion, and conservation-mindedness.

Stochasticity: Adjustments and stochastic variability are added to key agricultural variables, which include crop yields, production costs, cash rent values, and opportunity costs associated with conservation land in order to account for economic and environmental randomness within the system. Random factors for these variables are drawn from uniform continuous distributions that are based on field data of crop yields, empirical survey data, and estimates published by Iowa State University Extension and Outreach (Section 3.7). Changes in these distributions are also accounted for, depending on crop price levels.

Learning: As will be outlined further in section 3.2.9, each year, the farmer agents calculate profit differences between crop production and conservation subsidies. Farmer agents save this profit difference information from the beginning of the simulation and use it to adjust their decision-making space on an annual basis. The profit difference information is based on past crop prices, production costs, and conservation subsidies.

Agent Interaction: Interaction occurs between the city and farmer agents, as well as between the agents and the environment. The most critical interaction is between the farmer agents and city agent. The city agent is affected by river discharge through flood damage. Based on the city agent's objective to reduce flooding potential, the city agent offers a subsidy to farmer agents to convert land from agricultural production to conservation. The city agent

contacts farmers in random order yearly to determine if the farmer agents have decided to implement further conservation land. Farmer agent land allocation affects the CN parameter in the hydrology model, which affects runoff in the watershed. Runoff subsequently affects river discharge, forming a feedback loop between the environment, city, and farmer agents. The market agent also affects the city and farmer agents directly and indirectly. The farmer agent's profits and decisions are impacted by past and future crop prices. The city agent's set subsidy rate is dependent on cash rent values, which are based on the market.

Observation: The model outputs total conservation land for each simulation year, the city agent's yearly conservation goal, the mean of the decision-making variables for the farmer agents, maximum annual discharge, and 50^{th}, 75^{th}, and 90^{th} percentile discharge for the entire simulation period.

3.2.5 Model Initialization

Prior to each simulation, the location, decision-making and behavioral characteristics, and soil types of each farmer agent are defined. Farmer agents are equally distributed among the subbasins based on the total number of farmer agents desired. If the number of farmer agents is set to 100 and hydrology module contains 10 subbasins, the model allocates 10 farmer agents to each subbasin. The land within the subbasin is equally divided among the 10 farmer agents. The actual number of farmer agents in each particular subbasin can be specified if data is available.

Next, the parameters governing the farmer agent behavior and decision-making are stochastically defined. The $Cons_{max}$ parameter (Section 3.2.2.2) is randomly drawn from a uniform distribution: $\mathcal{U}(0, 0.1)$, with bounds of the distribution based on the conservation practice used (Section 3.2.9.1). Decision weights that govern the farmer decision making (Section 3.2.9) are implemented in a similar fashion, with each parameter initialized from a

uniform distribution: $\mathcal{U}(0,1)$. Currently, these decision weights are initialized from this range due to lack of data for explicitly defining the distribution of each weight. Lastly, soil types and the area of land associated with each soil type are randomly assigned to each farmer agent upon model initialization. Assigning different soil types creates heterogeneous conditions under which farmer agents must operate (Section 3.2.8) and affects the profitability of each farmer agent differently.

3.2.6 Model Input

3.2.6.1 Economic Inputs

The agent-based models require inputs of historical crop prices ($/MT), production costs ($/Ha), cash rental rates ($/Ha), and federal government subsidy estimates ($/Ha). An example of these model inputs is shown in figure 3.3 in comparison to mean Iowa crop yields.

3.2.6.2 Production Costs

Production costs are treated as a time series input, with total costs per hectare for each year represented by one lumped value. Production costs used in this model application include machinery, labor, crop seed, chemicals, and crop insurance (Plastina, 2017b). In addition, it is assumed that all farmer agents rent their land, which significantly increases expenses as land rental costs account for approximately half of total production costs (Plastina, 2017b).

3.2.6.3 Conservation Subsidy and Costs

The conservation subsidy is based on the Conservation Reserve Program Contour Grass Strips practice (CP-15A) which includes annual land rental payments and 90% cost share for site preparation and establishment [USDA Conservation Reserve Program Practice CP-15A, 2011]. Subsidies are calculated using annual inputs of historical cash rental rates. The cost of

establishing and maintaining conservation land is based on analysis conducted by Tyndall et al., (2013). These costs are adjusted based on the land quality of each farmer agent (Section 3.7.2, 3.7.3).

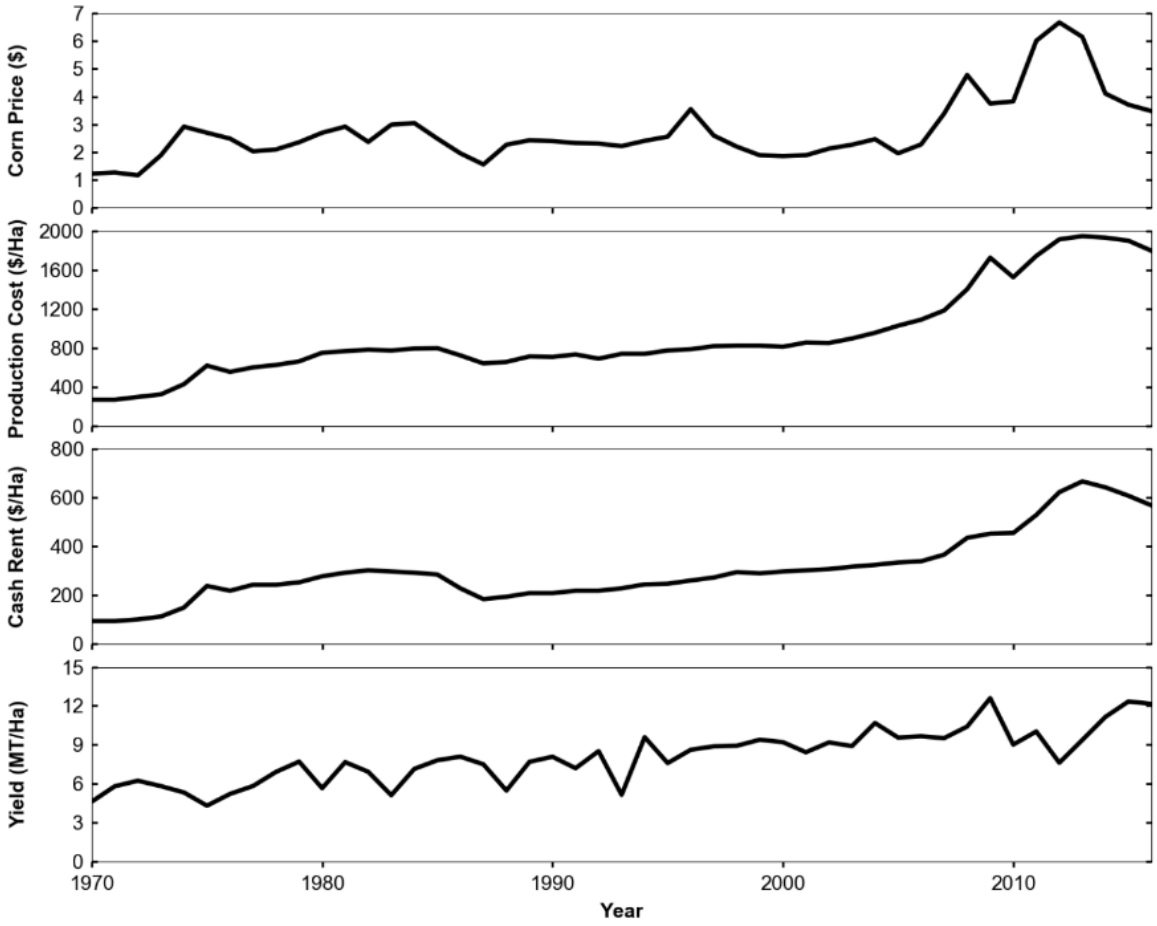

Figure 3.3. Example input time series of corn price, production cost, and cash rent as compared to mean crop yields.

3.2.6.4 Federal Government Subsidies

Calculation for federal government crop subsidies for individual farmer agents were not included in the agent-based model due to the complexity and variety of commodity programs available (i.e., Price Loss Coverage, Agricultural Risk Coverage, etc.), each of which focuses on different aspects of revenue protection (i.e., protection against low crop prices, protection

against revenue loss). Rather, federal crop subsidies are input to the model and applied to each farmer agent.

3.2.6.5 Environmental Variables

The hydrology module requires hourly liquid precipitation (mm) as an input in order to capture short-term heavy rainfall events. The crop yield module requires inputs of mean monthly precipitation and temperature to estimate crop yields (Section 3.2.8). The module calculates mean monthly precipitation based on the hourly precipitation input, however, the user must provide an input of mean monthly temperatures (C).

3.2.7 Hydrology Module

In the hydrology module, basin runoff is computed using the SCS curve number (CN) method, runoff is converted to basin outflow using the SCS unit hydrograph (SCS-UH) method, and channel flow is routed through reaches in the river network using the Muskingum method (Mays, 2011). These methods were chosen because they are employed in an application of the U.S. Army Corps of Engineers' Hydrologic Modeling System (HEC-HMS) (Scharffenberg, 2013) by the City of Ames, Iowa for flood forecasting (Schmeig et al., 2011), therefore, realistic parameter sets for an agricultural watershed in the Iowa were available. The hydrology module allows simulation of a single basin or multiple sub-basins. A single area-weighted CN parameter is required for each subbasin and is the only parameter that changes during simulation. The SCS-UH method requires specification of sub-basin area, time lag, and model timestep. The Muskingum method requires specification of three parameters for each reach within the river network: Muskingum X, Muskingum K, and the number of segments over which the method will be applied within the reach.

CN values derived by Dziubanski et al. (2017) (Chapter 2) using data from native prairie strips field studies are applied for the primary landcover types: a CN = 82 is used for 100% row crop production; and a CN = 72 is used for the conservation option implemented by the farmer agents (10% native prairie strips with 90% row crop production, Section 3.2.9.1). Urban areas are given a CN value of 90 which is derived from the standard lookup tables for residential areas with lot sizes of 0.051 hectares or less, soil group C (USDA-Natural Resources Conservation Service, 2004).

The model accepts point-scale rainfall data (e.g., rain gauge data) and calculates mean areal precipitation using the Thiessen Polygon gauge weighting technique (Larry W. Mays, 2011). The Thiessen weights are entered as parameters to the module. For the initial testing presented in this paper, uniform precipitation over the entire watershed was assumed.

Output from the hydrology module is discharge at the watershed outlet ($m^3 s^{-1}$). The hydrology module is run continuously but is designed primarily for simulation of peak flows which generally occur during the summer in the study region; therefore, for simplicity, a constant baseflow is assumed and snow is ignored. Runoff, river routing processes, and discharge are computed on a timestep identical to the input rainfall data. The model is currently set up to run at an hourly timestep, but is capable of running at a 30-minute timestep.

3.2.8 Crop Yield Module

Crop yields are modeled with a multiple regression equation that takes into account monthly precipitation and temperature. The regression equation, which was developed using historical crop yield and meteorological data for Iowa from 1960-2006, can be represented as (Tannura et al., 2008):

$$yield_t = \beta_0 + \beta_1(year_t) + \beta_2(September\ through\ April\ precipitation) + \beta_3\ (May\ precipitation) + \beta_4(June\ precipitation) + \beta_5(June\ precipitation)^2 + \beta_6(July\ precipitation) + \beta_7(July\ precipitation)^2 + \beta_8(August\ precipitation) + \beta_9(August\ precipitation)^2 + \beta_{10}(May\ temperature) + \beta_{11}(June\ temperature) + \beta_{12}(July\ temperature) + \beta_{13}(August\ temperature) + \varepsilon_t \quad (3.1)$$

The above regression model is only appropriate for reproducing mean historical crop yields. Since each farmer's land can be composed of different soil types, adjustments are applied to the crop yield for each soil type to account for differences in soil productivity (Section 3.7.4).

3.2.9 Farmer Agent Module

3.2.9.1 Conservation option

The conservation option implemented by farmer agents is native prairie strips, a practice in which prairie vegetation is planted in multiple strips perpendicular to the primary flow direction upland of and/or at the farm plot outlet (Chapter 2; Dziubanski et al., 2017; Helmers et al., 2012; Zhou et al., 2010). Prairie strips have been shown to reduce runoff by an average of 37% (Hernandez-Santana et al., 2013), and have additional benefits of reducing nutrients (Zhou et al., 2014) and sediments (Helmers et al., 2012) in runoff.

3.2.9.2 Farmer agent land use decision process

Rules governing agent decision-making need to realistically capture human behavior without creating an excessively complex model (An, 2012; Zenobia et al., 2009). The two dominant techniques of defining how agents make decisions within their environment include constrained optimization and heuristics (Schreinemachers and Berger, 2006, 2011). In optimization, agents are typically designed to determine optimal resource allocation or

production plans such that profit is maximized and constraints are obeyed (Berger and Troost, 2014). Example studies using optimization include Becu et al. (2003), Ng et al. (2011), Schreinemachers and Berger (2011). In heuristics, agents are set up to use "rules" to determine their final decision (Pahl-wostl and Ebenhöh, 2004; Schreinemachers and Berger, 2006). The "rules" are typically implemented using conditional statements (e.g. if-then). Example studies using heuristics include Barreteau et al. (2004), Le et al. (2010), Matthews (2006), van Oel et al. (2010).

We take a slightly different approach from the aforementioned studies by modeling agent decision making using a nudging concept originating in the field of data assimilation (Asch et al., 2017). Agents nudge their decision based on outcomes (i.e. flood damage, farm profitability) from the previous year. Information relevant to an individual agent is mapped into the decision space through a function that updates the prior decision to create a new (posterior) decision for the current year. The approach used for both agents is different from optimization in that the agents are not trying to determine the best decision for each year. These agents try to find a satisfactory solution for the current year, and are thus termed "satisficers" rather than optimizers (Kulik and Baker, 2008).

At the start of each calendar year, a farmer agent decides how to allocate his/her land between production and conservation based on four variables: conservation goal, crop price projection, past profits, and risk-aversion. These factors were chosen based on numerous studies indicating profits, economic incentives, conservation beliefs, beliefs in traditional practices, and observable benefits to be the key factors influencing on-farm decision making related to conservation adoption (Arbuckle, 2013; Burton, 2014; Hoag et al., 2012; Nowak, 1992; Pfrimmer et al., 2017).

A farmer agent's decision of the total amount of land to be allocated into conservation, C_t , for the current year t is:

$$C_t = W_{risk-averse}[C_{t-1:t-X}] + W_{futures}[D_{t-1} + \delta C_{futures}] + W_{profit}[D_{t-1} + \delta C_{profit}] + W_{cons}[D_{t-1} + \delta C_{cons}] \quad (3.2)$$

where $C_{t-1:t-X}$ is the mean total amount of land allocated to conservation during the previous X years, D_{t-1} is the prior conservation decision (total amount of land the farmer would have liked to implement in conservation) in year $t-1$, $\delta C_{futures}$ is the decision based on crop price projections, δC_{profit} is the decision based on past profit, and δC_{cons} is the decision based on the conservation goal of the farmer (Table 3.1). Parameter X represents the concept of memory, where one farmer agent might consider their history of conservation land implemented over the last year, while another farmer agent might consider their conservation land implemented over, for example, the last 5 years. Decision weights alter how each of the four components factor into the farmer agent's decision: $W_{risk-averse}$ reflects the unwillingness to change past land use, $W_{futures}$ reflects the consideration of future price projections, W_{prof} reflects the consideration of past profits, and W_{cons} is the agent's consideration of his/her conservation goal (Table 3.2). Upon initializing each farmer agent, values are allocated for each decision weight such that:

$$W_{risk-averse} + W_{futures} + W_{profit} + W_{cons} = 1 \quad (3.3)$$

The above decision scheme allows for varying decision weights, thus one farmer's decision may be heavily weighted by future crop prices, whereas another farmer's decision may be heavily weighted by past profits. If majority of a farmer's decision is based on $W_{risk-averse}$, then that farmer is less inclined to change his/her previous land use.

Table 3.1. Variables in farmer agent equations.

Farmer Agent Variables	Description	Unit
$C_{t-1:X}$	Mean total amount of land allocated to conservation during the previous X years	Hectares
D_{t-1}	Previous year's conservation land decision	Hectares
$\delta C_{futures}$	Conservation decision based on future crop price	Hectares
δC_{profit}	Conservation decision based on past profit	Hectares
δC_{cons}	Conservation decision based on conservation goal	Hectares
$Profit_{diff}$	Differences in profit between a hectare of crop and a hectare of conservation land	($/Hectare)
$Hectares_{tot}$	Total land owned by farmer agent	Hectares
$Profit_{crop}$	Profit derived from a hectare of crop land	($/Hectare)
$Profit_{cons}$	Profit derived from a hectare of conservation land	($/Hectare)
$CropPrice_{t-1}$	Crop price for the previous year t-1	($/MT)
$Yield_{t-1}$	Average farm yield per hectare for the previous year t-1	(MT/Acre)
$ProdCost_{t-1}$	Production cost for the previous year t-1	($/Hectare)
$FedSub_{t-1}$	Federal subsidy for the previous year t-1	($/Hectare)
$CropIns_{t-1}$	Crop insurance for the previous year t-1	($/Hectare)
$ConsSubsidy_{t-1}$	Conservation subsidy rate for the prevous year t-1	($/Hectare)
$Cost_{prairie}$	Cost of establishing and maintaining native prairie	($/Hectare)
$CropPrice_t$	Crop price for the current year t	($/MT)
P75	Third quartile of profit difference	($)
P50	Median of profit difference	($)
P25	First quartile of profit difference	($)
maxChange	Conservation change as a fraction of $Cons_{max}$	Dimensionless
Gross Indemnity	Insurance payout per hectare	($/Hectare)
Rev Guarantee	Guaranteed revenue per hectare	($/Hectare)
Actual Rev	Actual revenue per hectare	($/Hectare)
Projected Price	Projected crop price for the current year t	($/MT)
Harvest Price	Actual crop price at time of harvest	($/MT)
Coverage Level	Insurance coverage level	Dimensionless
TrendAdj APH Yield	10 year mean historical yield adjusted for trends in crop yields	(MT/Hectare)
Harvest Yield	Realized yield at time of harvest	(MT/Hectare)
Adjustment Factor	Factor used for adjusted historical crop yields based on trend	Dimensionless
$ProdCostHist_t$	Historical production cost for year t	($/Hectare)
ProdCostAdjust(CSR2)	Production cost adjustment based on CSR2 value	Dimensionless
CashRentRandom($CropPrice_t$)	Cash rent stochastic varaibility based on crop price magnitude	Dimensionless
InputCostRandom	Input cost stochastic variability	Dimensionless
OppCost	Opportunity cost associated with converting land to conservation	($/Hectare)
OppCostIncreasedPerCSR2	Increase in opportunity cost per CSR2 point	($/Hectare)
WeightedAvgCSR2	Weighted average CSR2 value of a farmer agent's landscape	Dimensionless
Establishment	Establishment costs associated with conversion to conservation land	($/Hectare)
Maintenance	Maintenance costs associated with conversion to conservation	($/Hectare)

Table 3.2. Primary agent model parameters in decision-making equations.

Agent Model Parameters	Description	Range
$W_{risk\text{-}averse}$	Weight placed on farmer agent's previous land use	0.0 - 1.0
$W_{futures}$	Weight placed on farmer agent's decision based on future crop price	0.0 - 1.0
W_{profit}	Weight placed on farmer agent's decision based on past profit	0.0 - 1.0
W_{cons}	Weight place on farmer agent's decision based on his conservation goal	0.0 - 1.0
$Cons_{max}$	Farmer's conservation goal - used to describe the farmer's conservation-mindedness	0.0 - 0.1
ConsGoal	Conservation goal at maximum flood damage	0.0 - 0.1

The decision components for past profit and future crop prices are based on a partial budgeting approach that compares land use alternatives. Under this budgeting approach, farmer agents take into account added and reduced income, as well as added and reduced costs from changing an acre of land from crop production to conservation (Tigner, 2006). The result from performing this budget indicates the net gain or loss in income that a farmer agent may incur if they make the land conversion.

The past profits decision is solely based on outcomes that have been fully realized for the previous year. In this decision, the land allocated to conservation is based on the net amount of money that could have been earned per hectare of conservation land versus crop land and is calculated as:

$$\delta C_{profit} = \left[A * \ Profit_{diff}{}^{2} + B * \ Profit_{diff} + C\right] \cdot Cons_{max} \cdot Hectares_{tot} \qquad (3.4)$$

where $Profit_{diff}$ is the difference in profit between a hectare of cropland and a hectare of conservation land (Table 3.2), $Cons_{max}$ is the farmer agent's maximum conservation parameter, $Hectacres_{tot}$ is the area of the agent's land, and A, B, C are equation coefficients discussed later.

$Profit_{diff}$ is calculated as:

$$Profit_{diff} = \ Profit_{crop} - \ Profit_{cons} \qquad (3.5)$$

where,

$$Profit_{crop} = (CropPrice_{t-1} \cdot Yield_{t-1}) - ProdCost_{t-1} + FedSub_{t-1} + CropIns_{t-1} \quad (3.6)$$

and,

$$Profit_{cons} = ConsSubsidy_{t-1} - Cost_{prairie} \quad (3.7)$$

$Profit_{crop}$ is the profit received for cropland in the previous year (Table 3.1), $CropPrice_{t-1}$ is the realized crop price for the previous year, $Yield_{t-1}$ is the farmer's realized mean yield (per hectare) from the previous year, $ProdCost_{t-1}$ is the crop production cost during the previous year, $FedSub_{t-1}$ is the amount of federal subsidies the farmer received in the previous year, $CropIns_{t-1}$ is the total amount of crop insurance received in the previous year, $Profit_{cons}$ is the profit received for conservation land in the previous year, $ConsSubsidy_{t-1}$ is the conservation subsidy established for the previous year, and $Cost_{prairie}$ is the cost associated with establishing and maintaining conservation land (Section 3.7.3).

The future crop prices decision is based on a combination of past performance information and projected future crop prices. Equations (3.4), (3.5) and (3.7) are used to calculate the land allocated to conservation based on future crop price, $\delta C_{futures}$, with equation (3.6) being replaced with the following:

$$Profit_{crop} = (CropPrice_{t} \cdot Yield_{t-1}) - ProdCost_{t-1} + FedSub_{t-1} + CropIns_{t-1} \quad (3.8)$$

where $CropPrice_t$ is the projected crop price for the upcoming growing season (Table 3.1). $CropPrice_t$ is randomly selected given a mean (in this model based on historical crop prices), a standard deviation of 10%, and assuming a normal distribution.

The first term in equation (3.4) is a second-degree polynomial of form $Ax^2 + Bx + C = y$, therefore three equations need to be simultaneously solved to determine coefficients A, B, C. δC_{profit} and $\delta C_{futures}$ can take on values between -100% to 100% depending upon whether

the farmer agent observes a positive or negative $Profit_{diff}$. If the farmer agent observes a positive $Profit_{diff}$, the agent uses all historical positive $Profit_{diff}$ values from the start of the simulation through $t-1$ to solve for the coefficients using the following system of equations:

$$\begin{aligned} A(P75)^2 + B(P75) + C &= -maxChange \\ A(P50)^2 + B(P50) + C &= -0.5maxChange \\ A(P25)^2 + B(P25) + C &= 0 \end{aligned} \tag{3.9}$$

where P75, P50 and P25 are the third quartile, median, and first quartile of the historical positive $Profit_{diff}$ values (Table 3.1), respectively, and $maxChange$ is the maximum allowed change in conservation land in any given year, which is equal to 1.0 (up to 100% change possible). When $Profit_{diff}$ is positive (i.e. greater profit was earned from crop production than conservation land), the farmer agent will potentially decrease the amount of land in conservation. A similar process occurs when the farmer observes a negative $Profit_{diff}$; however, the system of equations now becomes:

$$\begin{aligned} A(P25)^2 + B(P25) + C &= maxChange \\ A(P50)^2 + B(P50) + C &= 0.5maxChange \\ A(P75)^2 + B(P75) + C &= 0 \end{aligned} \tag{3.10}$$

Under negative $Profit_{diff}$, conservation land is potentially increased because the farmer earned a lower revenue through crop production.

Equations 3.9 and 3.10 are illustrated in Figure 3.4. Half of the maximum allowable percent increase in conservation land ($+0.5maxChange$) is assumed to correspond to the median historical negative $Profit_{diff}$, whereas half of the maximum allowable percent decrease in conservation land ($-0.5maxChange$) corresponds to the median historical positive $Profit_{diff}$ (Figure 3.4). We assume that farmer agents will not change land use when a very

small profit difference between the two possible options is observed because changing land use requires extra upfront time and resources (Duffy, 2015). Similarly, we assume that farmer agents will fully implement the maximum land conversion possible prior to reaching the most extreme $Profit_{diff}$ values. Therefore, an increase in conservation land begins to occur when the negative $Profit_{diff}$ value is less than the Q75 of historical negative $Profit_{diff}$ and reaches a maximum (100% change) when the negative $Profit_{diff}$ reaches Q25 (black curve in Figure 3.4). A decrease in conservation land begins to occur when the positive $Profit_{diff}$ is greater than Q25 of historical positive $Profit_{diff}$ and reaches a maximum (-100%) when the positive $Profit_{diff}$ reaches Q75 (gray curve in Figure 3.4). A farmer increases or decreases conservation land as a fraction of the $Cons_{max}$ parameter (equation 3.4).

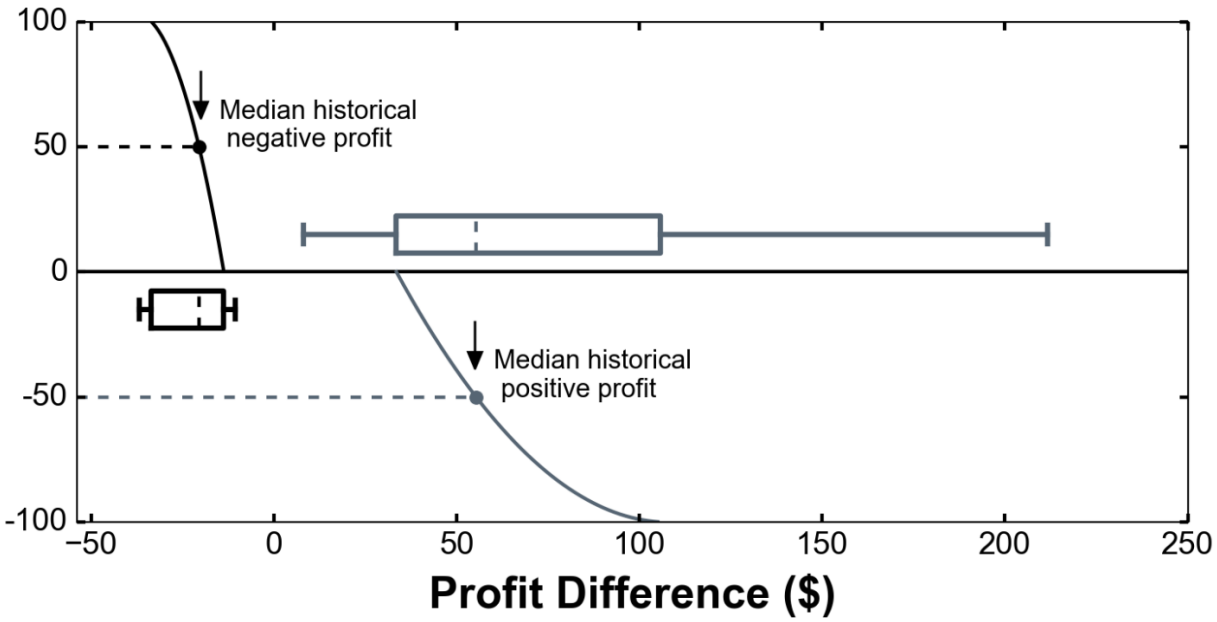

Figure 3.4. Example of percent conservation change for δC_{profit} and $\delta C_{futures}$. Gray curves indicate negative percent change (decrease conservation land), black curves indicate positive percent change (increase conservation land).

The amount of conservation land the farmer decides to allocate based on his/her conservation goal is strictly a function of the agent's $Cons_{max}$ parameter and is computed by:

$$\delta C_{cons} = \left(\frac{maxChange * 2.0}{0.1} \cdot Cons_{max} - maxChange\right) \cdot Cons_{max} \cdot Acres_{tot} \qquad (3.11)$$

where all variables are as previously defined (Table 3.1). If a farmer's $Cons_{max}$ parameter is 0.1, he will decide to increase conservation land by 100% of the maximum possible defined by $Cons_{max}$ (e.g. 10% of total farm hectares if $Cons_{max} = 0.1$, Figure 3.5), and at a $Cons_{max}$ parameter of 0, the farmer will decrease his conservation land by 100% of the maximum conservation land, which in this case is 0% of total farm hectares since $Cons_{max} = 0$. Therefore, if a farmer agent owns a total of 161.8 hectares of land, is fully conservation-minded (conservation parameter = 0.1), solely bases his decision on his conservation-mindedness ($W_{cons} = 1$), and $maxChange$ = 1.0, then δC_{cons} will equate to 16.2 hectares and his conservation land will increase by this amount if accepted by the city agent.

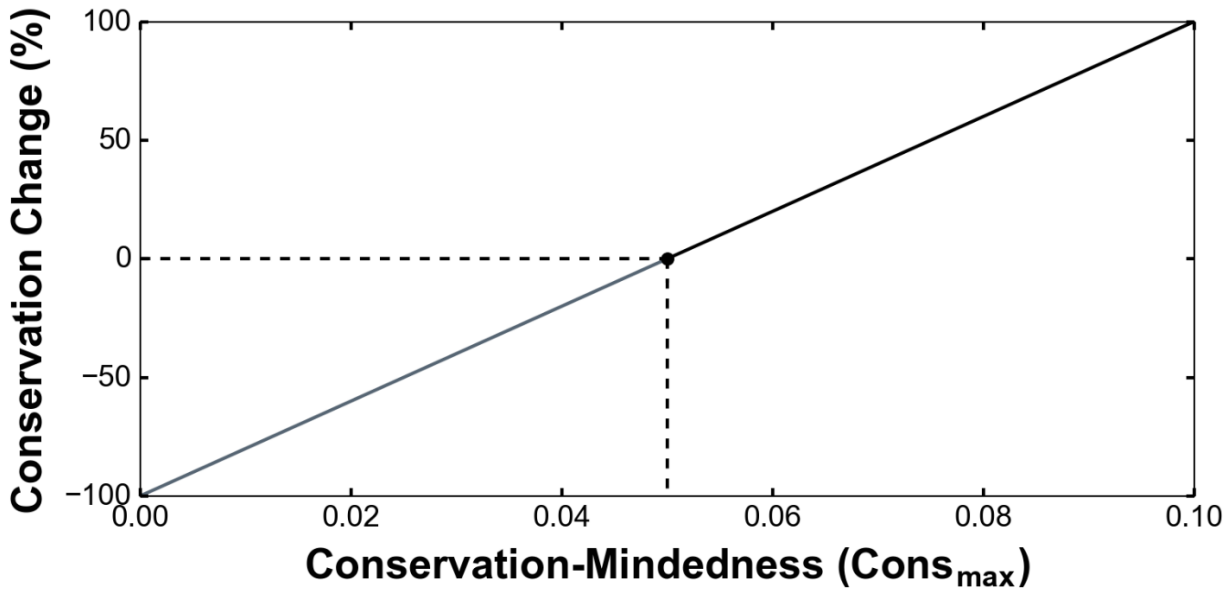

Figure 3.5. Example of percent conservation change for δC_{cons}. Gray curves indicate negative percent change (decrease conservation land), black curves indicate positive percent change (increase conservation land).

3.2.10 City Agent Module

At the end of each year, the city agent collects discharge data and calculates the damage associated with the maximum discharge at the outlet for that year. Flood damages are calculated using a flood damage function defined by Tesfatsion et al. (2017):

$$FDam = \frac{FDmax}{1 + \exp[-(\text{discharge} - \text{Q50})/dQ)]} \tag{3.12}$$

where $FDam$ is the total flood damage in dollars ($) (Table 3.3), $FDmax$ is the maximum flood damage that can be incurred in dollars ($), Q50 is the flow at which damage is 50% of the maximum, and dQ is the width of the transition of the flood damage curve. $Q50$ is defined as:

$$Q50 = \frac{Q_{min} + Q_{max}}{2.0} \tag{3.13}$$

where Q_{min} is the flow at which damage is 1% of the maximum damage and Q_{max} is the flow at which damage is 99% of the maximum damage. Currently, Q_{min} is set to 229.45 m^3/s and Q_{max} is set to 501.43 m^3/s based on the 10 year flood stage and 100 year flood stage, respectively, for Squaw Creek at Ames, IA. Maximum damage is set to $50 000 000 based on estimates of flood damage during the 2010 Ames, IA flood. dQ specifies how rapidly flood damages accrue from minor flood stage to maximum flood stage (Tesfatsion et al., 2017):

$$dQ = \frac{Q_{max} - Q_{min}}{9.2} \tag{3.14}$$

The flood damage for the previous year $t - 1$ is used to compute the conservation goal of the city agent for the current year t.

The conservation goal of the city agent is calculated as:

$$G_t = G_{t-1} + (A_{tot} - C_{tot}) \cdot P \tag{3.15}$$

$$P = P_{new} \cdot FDam \tag{3.16}$$

$$P_{new} = \frac{ConsGoal}{FDmax} \tag{3.17}$$

where G_t is the conservation goal for the new year t, G_{t-1} is the unfulfilled hectares in conservation from the previous conservation goal for year $t-1$, A_{tot} is the total land area in the catchment, C_{tot} is the total number of hectares currently in conservation, P is the percentage of new production land added into conservation, P_{new} indicates how much land to add into conservation based on the flood damage $FDam$ for year $t-1$, and $ConsGoal$ is a parameter that indicates the new percentage of conservation land to be added if maximum flood damage occurs (Table 3.2). Currently, $ConsGoal$ is set to 5% of total land area in the watershed when maximum damage occurs. This goal stays constant through the course of the entire simulation period.

Table 3.3. Variables in city agent equations.

City Agent Variables	Description	Unit
FDam	Current year's flood damage	($)
FDmax	Maximum attainable flood damage	($)
Q50	Discharge at with flood damage if 50% of maximum	(m^3/s)
Q_{min}	Discharge at with flood damage if 1% of maximum	(m^3/s)
Q_{max}	Discharge at with flood damage if 99% of maximum	(m^3/s)
dQ	Width of transition of flood damage curve	(m^3/s)
G_t	Government agent conservation goal for the current year t	Hectares
G_{t-1}	Unfullfilled conservation land from the previous year's t-1 conservation goal	Hectares
A_{tot}	Total agricultural land in watershed	Hectares
C_{tot}	Total land currently in conservation	Hectares
P	Total conservation land to be added to the goal as a percentage of production land	Dimensionless
P_{new}	Variable describing change in conservation goal with flood damage	(1/$)

3.2.11 Scenario Analysis

The study watershed is modeled after the Squaw Creek basin (~56200 Ha) located in central Iowa, USA. This basin is characterized by relatively flat hummocky topography and poorly drained soils with a high silt and clay content (~30-40% silt and clay) (Prior, 1991;

USDA-Natural Resources Conservation Service (USDA-NRCS), 2015). The predominant land use is row crop agriculture (~70% of the total watershed area) with one major urban center at the outlet (Ames, Iowa), and several small communities upstream. Average annual precipitation is 32 inches, with the heaviest precipitation falling during the months of May and June. The watershed is divided into fourteen subbasins and hydrologic model parameters are obtained from Schmeig et al. (2011).

In this model application, 100 farmer agents are implemented (~7 farmers per subbasin) with 121.4 hectares total for each farmer. Six scenarios are run: historical (time trend of yield kept at historical level) and low yield (time trend of yield decreased by 50%), high and low corn prices ($\pm 25\%$ from historical prices) and high and low conservation subsidies (annual rental payments of 125% and 75% of historical cash rent). In addition, four different farmer decision schemes are created in which an 85% weight was assigned to one decision variable, with all other variable weights set to 5% (Table 3.4). Each scenario is tested with each decision scheme and system outcomes under different farmer behaviors are assessed.

Table 3.4. Decision weighting scheme tested with each scenario.

Decision Scheme	Decision Weight			
	Conservation Goal	Futures	Past Profit	Risk Aversion
Conservation	**0.85**	0.05	0.05	0.05
Future price	0.05	**0.85**	0.05	0.05
Past profit	0.05	0.05	**0.85**	0.05
Risk averse	0.05	0.05	0.05	**0.85**

To test the sensitivity of the hydrologic system to farmer types, the conservation parameter ($Cons_{max}$) of the farmer agents is varied using a stratified sampling approach. Each farmer agent is randomly assigned a $Cons_{max}$ value from a predefined uniform distribution with

a range of 0.04. The lowest distribution has a range of -0.01 – 0.03 and the highest distribution has a range of 0.075 – 0.115. Any farmer agent that is assigned a parameter value less than 0 or greater than 0.1 is modified to have a value of 0 or 0.1, respectively. Twelve simulations are performed for each conservation parameter interval, with a total of 17 conservation parameter intervals. Thus, the first 12 simulations consist of farmer agents with $Cons_{max}$ chosen from -0.01 – 0.03. For the next 12 simulations, the distribution bounds are shifted up by 0.005 with $Cons_{max}$ chosen from -0.005 – 0.035. A total of 204 simulations are conducted for each decision scheme under each scenario (Table 3.4).

Each simulation is run using 47 years of historical climate and market data, with the exception of federal crop subsidies, which are based on 16 years of historical estimates produced by Iowa State University Agricultural Extension (Hofstrand, 2018; Table 3.5). It is assumed that federal crop subsidy payments from 1970-2000 are similar to levels seen from year 2000-2005 due to relative stability in long-term crop prices and production costs. The hourly 47 year precipitation time series data was obtained from the Des Moines, Iowa airport Automated Surface Observing System. Historical 47 year time series of corn prices, crop production costs, and land rental values are used as economic inputs into the model and where obtained from Iowa State University Agricultural Extension and Illinois FarmDoc (Table 3.5).

Table 3.5. Model Inputs.

Model Inputs	Years	Unit
Historical Cash Rent	1970-2016	($/Hectare)
Federal Subsidies	2000-2016	($/Hectare)
Historical Production Costs	1970-2016	($/Hectare)
Historical Corn Prices	1970-2016	($/MT)
Precipitation	1970-2016	(mm/hr)

3.3 Results

The 90th percentile peak discharge is 296.4 m^3/s when no conservation is occurring in the watershed (Figure 3.6). The 90th percentile peak discharge decreases for all four decision schemes and under all scenarios as the average conservation-mindedness ($Cons_{max}$) of the population increases (Figure 3.6). The low crop price scenario produces a larger decline in peak discharge compared to the high crop price scenario, with the exception of the conservation decision scheme (85% weight on conservation) in which both low and high crop price scenarios produce a similar ensemble pattern (Figure 3.6a).

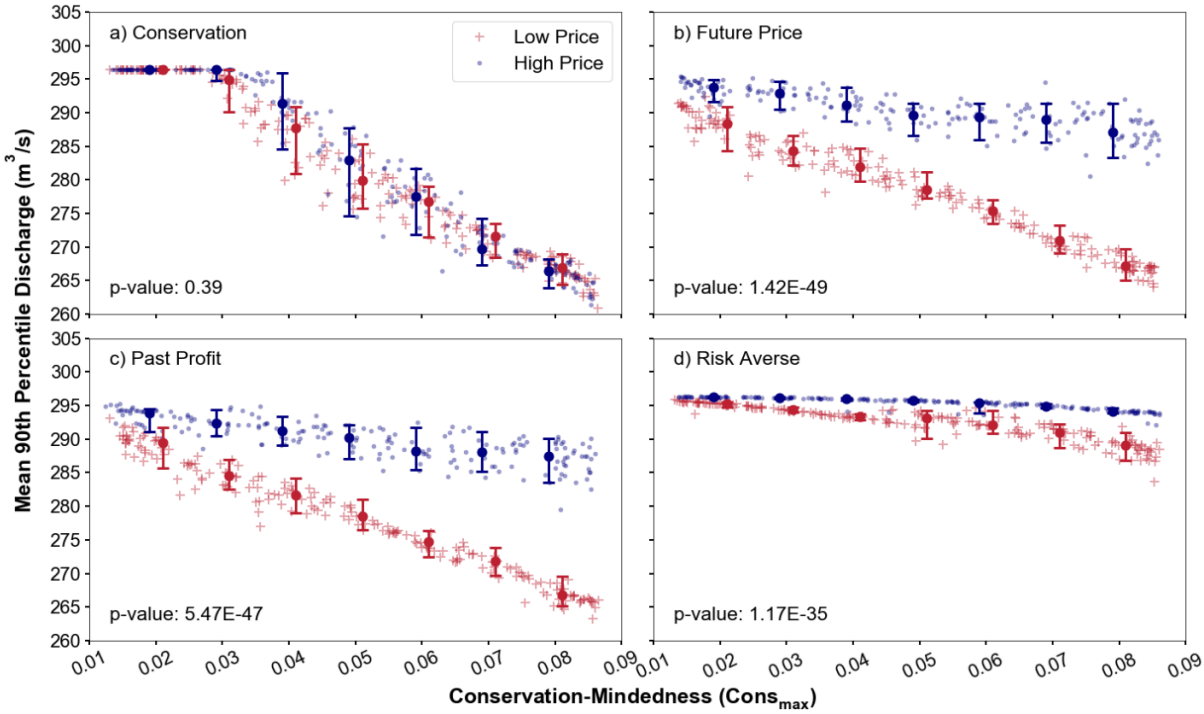

Figure 3.6. Mean 90th percentile discharge for high and low crop price scenarios under a) 85% weight on conservation goal, b) 85% weight on future price, c) 85% weight on past profit, and d) 85% weight on risk aversion.

Under low crop prices, peak discharge reaches an average reduction of 8.0% (23.9 m^3/s) when the average $Cons_{max}$ is 0.08-0.09 (conservation-minded population) and 4.7% (13.9 m^3/s) when the average $Cons_{max}$ is 0.04-0.06 (mixed population). These decrease in peak

discharge corresponds with the 800-1000 hectares and 400-600 hectares converted to conservation by the conservation-minded and mixed farmer populations, respectively (Figure 3.7a, c, e, g). The production-minded populations ($Cons_{max}$ ~0.01-0.02) implement less than 200 hectares during the entire simulation period. These acreage values represent 6.5-8.2%, 3.3-5.0%, and less than 2.0% of the entire watershed for the conservation-minded, mixed, and production-minded groups, respectively. Given that 10% of the watershed would be in conservation if native prairie strips were fully implemented, about 65-80% of a conservation-minded population fully implements the practice over the simulation period under low crop prices.

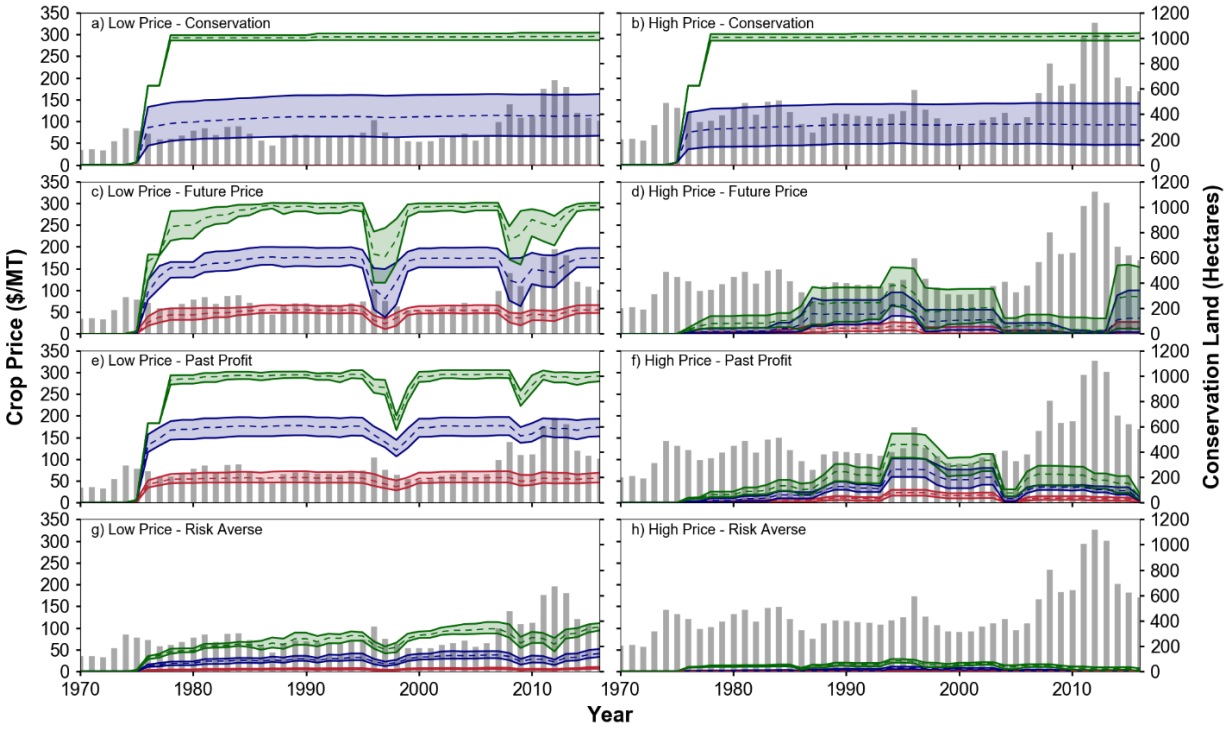

Figure 3.7. Range of simulated conservation land within the watershed under low (left column) and high (right column) crop prices for conservation-minded populations (green), mixed populations (blue) and production-minded populations (red). Crop prices are plotted as bars for each crop price scenario. Results are for decision schemes of 85% weight on conservation behavior (a, b), 85% weight on future price (c, d), 85% weight on past profit (e, f), and 85% weight on risk aversion (g,h).

Under the high crop prices, mean peak discharge decreases by no more than 9 m^3/s (3.1%) under the future price and past profit weighting schemes for the highly conservation-minded population (Figure 3.6b and c, respectively), with an even smaller reduction seen for the risk-averse scenario. This represents approximately a 47% smaller decrease in the peak discharge when crop prices are high and the population is conservation-minded. Discharge remains largely unchanged for these decision schemes because generally less than 200 hectares of land is allocated for conservation when corn prices are high (Figure 3.7d, f, and h).

Relative to the conservation decision scheme, corn prices factor more heavily into the future price and past profit decision schemes, producing a large spread between the discharge outcomes under the two corn price scenarios. Mean peak discharge decreases by an average of 2-3% (~7-8 m^3/s) for production-minded populations and up to 10% (~29.6 m^3/s) for conservation-minded populations for both decision schemes under low prices (Figure 3.6b and c). In this case, conservation subsidies allow the farmer agents to approach break even because they are guaranteed a subsidy that covers the cash rent for that land, whereas crop production leads to potential losses due to corn prices being low relative to production costs. Even in these scenarios where farmer agents are heavily considering profit related variables, populations dominated by production-minded farmer agents are still inclined to leave land in production (Figure 3.7c and e).

Under historical and low crop yield scenarios, the 90^{th} percentile peak discharge decreases by an average of 6.9% (20.4 m^3/s) and 8.0% (23.7 m^3/s), respectively, for the conservation-minded populations (Figure 3.8). This is similar to changes observed for the low crop price scenario (Figure 3.6). The low crop yield and low crop price scenarios also had similar amounts of land conversion (Figure 3.7a,c,e,g and 3.9 a,c,e,g). More conservation land

is established under the historical yield scenario (which is using historical crop prices) compared to the high crop price scenario (which uses historical yields) (Figure 3.7 b,d,f,h and 3.9 b,d,f,h). As a result, mean peak discharge decreases by 38% more in the historical yield scenario compared to the high crop price scenario for the conservation-minded population.

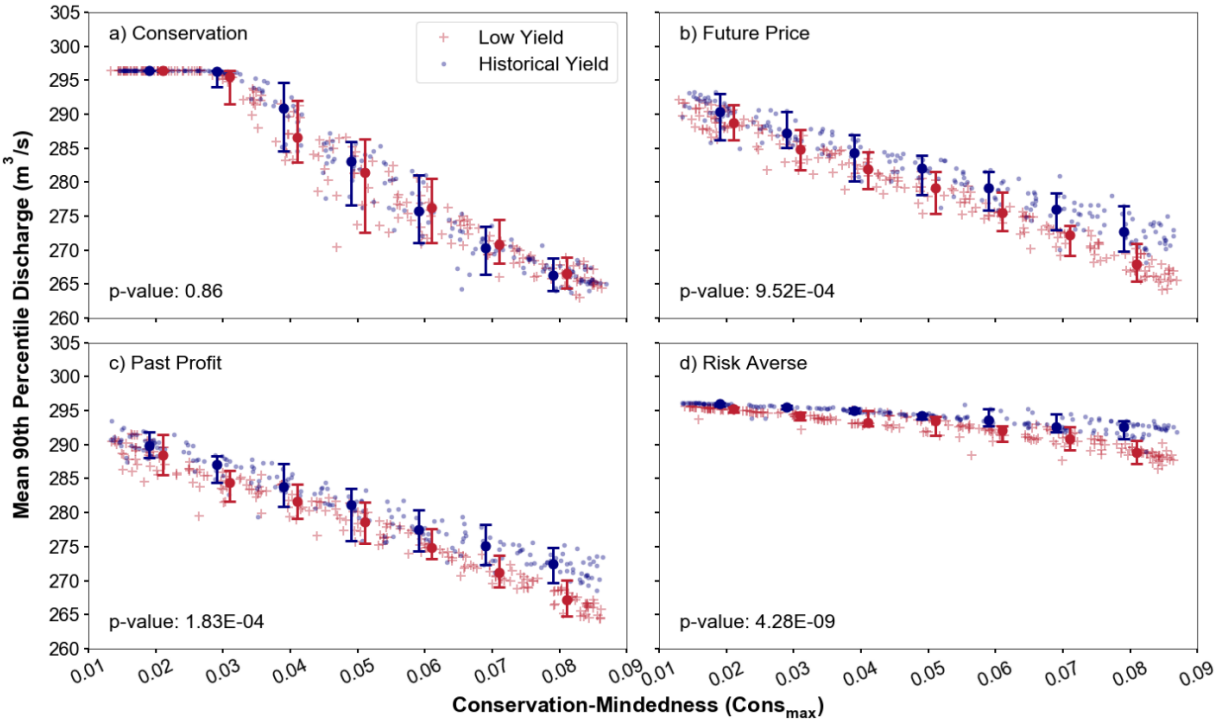

Figure 3.8. Mean 90th percentile discharge for historical and low yield scenarios under a) 85% weight on conservation goal, b) 85% weight on future price, c) 85% weight on past profit, and d) 85% weight on risk aversion.

A difference in the variability in land conversion patterns occurs between the historical and low crop yield scenarios, particularly under the past profit and future price weighting schemes (Figure 3.9 c-d, e-f). When the trend in yields is low, conservation land remains relatively consistent during the entire simulation for all populations (Figure 3.9 c,e). For instance, conservation land remains at approximately 600 Ha for the mixed population after year 1985. Under historical yields, more inter-annual variability is seen with conservation land changing by 200 Ha over the course of several years many times throughout the simulation

period. This pattern, however, is not reflected through changes to the mean 90th percentile discharge.

Under the low and high subsidies scenarios (not shown), the 90th percentile peak discharge decreases by an average of 6.0% (18.0 m^3/s) and 7.3% (21.6 m^3/s), respectively, for conservation-minded populations. Thus, low subsidies show the second smallest overall change in peak discharge next to high crop prices. The high and low subsidies scenarios produce a greater overall fluctuation in the number of hectares in conservation land. Increasing the subsidy by 25% from historical levels does not result in a consistent 1000 Ha of conservation land implemented when the population is conservation minded, rather, the conservation land varies over time, similar to the historical yield scenario, and generally hovers in the 800-1000 Ha range. Low subsidies result in even greater variability in conservation land, with changes of 200-300 Ha seen over short time spans of a few years. However, as was seen under the historical yield scenario, these variations do not translate to substantial changes in mean peak discharge.

The risk averse decision scheme produces the smallest changes in peak discharge under all scenarios, with an average decrease of less than 1% (3 m^3/s) and 2% (6 m^3/s) for mixed and conservation-minded populations, respectively (Figure 3.6d, 3.8d). In this scheme, a farmer's past practices outweighs the motivation to convert land based on what past profit or future crop prices may suggest. As a result, the farmer agents implement conservation land more slowly. For instance, with a conservation-minded group of farmer agents with 85% weight on future prices or past profit, conservation land reaches a relative stability of ~1000 hectares by year 1980 under low crop prices (Figure 3.7c and e). When risk aversion is heavily weighed, conservation land gradually increases throughout the entire simulation period, reaching its

highest level of ~400 Ha at the end of the simulation period for the low crop price and low yield scenario (Figure 3.7h, 3.9h). In all other scenarios, the conservation land remains at relative equilibrium below 200 Ha.

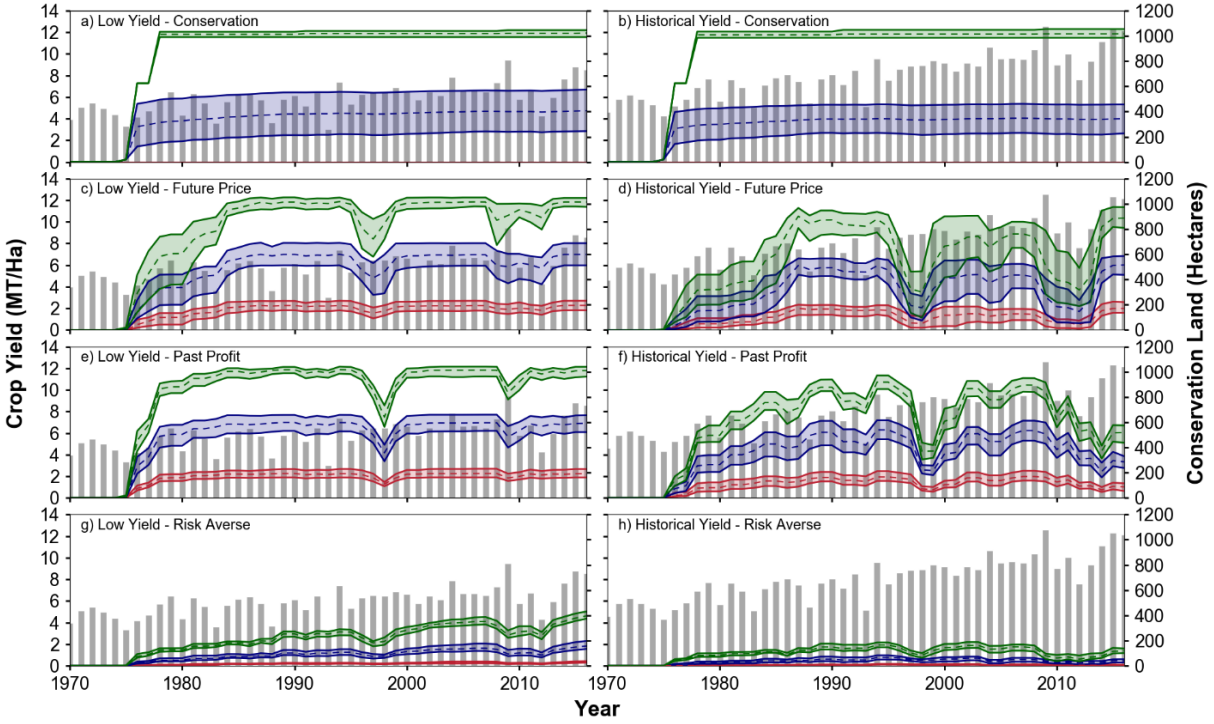

Figure 3.9. Range of simulated conservation land within the watershed under low (left column) and historical (right column) crop yields for conservation-minded populations (green), mixed populations (blue) and production-minded populations (red). Yearly crop yields are plotted as bars for crop yield scenario. Results are for decision schemes of 85% weight on conservation behavior (a, b), 85% weight on future price (c, d), 85% weight on past profit (e, f), and 85% weight on risk aversion (g,h).

To gain an understanding of how each of the scenarios differs from the historical 1970-2016 period, the mean peak discharge is compared against the historical yield scenario, which does not modify any economic or agricultural variables (Figure 3.10). Overall, crop prices had the largest impact on mean peak discharge while changes in subsidies had the smallest overall impact. When crop prices were low, mean peak discharge decreased by 1-2% for mixed populations and 2-3% for conservation-minded populations under the future price and past

profit schemes (Figure 3.10a). High crop prices result in an increase in peak discharge from the historical yield scenario, with an increase of 2-4% for mixed populations, and 5-6% for conservation-minded populations. Subsidy scenarios produced a similar result, where a larger change (increase) in mean peak discharge occurs under low subsidies than under high subsidies. This indicates that high crop prices are a major factor in reducing willingness of the farmer agents to accept conservation subsidies.

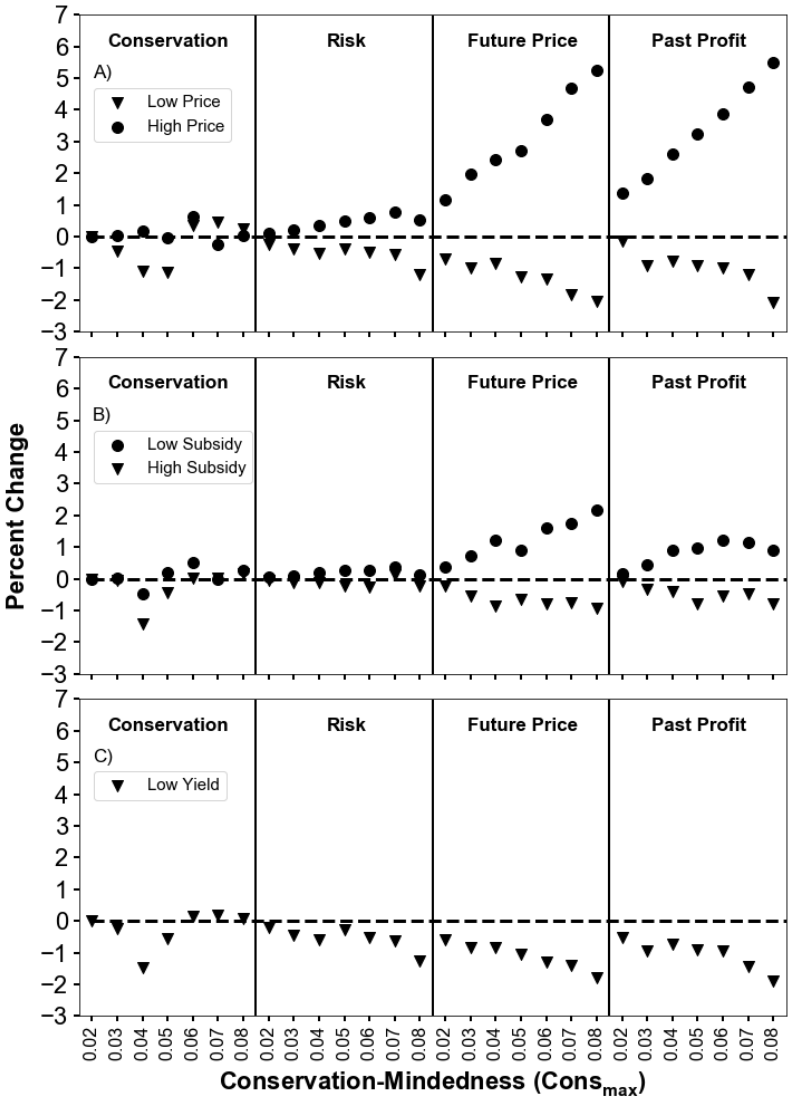

Figure 3.10. Percent Change in median 90th percentile discharge from the historical yield scenario for a) high and low crop prices, b) high and low subsidies, c) low yield for the conservation, risk, future price, and past profit weighting schemes.

Overall, the current government conservation goal of 5% at maximum flood damage did not have a significant impact on the trends in conservation land, but did impact the total amount of land implemented. Following two major flooding events, the government goal increases from less than 20 Ha in 1975 to 620 Ha on average in 1976. A similar event in 1977 increases the government goal by another 500 Ha. These increases in the government conservation goal do correspond to the large and rapid onset of conservation land seen during those year (Figure 3.7a,c,e; 3.9a,c,e). Under the conservation-minded populations, the government goal is nearly fulfilled, particularly if crop prices are low, or subsidies are high. In these cases, the goal remains below 200 Ha for extended periods when crop prices are relatively stable. The only case where the government goal limits the amount of land implemented is under the conservation weighting scenarios. Under production-minded populations, the government goal increases to approximately 1000-1200 Ha following the flood events mentioned earlier and remains relatively stable thereafter.

3.4 Model Verification

Calibrating and verifying the social part of social-hydrologic models is difficult due to reasons that include lack of sufficiently detailed empirical data or system complexity at various scales (An, 2012; Ormerod and Rosewell, 2009; Troy et al., 2015). Validation of agent-based models is usually performed on the micro and macro levels. The micro level involves comparing individual agent behaviors to real world empirical data whereas the macro level involves comparing the model's aggregate response to system-wide empirical data (An et al., 2005; Berger, 2001; Troy et al., 2015; Xiang et al., 2005). Troy et al., (2015) suggests that one or a few model simulations out of an ensemble of simulations should match the real-world observed data.

We conduct a macro-level model verification by comparing modeled conservation land to the historical percent of conservation land implemented in Iowa, with specific focus on determining if certain ensemble members correlate closely with the observed data. Comparing against total conservation land in Iowa was most appropriate because the economic inputs used represent statewide averages from Iowa data (i.e. cash rent input was the mean cash rent for Iowa, not the mean for any particular county or region within Iowa).

Analyzing the historical yield simulations (i.e. no economic modifications) for the future price and past profit scenarios shows that trends in the simulated conservation land generally align with trends in the observed conservation land (Figure 3.11). Simulated conservation land is not maintained following a rise in crop prices in the mid-1990s and from 2006-2013, which is similar to the observed data. The drop in conservation land occurs because the subsidy rate is not modified in response to market forces to incentivize the farmer (Newton, 2017). In 2008 and 2011, corn prices rose to a record high values, and farmer in the Midwest U.S. (e.g., Iowa, Minnesota) were converting significant portions of CRP land back into crop production (Marcotty, 2011; Secchi and Babcock, 2007). It is estimated that when corn prices rise by $1.00, 10-15% of CRP land in Iowa is converted back to production (Secchi and Babcock, 2007). The total amount of conservation land is best matched by the conservation-minded population, but the changes in conservation land are best matched by the mixed population. Adding in additional factors, such as the Federal Market Loss Assistance and Loan Deficiency Payments, may improve results. Further, it is possible to improve the simulation via model calibration, such as adjusting the farmer decision weights, parameter X, and decision curves for the past profit, future price, and conservation variable. However, it may be difficult to find sufficient data sets to support a robust calibration of this type of model. For modeling land use decisions,

data is typically available at the aggregate level rather than at the individual agent level (An, 2012; Parker et al., 2008) This introduces difficulty in trying to verify farm-level decisions with respect to farm-level finances.

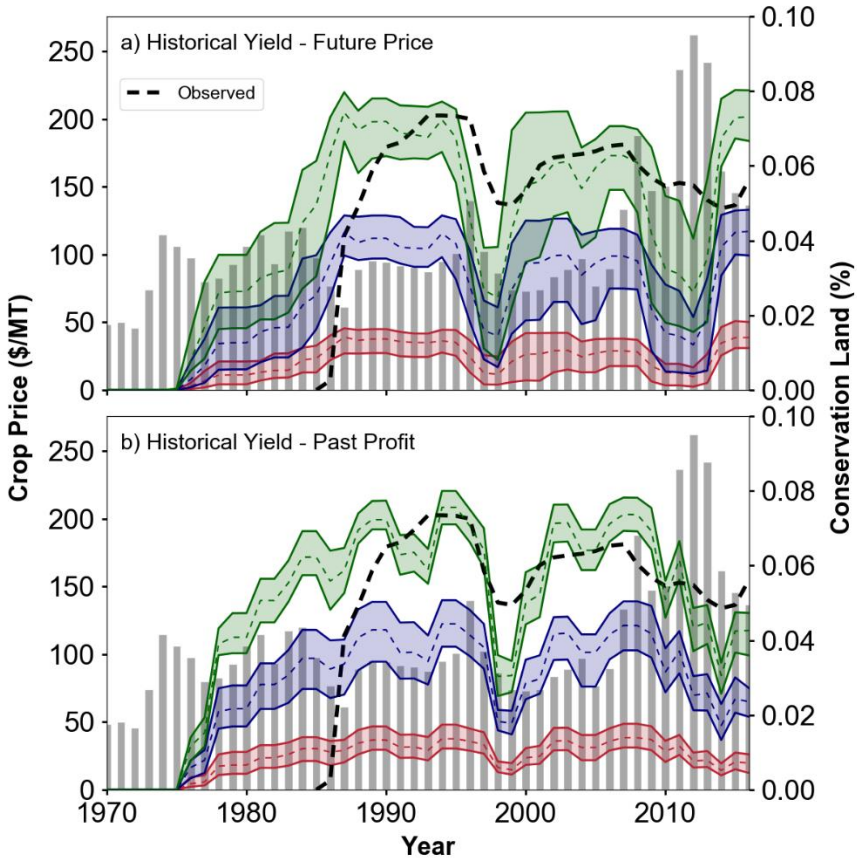

Figure 3.11. Range of simulated conservation land under historical conditions for conservation-minded populations (green), mixed populations (blue) and production-minded populations (red) in comparison to observed historical conservation land in Iowa. Crop prices are plotted as bars for reference. Results are for decision schemes of 85% weight on future price (a), and 85% weight on past profit (b).

The onset of significant land conversion in the model is offset from the observations. Conservation land in both weighting scenarios is implemented in the mid-1970s, while conservation land in the observation is implemented in the late-1980s. The CRP program did not come into existence until 1985, which explains this difference. Shifting the simulated conservation land time series forward in time against the observed conservation land and

calculating pearson's r, we find that the future price decision scheme is offset by about two years (Figure 3.12a). After shifting forward two years, a few simulations indicate a pearson's r of 0.7-0.8 (Figure 3.12a). In contrast, the past profit decision scheme did not show a stronger correlation until the simulations are shifted forward by 10 years (i.e. the first year conservation land is implement is in line with the first year CRP land is implemented) (Figure 3.12b). Under this decision scenario, the correlation was particularly strong for the conservation-minded population, with conservation land increasing to 4% in roughly 2-3 years following a slightly smaller drop in crop prices, as occurred under the CRP program from 1985-1987.

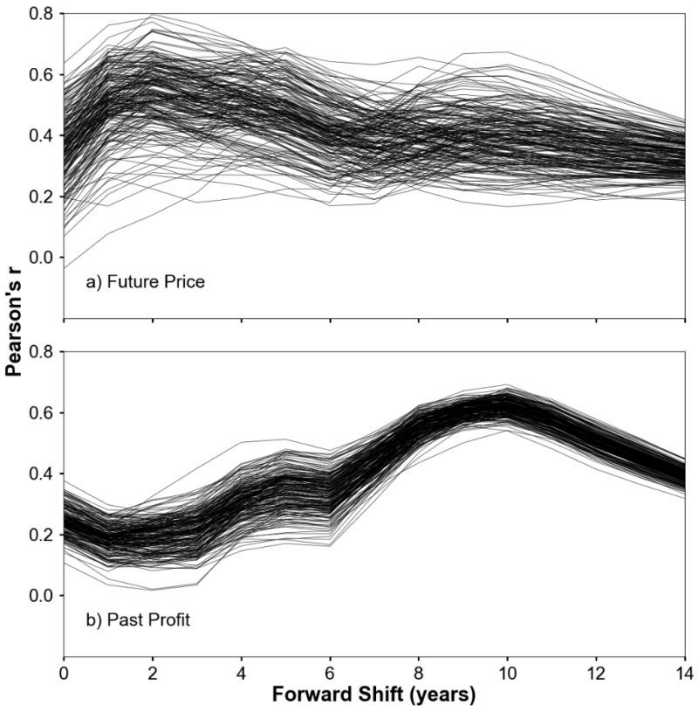

Figure 3.12. Pearson's correlation coefficient for simulations under historical conditions shifted forward against observed conservation land in Iowa. Results are for decision schemes of 85% weight on future price (a), and 85% weight on past profit (b).

Overall macro level validation does provide evidence that the model captures changes in CRP land during the appropriate time periods, however, it does not provide evidence that any individual agent's decisions are valid. Since micro level farm-specific data was not available,

validation on the micro level was not performed. The next step in the model validation process could include gathering detailed survey data or iterative participatory modeling with local agricultural stakeholder to validate farm level decision making within the model.

3.5 Conclusions

Scenarios of historical and low crop yields, as well as high and low corn prices and conservation subsidies, were simulated for an agricultural watershed in the Midwest US corn-belt using an agent-based model of farmer decision making coupled to a simple rainfall-runoff hydrologic model. The influence of different farmer agent decision components on model outcomes was also explored. Model results demonstrate causations and correlations between human systems and hydrologic outcomes, uncertainties, and sensitivities (specifically focused on high flows).

The primary findings from this study are:

- Crop prices had the largest impact on mean peak discharge, with a 47% larger reduction in mean peak discharge under low crop prices in comparison to high crop prices.
- Changes in subsidy rates and crop yields produce similar changes in mean peak discharge. Approximately a 15-20% difference was realized between high and low subsidies, and historical and low yields.
- Despite the potential benefits of subsidy payments during low corn prices, farmer agents that have low conservation-mindedness keep land in production.
- Farmer agents were more inclined to eliminate conservation land – a 5-6% increase in mean peak discharge was indicated under high crop prices, while only a 2-3% decrease in

mean peak discharge was indicated under low crop prices, in comparison to the historical baseline simulation (i.e. historical yield scenario).

- Heavily weighing a farmer agent's future price or past profit decision variables produces the largest difference in mean peak discharge between scenarios. For instance, under these weighting scenarios, a 7% difference in mean peak discharge is seen between high and low crop prices as opposed to a 0-2% difference under the risk averse or conservation weighting schemes.
- A large risk aversion has the smallest impact on mean peak discharge with less than a 2% decrease in mean peak discharge seen under all scenarios.
- Weighting the conservation decision variable heavily results in similar conservation land and peak discharges in the watershed over time regardless of changes in crop price, yield, or subsidy. In this case, farmer agents' preferred land use is dominating their decisions.
- The model does correlate with observed conservation land in Iowa. A 0.7-0.8 pearson's r was noted under the future price weighting scenario for a few select simulations.

The social-hydrologic modeling approach allows identification of trends and tipping points of a system that would most likely not be captured by the standard modeling approach (Montanari et al., 2013; Sivapalan et al., 2012). In this study, relationships between seemingly unrelated variables (e.g., crop prices, conservation-mindedness, and peak flows) were revealed. For example, connections between the mean 90th percentile peak discharge of a watershed and crop prices were revealed and explained.

The current model design contains several limitations in both the hydrologic and agent-based models that will need to be addressed in future model development. The curve number values that were used to represent the conservation option were derived for small agricultural

plots of approximately 0.5-3 Ha in size. The question remains whether these CN values can be scaled up to the size of a several hundred hectare farm plot and still produce feasible discharge results. In addition, there is no explicit spatial representation of farmer agents within each subbasin, Coupling the agent-based model to a more robust hydrologic model may reduce some of these hydrologic limitations.

From the agent-based modeling standpoint, the decision-making of the farmer and city agent could be made more sophisticated by introducing certain state variables, further decision components and longer planning horizons. Studies have identified variables such as farm size, type of farm, age of farmer, off farm income, neighbor connections, land tenure agreement, education from local experts, among others, to be significant in determining adoption of conservation practices (Arbuckle, 2017; Daloğlu et al., 2014; Davis and Gillespie, 2007; Lambert et al., 2007; Mcguire et al., 2015; Ryan et al., 2003; Saltiel et al., 1994; Schaible et al., 2015). The functionality of the city agent could be expanded by introducing a method for adjusting the conservation goal through time or introducing cost-benefit analysis capabilities. Cost-benefit capabilities would allow the city agent to make more advanced decisions such as choosing among a variety of flood reducing investments (Shreve and Kelman, 2014; Tesfatsion et al., 2017).

Lastly, future work with the modeling system could also focus on addressing model calibration. Using the current observed conservation land can be used as a starting point for calibrating farmer agent decision-making parameters; however, more detailed survey data or collaboration with agricultural stakeholders may be necessary to obtain a full validation of individual agent decision-making.

One of the strength of agent-based models is being able to explore feedbacks not only from the human system to the hydrologic system, but additionally being able to explore how the hydrologic system affects the response of the human system (An, 2012). This study did not explore the feedbacks from the hydrologic system to the human system in detail but could be another focus of future work.

3.6 Acknowledgments

Funding for this project was provided by an Iowa State University College of Liberal Arts and Sciences seed grant. We would like to thank all other seed grant participants, including Jean Goodwin, Chris R. Rehmann, William W. Simpkins, Leigh Tesfatsion, Dara Wald, and Alan Wanamaker.

3.7 Appendix A

3.7.1 Farmer Agent Crop Insurance

The crop insurance protection in the model follows the Revenue Protection (RP) plan, which is one of several insurance options set forth by the USDA Agricultural Risk Management agency in the Common Crop Insurance policy. RP accounts for 95-100% of the insurance plans chosen by farmers in the U.S corn belt (Schnitkey, 2017). Each farmer agent is on the RP crop insurance plan at an 80% coverage level with insurance premiums factored into the crop production costs. The RP plan protects farmer agents against poor yields and suppressed crop prices. In a given year, the insurance payout per hectare (Gross Indemnity) at an 80% coverage level for corn crop is calculated as (Plastina, 2014a):

$$Gross\ Indemnity\ = Rev\ Guarantee - Actual\ Rev \tag{3.18}$$

where,

$$Rev\ Guarantee = max(Projected\ Price, Harvest\ Price) * Coverage\ Level * TrendAdj\ APH\ Yield \quad (3.19)$$

and,

$$Actual\ Rev = Harvest\ Price * Harvest\ Yield \quad (3.20)$$

The trend-adjusted actual production history (APH) yield is calculated as (Plastina, 2014b):

$$TrendAdj\ APH\ Yield = \frac{\sum_{n=1}^{n=10} Yield_{t-n} + AdjustmentFactor \cdot n}{10} \quad (3.21)$$

where $Yield_{t-n}$ is the historical yield for year $t-n$, with year t being the current year. The yield is based on the mean yield of the previous 10 years. For each year, the yield is adjusted upward by $AdjustmentFactor \cdot n$, where n is the number of years back in time from the current year. The most recent adjustment factors for Iowa have ranged from 1.90 -2.40 (Plastina, 2014b), with an $AdjustmentFactor$ value of 2.0 used in the model. The mean of the adjusted yields then gives the trend-adjusted APH yield.

3.7.2 Stochastic Variability of Agricultural Economic Variables

Differences in land quality causes production costs to range by approximately 20% between low and high quality land, with 50-60% of the difference due to cash rental rates, and 30-40% of the difference due to crop production inputs (i.e seed, fertilizers, crop insurance) (Plastina, 2017b). To account for the impact of land quality, crop production costs are adjusted and stochastically varied using values and ranges derived from historical crop production costs for 2000-2018 and Cash Rental Rates from Iowa surveys for 2002-2017 (Plastina, 2017b, 2017a).

The production costs of the farmer agent are adjusted up or down based on the agent's Corn Suitability Rating (CSR2) value. The CSR2 index is based on the soil and particle size classes, field condition, and soil depth and values are available from the NRCS SSURGO database. A weighted mean CSR2 value is calculated for each farmer agent according to the fraction of soil types present on the agent's land (Section 3.7.4). Based on the 2015-2017 Iowa State University Land Value surveys (Zhang, 2017), low, medium, and high quality CSR2 values were determined to be 61, 74, and 86, respectively. Assuming that the historical average production costs correspond to medium quality land, a farmer agent's production costs are scaled linearly using a 10% decrease in the median cost for the lowest quality land and a 10% increase in the median cost for the highest quality land.

Stochastic variability was added to the production costs based on variability in cash rent and crop production input prices. Cash rent variability was found to be consistent across land qualities, but showed a remarkable increase in range between low and high crop prices. The 25th percentile of cash rent linearly decreased from -10% to -40% from the average value between a crop price of \$2.00 and \$7.00, and was represented through the regression equation:

$$Decrease = -0.0449x - 0.0982 \tag{3.22}$$

The 75th percentile of cash rent linearly increased from +10% to +45% from the average value between \$2.00 and \$7.00, and was represented through the regression equation:

$$Increase = 0.0565x + 0.0780 \tag{3.23}$$

Based on the crop price, the stochastic variability added to the cash rent is randomly drawn from the uniform distribution: $\mathcal{U}(Decrease, Increase)$. Further, it is assumed that cash rents are unlikely to vary significantly from below to above the mean cash rent from one year to the next. Therefore, the final variability added to the cash rent is based on a weighted average

between the previous year's and current year's variability, with equal weight place on both years.

The inputs portion of the production costs (i.e. cost of seed, fertilizer, crop insurance, etc.) was found to increase and decrease by ~3-4% of the total historical production costs between medium and high quality land, and medium and low quality land, respectively. It was assumed that variability in the input costs could range between +1.5% and -1.5% of the total production costs. Thus, input variability was randomly drawn from a uniform distribution: $\mathcal{U}(-0.015,0.015)$.

The final production cost is represented by the equation:

$$\begin{aligned} ProdCost_t = [ProdCostHist_t \cdot ProdCostAdjust(CSR2)] \\ +CashRentRandom(CropPrice_t) \\ +[ProdCostHist_t \cdot InputCostRandom] \end{aligned} \quad (3.24)$$

where $ProdCost_t$ is the final adjusted production cost for year t, $ProdCostHist_t$ is the historical production costs, $ProdCostAdjust(CSR2)$ is the production cost adjustment based on CSR2 value, $CashRentRandom(CropPrice_t)$ is the stochastic variability added to cash rent based on equations crop price magnitude (equations 3.22, 3.23), and $InputCostRandom$ is stochastic variability added to input costs.

3.7.3 Opportunity Cost Adjustment

Because production costs vary based on land quality, opportunity costs are adjusted up or down such that farmer agents with higher (lower) land quality will have higher (lower) opportunity costs associated with implementing conservation land.

The famer agent's cost of implementing the native prairie strips in this model is based on financial analysis conducted by (Tyndall et al., 2013). Farmer agents consider three key cost variables associated with implementing conservation land: cost of establishing the prairie (i.e.

materials, site preparation and planting), cost of maintaining the prairie through annual mowing or burning, and cost of forgone revenue from the land taken out of crop production. Tyndall et al., (2013) shows that opportunity costs account for 53% of total costs of native prairie strips for low quality land and scale up to 88% for high quality land. On the other hand, establishment costs account for 10% or less of total costs for high quality land and scale up as land quality decreases.

For simplicity purposes, we assume opportunity costs are 90% of $Cost_{prairie}$ under high quality land and 60% of $Cost_{prairie}$ under low quality land. The remaining percentage of $Cost_{prairie}$ is assumed to be split evenly between establishment and maintenance costs. The final opportunity cost for farmer agents with land between low and medium quality is calculated as:

$$OppCost = OppCostIncreasedPerCSR2 \cdot WeightedAvgCSR - 0.104 \quad (3.25)$$

where $OppCostIncreasedPerCSR2$ is the increase in opportunity costs per point increase in the CSR2 value (i.e. slope), and the value -0.104 is the intercept which gives an opportunity cost of 60% of total costs at a CSR2 value of 61. A similar equation is used for finding the opportunity cost between medium and high quality land, with the difference being the intercept coefficient.

The final cost per acre of implementing conservation land is calculated using the following equation:

$$Cost_{prairie} = OppCost + Establishment + Maintenance \quad (3.26)$$

where $OppCost$ is based on the cash rent input (Section 3.2.6), and establishment and maintenance costs are calculated as:

$$\frac{Establishment}{Maintenance} = CashRent \cdot \frac{\frac{1-0.9}{2}}{0.9} \quad (3.27)$$

3.7.4 Soil Crop Yield Adjustment and Stochastic Variability

A farmer agent's land can be defined by up to 8 different soil types at different percentages. The soil types used are common to the Squaw Creek watershed: Nicollet Loam (1-3% slope), Clarion Loam (2-5% slope), Webster clay loam (0-2% slopes), Canisteo clay loam (0-2% slopes), Clarion loam (5-9% slopes, moderately eroded), Harps loam (1-3% slopes), Clarion loam (5-9% slopes), and Okoboji mucky silt loam (0-1% slopes). To account for differences in soil crop productivity, adjustments were developed using field scale data spanning 1995-2006 from 10 fields in central Iowa (A. VanLoocke, personal comm., July 2015). Mean yearly yields were derived for each soil type over the course of the 11 year period. The mean yearly yields were compared against mean historical central Iowa crop yields for the same period to determine whether a particular soil type tends to produce a crop yield higher or lower than the historical mean. Soil type adjustments were then derived by taking the mean of the differences between the mean yearly yield and mean historical yield. In general, the soils displayed on average a 0.35 Mt/Ha higher yield over mean historical Central Iowa yields. For Clarion loam (5-9% slopes, moderately eroded), yields were approximately 0.11 MT/Ha lower than the mean Central Iowa yield, while Nicollet Loam (1-3% slope) on average produced 0.63 MT/Ha higher yields. All other soil type displayed differences in mean yield between these values. The adjustment factors were added to the crop yield for each soil type over the entire simulation period. Thus, it was assumed that these yield factors remain constant through time.

Stochastic variability is added to the yield for each soil type to account for other factors that influence crop productivity. Stochastic variability was drawn from a uniform distribution

between the range of mean differences of the 5th and 95th percentiles and added to the soil yield for that year. For example, the 5th and 95th percentiles of yields for Nicollet Loam were on average 0.9 MT/Ha lower and 0.95 Mt/Ha higher than the mean yearly yield for Nicollet loam. Thus, after adjusting the soil yield up by 0.63 MT/Ha, stochastic variability was then added from the uniform distribution: $\mathcal{U}(-0.9,0.95)$.

3.8 References

Ahn, K. H. and Merwade, V.: Quantifying the relative impact of climate and human activities on streamflow, J. Hydrol., 515, 257–266, doi:10.1016/j.jhydrol.2014.04.062, 2014.

An, L.: Modeling human decisions in coupled human and natural systems : Review of agent-based models, Ecol. Modell., 229, 25–36, doi:10.1016/j.ecolmodel.2011.07.010, 2012.

An, L., Linderman, M., Qi, J., Shortridge, A. and Liu, J.: Exploring Complexity in a Human–Environment System: An Agent-Based Spatial Model for Multidisciplinary and Multiscale Integration, Ann. Assoc. Am. Geogr., 95(1), 54–79, doi:10.1111/j.1467-8306.2005.00450.x, 2005.

Arbuckle, J. G.: Farmer Attitudes toward Proactive Targeting of Agricultural Conservation Programs, Soc. Nat. Resour., 26(6), doi:10.1080/08941920.2012.671450, 2013.

Arbuckle, J. G.: Iowa Farm and Rural Life Poll 2016 Summary Report, Ames, IA., 2017.

Asch, M., Boquet, M. and Nodet, M.: Nudging Methods, in Data Assimilation: Methods, Algorithms, and Applications, pp. 120–123, SIAM., 2017.

Axelrod, R. and Tesfatsion, L.: A Guide for Newcomers to Agent-Based Modeling in the Social Sciences, Handb. Comput. Econ., 2, 1647–1659, doi:10.1016/S1574-0021(05)02044-7, 2006.

Di Baldassarre, G., Viglione, A., Carr, G., Kuil, L., Salinas, J. L. and Blöschl, G.: Socio-hydrology: Conceptualising human-flood interactions, Hydrol. Earth Syst. Sci., 17(8), 3295–3303, doi:10.5194/hess-17-3295-2013, 2013.

Bao, Z., Zhang, J., Wang, G., Fu, G., He, R., Yan, X., Jin, J., Liu, Y. and Zhang, A.: Attribution for decreasing streamflow of the Haihe River basin, northern China: Climate variability or human activities?, J. Hydrol., 460-461, 117–129, doi:10.1016/j.jhydrol.2012.06.054, 2012.

Barreteau, O., Bousquet, F., Millier, C. and Weber, J.: Suitability of Multi-Agent Simulations to study irrigated system viability: application to case studies in the Senegal River Valley, Agric. Syst., 80(3), 255–275, doi:10.1016/j.agsy.2003.07.005, 2004.

Becu, N., Perez, P., Walker, a, Barreteau, O. and Page, C. L.: Agent based simulation of a small catchment water management in northern Thailand, Ecol. Modell., 170(2-3), 319–331, doi:10.1016/S0304-3800(03)00236-9, 2003.

Berger, T.: Agent-based spatial models applied to agriculture: A simulation tool for technology diffusion, resource use changes and policy analysis, Agric. Econ., 25(2-3), 245–260, doi:10.1016/S0169-5150(01)00082-2, 2001.

Berger, T. and Troost, C.: Agent-based Modelling of Climate Adaptation and Mitigation Options in Agriculture, J. Agric. Econ., 65(2), 323–348, doi:10.1111/1477-9552.12045, 2014.

Berger, T., Birner, R., Mccarthy, N., DíAz, J. and Wittmer, H.: Capturing the complexity of water uses and water users within a multi-agent framework, Water Resour. Manag., 21(1), 129–148, doi:10.1007/s11269-006-9045-z, 2006.

Bithell, M. and Brasington, J.: Coupling agent-based models of subsistence farming with individual-based forest models and dynamic models of water distribution, Environ. Model. Softw., 24(2), 173–190, doi:10.1016/j.envsoft.2008.06.016, 2009.

Borrill, P. and Tesfatsion, L.: Agent-based modeling: the right mathematics for the social sciences?, in The Elgar Companion to Recent Economic Methodology, pp. 228–258, New York, New York., 2011.

Burton, R. J. F.: The influence of farmer demographic characteristics on environmental behaviour: A review, J. Environ. Manage., 135, 19–26, doi:10.1016/j.jenvman.2013.12.005, 2014.

Daloğlu, I., Nassauer, J. I., Riolo, R. L. and Scavia, D.: Development of a farmer typology of agricultural conservation behavior in the american corn belt, Agric. Syst., 129, 93–102, doi:10.1016/j.agsy.2014.05.007, 2014.

Davis, C. G. and Gillespie, J. M.: Factors affecting the selection of business arrangements by U.S. hog farmers, Rev. Agric. Econ., 29(2), 331–348, doi:10.1111/j.1467-9353.2007.00346.x, 2007.

Duffy, M.: Conservation Practices for Landlords, Ames, IA., 2015.

Dziubanski, D. J., Franz, K. J. and Helmers, M. J.: Effects of Spatial Distribution of Prairie Vegetation in an Agricultural Landscape on Curve Number Values, JAWRA J. Am. Water Resour. Assoc., 53(2), 365–381, doi:10.1111/1752-1688.12510, 2017.

Elshafei, Y., Sivapalan, M., Tonts, M. and Hipsey, M. R.: A prototype framework for models of socio-hydrology: Identification of key feedback loops and parameterisation approach, Hydrol. Earth Syst. Sci., 18(6), 2141–2166, doi:10.5194/hess-18-2141-2014, 2014.

Grimm, V., Berger, U., Bastiansen, F., Eliassen, S., Ginot, V., Giske, J., Goss-Custard, J., Grand, T., Heinz, S. K., Huse, G., Huth, A., Jepsen, J. U., Jørgensen, C., Mooij, W. M., Müller, B., Pe'er, G., Piou, C., Railsback, S. F., Robbins, A. M., Robbins, M. M., Rossmanith, E., Rüger, N., Strand, E., Souissi, S., Stillman, R. a., Vabø, R., Visser, U. and DeAngelis, D. L.: A standard protocol for describing individual-based and agent-based models, Ecol. Modell., 198(1-2), 115–126, doi:10.1016/j.ecolmodel.2006.04.023, 2006.

Guo, Y. and Shen, Y.: Quantifying water and energy budgets and the impacts of climatic and human factors in the Haihe River Basin, China: 2. Trends and implications to water resources, J. Hydrol., 527, 251–261, doi:10.1016/j.jhydrol.2015.04.071, 2015.

Hawkins, R. H., Ward, T., Woodward, D. E. and Van Mullem, J.: Curve Number Hydrology: State of the Practice., American Society of Civil Engineers, Reston, VA., 2009.

Helmers, M. J., Zhou, X., Asbjornsen, H., Kolka, R., Tomer, M. D. and Cruse, R. M.: Sediment Removal by Prairie Filter Strips in Row-Cropped Ephemeral Watersheds, J. Environ. Qual., 41(5), 1531, doi:10.2134/jeq2011.0473, 2012.

Hernandez-Santana, V., Zhou, X., Helmers, M. J., Asbjornsen, H., Kolka, R. and Tomer, M.: Native prairie filter strips reduce runoff from hillslopes under annual row-crop systems in Iowa, USA, J. Hydrol., 477, 94–103, doi:10.1016/j.jhydrol.2012.11.013, 2013.

Hoag, D., Luloff, A. E. and Osmond, D.: How Farmers and Ranchers Make Decisions on Conservation Practices, Raleigh, NC., 2012.

Hofstrand, D.: Tracking the Profitability of Corn Production, Ames, IA., 2018.

Kulik, B. and Baker, T.: Putting the organization back into computational organization theory: a complex Perrowian model of organizational action, Comput. Math. Organ. Theory, 14, 84–119, doi:10.1007/s10588-008-9022-6, 2008.

Lambert, D. M., Sullivan, P., Claassen, R. and Foreman, L.: Profiles of US farm households adopting conservation-compatible practices, Land use policy, 24(1), 72–88, doi:10.1016/j.landusepol.2005.12.002, 2007.

Larry W. Mays: Water Resources Engineering, 2nd ed., John Wiler & Songs, Inc., Hoboken, NJ., 2011.

Le, Q., Park, S. and Vlek, P.: Ecological Informatics Land Use Dynamic Simulator (LUDAS): A multi-agent system model for simulating spatio-temporal dynamics of coupled human – landscape system 2. Scenario-based application for impact assessment of land-use policies, Ecol. Inform., 5(3), 203–221, doi:10.1016/j.ecoinf.2010.02.001, 2010.

Li, Z., Liu, W. Z., Zhang, X. C. and Zheng, F. L.: Impacts of land use change and climate variability on hydrology in an agricultural catchment on the Loess Plateau of China, J. Hydrol., 377(1-2), 35–42, doi:10.1016/j.jhydrol.2009.08.007, 2009.

Marcotty, J.: High crop prices a threat to nature?, StarTribune, 11th November [online] Available from: http://www.startribune.com/high-crop-prices-threat-to-nature/134566683/, 2011.

Matthews, R.: The People and Landscape Model (PALM): Towards full integration of human decision-making and biophysical simulation models, Ecol. Model., 194, 329–343, doi:10.1016/j.ecolmodel.2005.10.032, 2006.

Mcguire, J. M., Wright, L., Arbuckle, J. G. and Cast, A. D.: Farmer identities and responses to the social-biophysical environment, J. Rural Stud., 39, 145–155, doi:10.1016/j.jrurstud.2015.03.011, 2015.

Montanari, a., Young, G., Savenije, H. H. G., Hughes, D., Wagener, T., Ren, L. L., Koutsoyiannis, D., Cudennec, C., Toth, E., Grimaldi, S., Blöschl, G., Sivapalan, M., Beven, K., Gupta, H., Hipsey, M., Schaefli, B., Arheimer, B., Boegh, E., Schymanski, S. J., Di Baldassarre, G., Yu, B., Hubert, P., Huang, Y., Schumann, a., Post, D. a., Srinivasan, V., Harman, C., Thompson, S., Rogger, M., Viglione, a., McMillan, H., Characklis, G., Pang, Z. and Belyaev, V.: "Panta Rhei—Everything Flows": Change in hydrology and society—The IAHS Scientific Decade 2013–2022, Hydrol. Sci. J., 58(6), 1256–1275, doi:10.1080/02626667.2013.809088, 2013.

Montanari, A.: Debates-Perspectives on socio-hydrology: Introduction, Water Resour. Res., 51(6), 4768–4769, doi:10.1002/2015WR017430, 2015.

Newton, J.: Change on the Horizon for the Conservation Reserve Program?, [online] Available from: https://www.fb.org/market-intel/change-on-the-horizon-for-the-conservation-reserve-program (Accessed 15 January 2018), 2017.

Ng, T. L., Eheart, J. W., Cai, X. and Braden, J. B.: An agent-based model of farmer decision-making and water quality impacts at the watershed scale under markets for carbon allowances and a second-generation biofuel crop, Water Resour. Res., 47(9), doi:10.1029/2011WR010399, 2011.

Noel, P. H. and Cai, X.: On the role of individuals in models of coupled human and natural systems : Lessons from a case study in the Republican River Basin, Environ. Model. Softw., 92, 1–16, doi:10.1016/j.envsoft.2017.02.010, 2017.

Nowak, P.: Why farmers adopt production technology, Soil Water Conserv., 47(1), 14–16, 1992.

Van Oel, P. R., Krol, M. S., Hoekstra, A. Y. and Taddei, R. R.: Feedback mechanisms between water availability and water use in a semi-arid river basin: A spatially explicit multi-agent simulation approach, in Environmental Modelling & Software, vol. 25, pp. 433–443, Elsevier Ltd., 2010.

Ormerod, P. and Rosewell, B.: Validation and Verification of Agent-Based Models in the Social Sciences, Epistemol. Asp. Comput. Simul. Soc. Sci., 5466, 130–140, doi:10.1007/978-3-642-01109-2_10, 2009.

Pahl-wostl, C. and Ebenhöh, E.: Heuristics to characterise human behaviour in agent based models., 2004.

Parker, D. C., Hessl, A. and Davis, S. C.: Complexity, land-use modeling, and the human dimension: Fundamental challenges for mapping unknown outcome spaces, Geoforum, 39(2), 789–804, doi:10.1016/j.geoforum.2007.05.005, 2008.

Parunak, H. V. D., Savit, R. and Riolo, R. L.: Multi-agent systems and agent-based simulation, Proc. First Int. Work. Multi-Agent Syst. Agent-Based Simul., 10–25, doi:10.1007/b71639, 1998.

Pfrimmer, J., Gigliotti, L., Stafford, J. and Schumann, D.: Motivations for Enrollment Into the Conservation Reserve Enhancement Program in the James River Basin of South Dakota, Hum. Dimens. Wildl., 22(4), 1–8, doi:10.1080/10871209.2017.1324069, 2017.

Plastina, A.: Current Crop Insurance Policies, Ames, IA., 2014a.

Plastina, A.: Trend-Adjusted Actual Production History (APH), Ames, IA., 2014b.

Plastina, A.: Cash Rental Rates for Iowa 2017 Survey, Ames, IA., 2017a.

Plastina, A.: Estimated Costs of Crop Production in Iowa - 2017, Ames, IA., 2017b.

Prior, J.: Landforms of Iowa, 1st ed., University of Iowa Press, Iowa City, Iowa., 1991.

Reeves, H. W. and Zellner, M. L.: Linking MODFLOW with an agent-based land-use model to support decision making., Ground Water, 48(5), 649–60, doi:10.1111/j.1745-6584.2010.00677.x, 2010.

Ryan, R. L., Erickson, D. L. and De Young, R.: Farmers' Motivation for Adopting Conservation Practices along Riparian Zones in a Mid-western Agricultural Watershed, J. Environ. Plan. Manag., 46(1), 19–37, doi:10.1080/713676702, 2003.

Saltiel, J., Bauder, J. W. and Palakovich, S.: Adoption of Sustainable Agricultural Practices: Diffusion, Farm Structure, and Profitability, Rural Sociol., 59(2), 333–349, 1994.

Savenije, H. H. G. and Van der Zaag, P.: Integrated water resources management: Concepts and issues, Phys. Chem. Earth, 33(5), 290–297, doi:10.1016/j.pce.2008.02.003, 2008.

Schaible, G. D., Mishra, A. K., Lambert, D. M. and Panterov, G.: Factors influencing environmental stewardship in U.S. agriculture: Conservation program participants vs. non-participants, Land use policy, 46, 125–141, doi:10.1016/j.landusepol.2015.01.018, 2015.

Scharffenberg, W. A.: Hydrologic Modeling System User's Manual, United State Army Corps Eng. [online] Available from: http://www.hec.usace.army.mil/software/hec-hms/documentation/HEC-HMS_Users_Manual_4.0.pdf, 2013.

Schlüter, M. and Pahl-wostl, C.: Mechanisms of Resilience in Common-pool Resource Management Systems : an Agent-based Model of Water Use in a River Basin, Ecol. Soc., 12(2) [online] Available from: http://www.ecologyandsociety.org/vol12/iss2/art4/, 2007.

Schnitkey, G.: Revenue Protection (RP) Use on Corn in the Midwest, Champaign, Il., 2017.

Schreinemachers, P. and Berger, T.: Land use decisions in developing countries and their representation in multi-agent systems, L. Use Sci., 1(1), 29–44, doi:10.1080/17474230600605202, 2006.

Schreinemachers, P. and Berger, T.: An agent-based simulation model of human–environment interactions in agricultural systems, Environ. Model. Softw., 26(7), 845–859, doi:10.1016/j.envsoft.2011.02.004, 2011.

Secchi, S. and Babcock, B. A.: Impact of High Corn Prices on Conservation Reserve Program Acreage., Iowa Ag Rev., 13(2), 4–7 [online] Available from: http://search.ebscohost.com/login.aspx?direct=true&db=eih&AN=25148415&site=ehost-live DP - EBSCOhost DB - eih, 2007.

Shreve, C. M. and Kelman, I.: Does mitigation save? Reviewing cost-benefit analyses of disaster risk reduction, Int. J. Disaster Risk Reduct., 10, 213–235, doi:10.1016/j.ijdrr.2014.08.004, 2014.

Sivapalan, M. and Blöschl, G.: Time scale interactions and the coevolution of humans and water, Water Resour. Res., 51(9), 6988–7022, doi:10.1002/2015WR017896, 2015.

Sivapalan, M., Savenije, H. H. G. and Blöschl, G.: Socio-hydrology: A new science of people and water, Hydrol. Process., 26(8), 1270–1276, doi:10.1002/hyp.8426, 2012.

Steffens, K. J. and Franz, K. J.: Late 20th-century trends in Iowa watersheds: An investigation of observed and modelled hydrologic storages and fluxes in heavily managed landscapes, Int. J. Climatol., 32(9), 1373–1391, doi:10.1002/joc.2361, 2012.

Tannura, M. A., Irwin, S. H. and Good, D. L.: Weather, Technology, and Corn and Soybean Yields in the U.S. Corn Belt. [online] Available from: http://www.farmdoc.uiuc.edu/marketing/reports, 2008.

Tesfatsion, L., Rehmann, C. R., Cardoso, D. S., Jie, Y. and Gutowski, W. J.: An agent-based platform for the study of watersheds as coupled natural and human systems, Environ. Model. Softw., 89, 40–60, doi:10.1016/j.envsoft.2016.11.021, 2017.

Tigner, R.: Partial Budgeting: A Tool to Analyze Farm Business Changes, Ames, IA., 2006.

Tomer, M. D. and Schilling, K. E.: A simple approach to distinguish land-use and climate-change effects on watershed hydrology, J. Hydrol., 376(1-2), 24–33, doi:10.1016/j.jhydrol.2009.07.029, 2009.

Troy, T., Pavao-Zuckerman, M. and Evans, T.: Debates—Perspectives on socio-hydrology: Socio-hydrologic modeling: Tradeoffs, hypothesis testing, and validation, Water Resour. Res., 51, 4806–4814, doi:10.1002/2015WR017046, 2015.

Tyndall, J. C., Schulte, L. A., Liebman, M. and Helmers, M.: Field-level financial assessment of contour prairie strips for enhancement of environmental quality, Environ. Manage., 52(3), 736–747, doi:10.1007/s00267-013-0106-9, 2013.

USDA: Conservation Reserve Program. [online] Available from: www.nrcs.usda.gov/programs/crp, 2011.

USDA-Natural Resources Conservation Service (USDA-NRCS): National Engineering Handbook, Part 630, Washington, DC., 2004.

USDA-Natural Resources Conservation Service (USDA-NRCS): Field Office Technical Guide, [online] Available from: http://www.nrcs.usda.gov/wps/portal/nrcs/main/national/technical/fotg/ (Accessed 9 April 2016), 2015.

Viglione, A., Di Baldassarre, G., Brandimarte, L., Kuil, L., Carr, G., Salinas, J. L., Scolobig, A. and Blo¨schl, G.: Insights from socio-hydrology modelling on dealing with flood risk - Roles of collective memory, risk-taking attitude and trust, J. Hydrol., 518, 71–82, doi:10.1016/j.jhydrol.2014.01.018, 2014.

Vorosmarty, C. and Sahagian, D.: Anthropogenic Disturbance of the Terrestrial Water Cycle, Bioscience, 50(9), 753–765, doi:http://dx.doi.org/10.1641/0006-3568(2000)050[0753:ADOTTW]2.0.CO;2, 2000.

Wang, D. and Hejazi, M.: Quantifying the relative contribution of the climate and direct human impacts on mean annual streamflow in the contiguous United States, Water Resour. Res., 47(9), doi:10.1029/2010WR010283, 2011.

Xiang, X., Kennedy, R. and Madey, G.: Verification and Validation of Agent-based Scientific Simulation Models, Agent-Directed Simul. Conf., 47–55 [online] Available from: http://www.nd.edu/~nom/Papers/ADS019_Xiang.pdf, 2005.

Zenobia, B., Weber, C. and Daim, T.: Artificial markets : A review and assessment of a new venue for innovation research, Technovation, 29, 338–350, doi:10.1016/j.technovation.2008.09.002, 2009.

Zhang, A., Zhang, C., Fu, G., Wang, B., Bao, Z. and Zheng, H.: Assessments of Impacts of Climate Change and Human Activities on Runoff with SWAT for the Huifa River Basin, Northeast China, Water Resour. Manag., 26(8), 2199–2217, doi:10.1007/s11269-012-0010-8, 2012.

Zhang, W.: 2017 Iowa State University Land Value Survey: Overview, Ames, IA., 2017.

Zhou, X., Helmers, M. J., Asbjornsen, H., Kolka, R. and Tomer, M. D.: Perennial Filter Strips Reduce Nitrate Levels in Soil and Shallow Groundwater after Grassland-to-Cropland Conversion, J. Environ. Qual., 39(6), 2006, doi:10.2134/jeq2010.0151, 2010.

Zhou, X., Helmers, M. J., Asbjornsen, H., Kolka, R., Tomer, M. D. and Cruse, R. M.: Nutrient removal by prairie filter strips in agricultural landscapes, J. Soil Water Conserv., 69, 54–64, doi:10.2489/jswc.69.1.54, 2014.

CHAPTER 4

PROJECTIONS OF HYDROLOGIC CHANGE IN NORTH CENTRAL IOWA UNDER HUMAN AND CLIMATE INFLUENCES

A paper to be submitted to *Hydrologic and Earth System Sciences*

David J. Dziubanski[8,9], Kristie J. Franz[8], and Andy VanLoocke[10]

Abstract

The hydrologic system has increasingly been experiencing change due to human decision making within the landscape and changing precipitation patterns due to shifting climate. Quantifying the relative impacts of these two dominant components is necessary for understanding hydrologic response and for future flood and drought planning. In this study, the impact of climate and human decision-making on streamflow, specifically focusing on changes in conservation land, is quantified for the U.S. Midwest Corn Belt under future climate scenarios through use of a social-hydrologic modeling system. This modeling system combines an agent-based model (ABM) with a simple semi-distributed hydrologic model. The hydrologic model uses the curve number method to relate land cover to hydrologic response. Agents (based on two primary types) make decisions that affect land use within the watershed. A city agent aims to reduce flooding in a downstream urban area by paying farmer agents a subsidy for

[8] Graduate Research Assistant (Dziubanski) and Associate Professor (Franz), Department of Geological and Atmospheric Sciences, Iowa State University.
[9] Primary researcher and corresponding author.
[10] Assistant Professor, Department of Agronomy, Iowa State University.

allocating land towards conservation practices that reduce runoff, similar to the U.S. Conservation Reserve Program. Farmer agents decide how much land to convert to conservation based on factors related to profits, past land use, neighbor influence, and conservation-mindedness (willingness to convert land to conservation). The model is implemented for a watershed representative of the mixed agricultural/small urban area land use found in Iowa, USA. In this region, on-farm crop yields are affected by flooding in many poorly drained depressions called "prairie potholes." The modeling system additionally includes a simple module to capture the effects of on-farm flooding to decision-making. In this study, we simulate the watershed under two future climate scenarios of temperature and precipitation and quantify the changes to peak streamflow. Under the RCP 4.5 and RCP 8.5 scenarios, conservation land increases by approximately 20-60% and 40-60%, respectively. This results in a 4% and 7% decrease in mean 95th percentile discharge relative to scenarios where conservation land is treated as constant at the historical mean. If farmers are allowed to modify their behavior through time, a 10% and 16% decrease in mean 95th percentile discharge is seen under the RCP 4.5 and 8.5 scenarios. However, overall changes to peak discharge are dominated by future changes in precipitation, with climate scenarios depicting mean 95th percentile discharge to increase by 49% for the second half of the century if conservation land is kept constant at the historical mean.

4.1 Introduction

The hydrology of many river basins across the world is changing as a result of increasing pressure from climate change and human interventions (Christensen et al., 2004; Frans et al., 2013; Naik and Jay, 2011). Human activities alter the hydrologic system through land cover and land use alterations, river channel modification, urbanization, and changes in

agricultural practices (Carpenter et al., 2011; Chelsea Nagy et al., 2012; Cruise et al., 2010; Montanari et al., 2013; Sivapalan et al., 2012; Turner and Rabalais, 2003). However, changes in the hydrologic system are not exclusively caused by human modification. In 2008, Milly et al. (2008) stated that "stationarity is dead" due to the impacts of changing climate on the hydrologic system. They argue that increasing anthropogenic change of Earth's climate is altering precipitation patterns, which is in turn affecting runoff.

Numerous studies have indicated that temperature and precipitation extremes are increasing across the United States, and are projected to further increase under climate scenarios (Gutowski et al., 2007; Karl et al., 2009; Prein et al., 2017; Wuebbles et al., 2014; Zhang et al., 2013). Villarini et al. (2013) studied the trends in precipitation across the Central U.S. by utilizing data from 447 rain gauge stations located in a region stretching from Minnesota south to Louisiana. Their findings point to an increasing trend (93 stations increasing versus 3 stations decreasing) in the frequency of heavy rainfall events, particularly over northern states (Minnesota, Iowa, Illinois). Based on observed trends in temperature data for the March-October period, they conclude that the increasing precipitation intensity may be a consequence of increasing temperatures. Other studies have shown similar findings to Villarini et al. (2013). An earlier study by Kunkel et al. (1999) examined precipitation trends across the entire U.S for the 1931-1996 period and found that the most prominent increase in frequency of 1-yr precipitation events is centered around the Northern Midwest and Great Lakes region. Groisman et al. (2012) found a 40% increase in the frequency of daily rainfall events with precipitation above 154.9 mm in a similar region of the U.S. Under future climate scenarios, the frequency of extreme precipitation over the Midwest is projected to further increase due to increasing

atmospheric temperatures (Janssen et al., 2014; Karmalkar and Bradley, 2017; Prein et al., 2017; Wuebbles et al., 2014).

The changing precipitation patterns are altering the nature of runoff and flooding across the U.S (Mallakpour and Villarini, 2015). Mallakpour and Villarini (2015) investigated the trend of magnitude and frequency of flooding for the Central U.S. using data from 774 streamflow gauges with 50 or more years of data. While only 13% of the stations indicated an increasing trend in flood magnitude, 34% showed an increasing frequency of flood events, while only 9% of stations showed a decreasing frequency. The change in flood frequency will likely increase further under climate projections for the Central U.S. Naz et al., (2016) used the Variable Infiltration Capacity (VIC) model to project changes in runoff under precipitation scenarios from models in the Coupled Model Intercomparison Project Phase 5 (CMIP5) project. Their study showed runoff from basins in the Central U.S increasing by close to 30% for the spring and summer months. Many other studies have indicated that the potential for flood risk in many regions of the U.S, particularily the East half, will only increase under changing climate (Arnell and Gosling, 2016; Milly et al., 2002).

The human system has an equally important effect on changing the hydrologic nature of watersheds. For example, Schilling et al., (2010) determined that approximately 30% of the increase in water flux observed in the Mississippi river basin over the last 100 years can be attributed to dramatic increases in soybean acreage since 1940. Since hydrologic changes arise from climate and human factors, a number of recent hydrologic studies have placed importance on trying to decipher the relative contributions of these variables on changing river discharge (Ahn and Merwade, 2014; Frans et al., 2013; Naik and Jay, 2011; Tomer and Schilling, 2009; Wang and Cai, 2010; Ye et al., 2013). These studies use a variety of techniques, such as

modeling and statistical methods (e.g. linear regression), water balance approaches, trend analysis, and Budyko analysis to determine the percentage of the recent changes in streamflow that can be attributed to human-induced changes versus climate (Ahn and Merwade, 2014). However, the extent to which humans are altering streamflow varies by region. For instance, Ahn and Merwade (2014) found that 85% of streamflow stations in Georgia indicated a significant human impact on streamflow. On the other hand, Frans et al. (2013) found climate to be a dominating factor (> 90%) in runoff change in the Upper Mississippi River Basin. Yet another study by Tomer and Schilling (2009) for the Midwest suggested that change in land use was the primary driver of streamflow change in the 1960s and 1970s, but since then, climate has been the primary driver.

Given the wide range of results from these studies, social-hydrologic models that couple these two systems may allow for a more complete analysis of how changes in precipitation coupled with human decision-making on the landscape affect streamflow (Montanari et al., 2013; Sivapalan et al., 2012). The main objective of this study is to quantify the relative contribution of changing precipitation patterns and human activities on streamflow in the Midwest Corn Belt for the 2018-2097 period using a social-hydrologic model. The modeling system used consists of a simple hydrologic model capable of simulating peak stream flows and an agent-based model (ABM) of agricultural decision-making. The ABM consists of two primary agents (farmer and city) that interact through conservation contracts similar to the United States Department of Agriculture Conservation Reserve Program (CRP). We focus on streamflow changes in a watershed located in Central Iowa, USA. This watershed is representative of many watersheds located in the Midwest, with dominant agricultural land use upstream and an urban center located downstream. Five climate simulations of temperature and

precipitation from the North American CORDEX program are used to drive the model under two primary climate scenarios: representative concentration pathways 4.5 and 8.5 (RCP 4.5, RCP 8.5 (van Vuuren et al., 2011)). The response of the system under these climate scenarios is explored for the three following decision-making scenarios: conservation land remains at the historical mean, farmer agents are allowed to change conservation land through time, but their behavior remains stationary, and farmer agents are allowed to change conservation land through time and their behavior may change through time. Lastly, the impact of on-farm flooding from excess precipitation on decision-making is investigated.

4.2 Model Methodology

4.2.1 Model Summary

The main purpose of the model is to understand hydrologic evolution of streamflow in the Midwest Corn Belt under human decision-making and future scenarios of precipitation and temperature (Figure 4.1). The model consists of several modules that simulate different components of the system. A hydrology module proceeds in hourly timesteps to capture flood discharge events, a pothole module proceeds in hourly timesteps to simulate flooding and crop death in depressions on agricultural land, an agent-based model proceeds in monthly timesteps to capture agricultural and city decision-making, a crop module proceeds in annual timesteps to simulate crop yields, and a market agent module proceeds in annual timesteps to simulate crop markets and price forecasts.

The agent-based model consists of two primary agents, a farmer agent and a city agent. The farmer agent is characterized by a conservation parameter ($Cons_{max}$), which indicates the degree to which the farmer agent is "production-minded" or "conservation-minded" (McGuire et al., 2013). $Cons_{max}$ represents the maximum fraction of land a farmer is willing to put into

conservation. A minimum value of 0.0 indicates a purely production-minded farmer that is unwilling to convert any land into conservation. A maximum value of 10% ($Cons_{max}$ = 0.10) indicates a purely conservation-minded farmer that is willing to convert up to 10% of his/her production land into conservation. A farmer agent's decision-making is further characterized by decision weights. These decision weights describe the importance of different decision-making variables that the farmer agents take into account when deciding to adjust their land use (section 4.2.6.3). Lastly, the farmer agent's land is randomly characterized by different percentages of different soil types that define the crop productivity of that farmer agent's land (section 4.2.10.2).

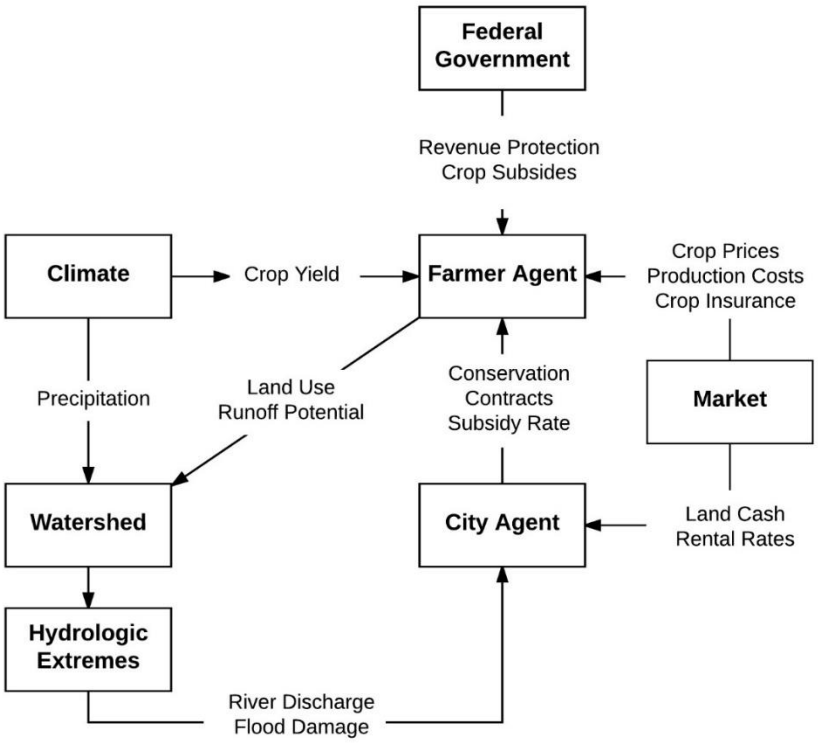

Figure 4.1. Flow of information within the coupled modeling system.

The city agent is defined by a conservation goal parameter ($ConsGoal$) that specifies that amount of new conservation land that the city agent would like to implement in order to reduce urban flooding downstream. This conservation goal varies based on the cash rental rate of agricultural land upstream (section 4.2.7).

4.2.2 Model Timeline

The agent-based model proceeds as follows. In January, the city agent determines how much land to allocate into conservation based on the previous year's flood damage (Figure 4.2). The farmer agent then calculates his/her preferred land division between production and conservation based on their conservation-mindedness, newly acquired information about the global market (crop prices, crop production costs, and crop insurance), crop subsidies provided by the city agent, as well as recent farm performance (profits and yields) (Figure 4.1).

In February, the city agent contacts farmer agents in random order to establish new conservation contracts if an unmet conservation goal remains or to renew any expiring contracts (Figure 4.2). If the farmer agent wants to add additional conservation acreage, a new contract is established. Each new contract is established for a 10 year period. However, if the farmer agent wants fewer conservation hectares, expiring contracts are renewed for a smaller number of hectares or are ended. The farmer is obligated to fulfill any contracts that have not yet expired (i.e. contracts less than 10 years old). Any new acreage that has been established in conservation in addition to currently active contracts is subtracted from the city agent's conservation goal that was established in January. The city agent contacts as many farmer agents as needed until the conservation goal is reached. If there are not enough farmer agents willing to enter into conservation contracts and the conservation goal is not reached, the goal rolls into the next year.

Because the farmer agents' land use decisions change on a yearly basis, it may be possible for the city agent to establish further contracts in the next year and fulfill the conservation goal.

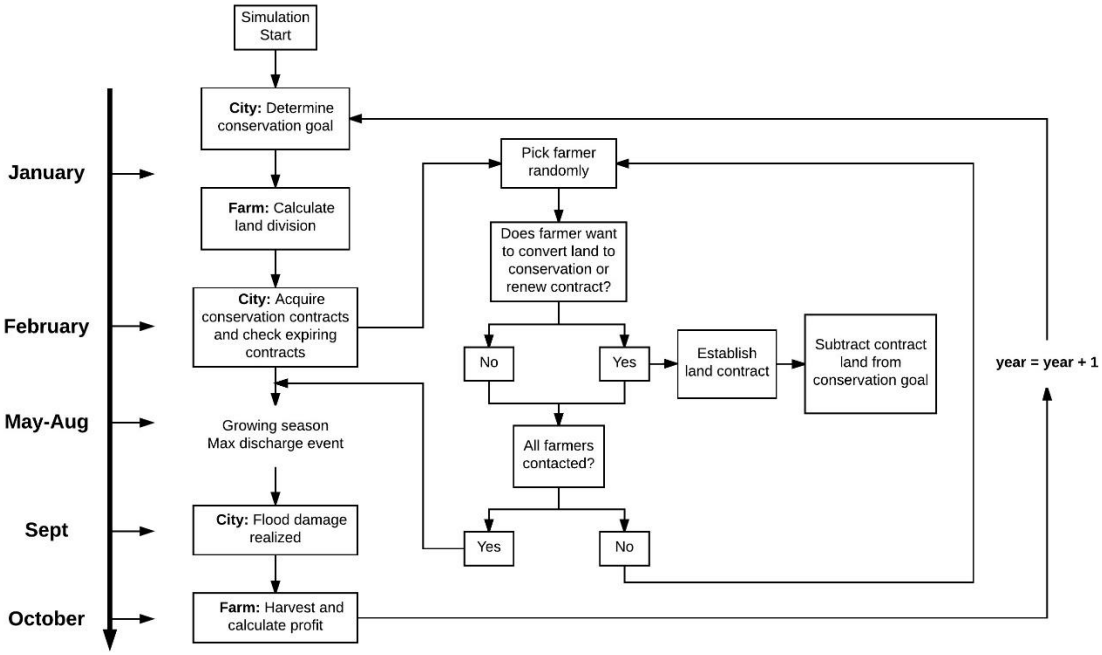

Figure 4.2. Timeline of agent decisions and actions within the coupled modeling system.

Prior to May, the farmer agent establishes any newly contracted conservation land on the historically poorest yielding land. No further decision making occurs during May through August, however, during this time, a maximum discharge event occurs. The associated flood damage cost is calculated in September and used by the city agent the following January to calculate whether any further conservation land should be added. If no flooding occurred, the conservation goal remains unchanged. In October, the farmer agent harvests his/her crop, and calculates yields and profits for that year.

4.2.3 Hydrology Module

The hydrology module is based on an application of the U.S. Army Corps of Engineers' Hydrologic Modeling System (HEC-HMS) (Scharffenberg, 2013) used by the City of Ames, Iowa for flood forecasting. The model was previously calibrated by Schmeig et al. (2011), therefore, realistic parameters were available for the watershed under study (section 4.2.10.1). The model is semi-distributed, with the capability to subdivide a watershed into multiple subbasins. The primary method used to compute runoff for each subbasin is the SCS curve number (CN) method. Runoff is subsequently computed to subbasin discharge using the SCS unit hydrograph (SCS-UH) method and routed downstream through the river channel using the Muskingum method (Mays, 2011). Each subbasin's landcover is described by a single are-weight CN. The CN value for each subbasin changes during the simulation as farm agents in the model modify their agricultural land between production and conservation. Several other model parameters are required for the subbasin discharge and routing methods. The SCS-UH method requires the user to define the subbasin area, time lag, and model timestep. The Muskingum method requires the Muskingum X and Muskingum K to be defined for each river reach, as well as the number of segments in the river reach. The hydrology module is run on an hourly timestep and is used to simulate peak flows in the system. Since the primary focus is on discharge that produces flood damage, a constant baseflow is specified for each subbasin and snowmelt is ignored. The module requires input of hourly precipitation (mm/hr), and the final output from the module is discharge at the watershed outlet ($m^3\ s^{-1}$).

CN values used in the hydrology module are based on values derived by Dziubanski *et al.*, (2017). In this study, CN values were computed using rainfall and runoff data for agricultural fields with varying percentages of native prairie strips. In the module, a CN value of

82 is used to define a 100% row crop field, a CN value of 72 is used to define the conservation practice implemented by the farmer agents (10% native prairie strips, 90% row crops), a CN of 90 is used to define urban area (based on standard lookup tables for residential areas with lot sizes of 0.051 hectares or less, soil group C, USDA-Natural Resources Conservation Service (USDA-NRCS), 2004), and a hypothetical CN of 15 was used for pothole land areas (section 4.2.4).

4.2.4 Pothole Module

Potholes in the model are described through mathematical profiles and an equation that indicates the current depth of ponding based on previous precipitation. Currently, three pothole profiles are specified in the Pothole module, named TYPE1, TYPE2, TYPE3, with profiles varying by area and depth. Each pothole profile is described by the parabolic equation:

$$y = a(x - h)^2 + k \tag{4.1}$$

where the vertex is represented by (h, k), and a is a positive coefficient that depends on the shape of the profile. The three potholes are assumed to have an area of 0.2 Ha (0.5 acres), 0.4 Ha (1 acre), and 0.8 Ha (2 acres), which equates to the potholes having a radius of 25.37 m (83.26 ft), 35.89 m (117.75 ft), and 50.75 m (166.52 ft), respectively. These area values are chosen based on recent studies that have shown the median pothole size to be 0.16 Ha, with areas ranging up to several hectares in sizes (Huang et al., 2011; Mcdeid, 2017; Wu and Lane, 2016).

Pothole TYPE1 has a depth of 0.3 m (1 ft), TYPE2 has a depth of 0.9 m (2.95 ft), and TYPE3 has a depth of 1.49 m (4.90 ft). These depths are chosen based on the range of pothole depths calculated for North Central Iowa (Upadhyay et al., 2018), and represent the shallowest, middle, and deepest potholes. The coefficient a for pothole TYPE1, TYPE2, and TYPE3 was

found to be 4.661×10^{-4} (1.419×10^{-4}), 6.987×10^{-4} (2.129×10^{-4}), 5.822×10^{-4} (1.1774×10^{-4}) for metric (imperial) units. These coefficient values correspond to a parabolic function passing through the points (25.37 m, 0.3 m), (35.89 m, 0.9 m), (50.75 m, 1.49 m).

The above pothole profiles are subsequently used to calculate the depth of flooding within each pothole throughout the growing season. For each pothole type, the depth of ponding is continuously tracked on an hourly basis based on the previous 24 hour precipitation total (mm). Depth of ponding in mm is represented by the equation (Edmonds, 2017):

$$depth\ (mm) = 0.7377 \cdot precip24hr + 125.04 \tag{4.2}$$

This depth of precipitation is input into inverse functions of the parabolic profiles to retrieve the extent of flooding within the pothole. If an area within the pothole is flooded by a minimum of a 12.7 mm (0.5 inches) for a 24 hour period or longer, complete crop death occurs. The final crop yield within the pothole area is then represented by:

$$yield_{pothole} = \left(1 - A_{flooded}\right) \cdot yield_{soil} \tag{4.3}$$

This equation represents the fraction of the normal yield that would occur if no flooding occurs. For example, if pothole TYPE1 experiences a flooding depth of 0.1 m at the center of the pothole for a 24 hr period, the full extent of flooding is $14.65\ m$ from the center and the extent of flooding $> 12.7\ mm$ is $13.68\ m$ from the center. This extent of flooding $> 12.7\ mm$ equates to 29% of the total area of the pothole. The final yield is $(0.71) \cdot yield_{soil}$.

In addition to affecting yields, the pothole area in the model affects the hydrologic response of the watershed. Each pothole in the model is assumed to be undrained (i.e. no surface tile drain inlet), thus the pothole acts like depression storage. The curve number value of

pothole land was set to 15 within the hydrology module. The low CN value assumes that the potholes may affect the runoff response through shallow interflow.

4.2.5 Crop Yield Module

Crop yields are modeled using a regression developed by Tannura *et al.*, (2008), which takes into account monthly precipitation and temperature. This regression was developed for Iowa using temperature and precipitation data from 1960-2006, and is represented as:

$$\begin{aligned} yield_t = {} & \beta_0 + \beta_1(year_t) + \beta_2(September\ through\ April\ precipitation) \\ & + \beta_3\,(May\ precipitation) + \beta_4(June\ precipitation) \\ & + \beta_5(June\ precipitation)^2 + \beta_6(July\ precipitation) \\ & + \beta_7(July\ precipitation)^2 + \beta_8(August\ precipitation) \\ & + \beta_9(August\ precipitation)^2 + \beta_{10}(May\ temperature) \\ & + \beta_{11}(June\ temperature) + \beta_{12}(July\ temperature) \\ & + \beta_{13}(August\ temperature) + \varepsilon_t \end{aligned} \tag{4.4}$$

The above regression model is only appropriate for reproducing mean historical crop yields for Iowa. Since each farmer's land can be composed of different soil types, adjustments and stochastic variability are applied to the crop yield for each soil type to account for differences in soil productivity. See Chapter 3 Section 3.7.4 for a more detailed description of these adjustments.

4.2.6 Farmer Agent Module

4.2.6.1 Conservation option

Farmer agents have the option of implementing native prairie strips on their landscape as a best management practice. Native prairie strips is a practice in which prairie vegetation is planted in strips perpendicular to the primary flow direction upland of and/or at the farm plot outlet (Dziubanski et al., 2017; Helmers et al., 2012; Zhou et al., 2010). Prairie strips reduce runoff by an average of 37% (Hernandez-Santana et al., 2013), and have additional

benefits of reducing nutrients (Zhou et al., 2014) and sediments (Helmers et al., 2012) in runoff.

4.2.6.2 Farm Agent Network

An added key function of the farmer agent module is the farmer agent network, which influences the diffusion of conservation adoption. It is well known that farmers trust their neighbors for providing reliable information about crop production (Arbuckle, 2017) and are heavily influenced by what their neighbors do (Davis and Gillespie, 2007; McGuire et al., 2013; Saltiel et al., 1994). In the farmer agent module, a probabilistic-based network is established. Each agent in a subbasin of n agents can make up to $n-1$ connections. The number of connections that an agent makes is randomly drawn from a binomial distribution (Newman et al., 2002) which describes the probability of forming k connections:

$$P(k) = \binom{n-1}{k} p^k (1-p)^{n-1-k} \qquad n \in \{0,..,n-1\} \tag{4.5}$$

where a farmer can make up to $n-1$ connections, each with the same success probability of p. Currently, p is set to 0.5 in the model, indicating a 50% probability of forming a connection with any one farmer. A second parameter that describes the farmer network is the connection strength, $ConnStrength$ (Granovetter, 1973). Once a farmer agent initiates a connection with another farmer agent, their connection strength is randomly chosen from the uniform distribution: $\mathcal{U}(0,1)$. The connection strength indicates the probability of the agents sharing their land use information during any given year. A farmer agent wanting to communicate with another farmer agent is defined by a random choice from a Bernoulli distribution with $p = ConnStrength$. If the choice of connection is a success for both farmer agents, they share information; however, if the choice of connection is a success for only one

farmer agent (i.e. one farmer agent wants to communicate with the other, but the other farmer agent does not want to communicate back), then the agents do not share information.

4.2.6.3 Farmer agent land use decision

In January of each year, a farmer agent decides how to divide his/her land between production and conservation based on five variables: conservation goal, future crop price projections, past profits, risk-aversion, and neighbor decisions from the previous year. These factors were chosen based on numerous studies indicating profits, economic incentives, conservation beliefs, neighbor connections, beliefs in traditional practices, and observable benefits to be the key factors influencing on-farm decision making related to conservation adoption (Arbuckle, 2017; Arbuckle, 2013; Burton, 2014; Daloğlu et al., 2014; Davis and Gillespie, 2007; Hoag et al., 2012; Lambert et al., 2007; Mcguire et al., 2015; Nowak, 1992; Pfrimmer et al., 2017; Ryan et al., 2003).

A farmer agent's decision of the total amount of land to be allocated into conservation, C_t , for the current year t is:

$$C_t = W_{risk-averse}[C_{t-1:t-X}] + W_{futures}[D_{t-1} + \delta C_{futures:Y}] + W_{profit}[D_{t-1} + \delta C_{profit:X}] + W_{cons}[D_{t-1} + \delta C_{cons}] + W_{neighbor}[C_{neighbor}] \quad (4.6)$$

where $C_{t-1:t-X}$ is the mean total amount of land allocated to conservation during the previous X years, D_{t-1} is the prior conservation decision (total amount of land the farmer would have liked to implement in conservation) in year $t-1$, $\delta C_{futures:Y}$ is the decision based on crop price projections for Y years into the future, $\delta C_{profit:X}$ is the decision based on the mean past profit of the previous X years, δC_{cons} is the decision based on the conservation goal of the farmer, and $C_{neighbor}$ is the weighted mean conservation land of the farmer agent's neighbors (Table 4.1, Table 4.2). Parameters X and Y represent the variation of years that farmer agent's might look

back or forward for decision making. For example, one farmer agent might consider his/her history of conservation land implemented over the last year, while another farmer agent might consider his/her conservation land implemented over the last 5 years. Similarly, one farmer agent might take into account future crop projections for the next 5 years, while another farmer agent might take into account crop projections for the next 10 years.

Decision weights alter how each of the five components factor into the farmer agent's decision: $W_{risk-averse}$ reflects the unwillingness to change past land use, $W_{futures}$ reflects the consideration of future price projections, W_{prof} reflects the consideration of past profits, W_{cons} is the agent's consideration of his/her conservation goal, and $W_{neighbor}$ reflects the importance that the agent places on his neighbor's decision. Upon initializing each farmer agent, values are allocated for each decision weight such that:

$$W_{risk-averse} + W_{futures} + W_{profit} + W_{cons} + W_{neighbor} = 1 \quad (4.7)$$

Table 4.1. Primary agent model parameters in decision-making equations.

Agent Model Parameters	Description	Range
$W_{risk\text{-}averse}$	Weight placed on farmer agent's previous land use	0.0 - 1.0
$W_{futures}$	Weight placed on farmer agent's decision based on future crop price	0.0 - 1.0
W_{profit}	Weight placed on farmer agent's decision based on past profit	0.0 - 1.0
W_{cons}	Weight place on farmer agent's decision based on his/her conservation goal	0.0 - 1.0
$W_{neighbor}$	Weight placed on farmer agent's decision based on his/her neighbor decisions	0.0 - 1.0
$Cons_{max}$	Farmer's conservation goal - used to describe the farmer's conservation-mindedness	0.0 - 0.1
X	Number of previous years a farmer agent takes into account for his/her land decision	1 - 5
Y	Number of future years a farmer agent takes into account for his/her land decision	5 - 10
$ConsGoal_{lower}$	Conservation goal at the 75th percentile of inflation-adjusted cash rent	0.0 - 0.1
$ConsGoal_{upper}$	Conservation goal at the 25th percentile of inflation-adjusted cash rent	0.0 - 0.1

The above decision scheme (equation 4.7) allows for varying decision weights. Thus, one farmer may heavily weight future crop price projections, whereas another farmer may be heavily weight past crop profits. If majority of a farmer's decision is based on $W_{risk-averse}$, then that farmer is less inclined to change his/her previous land use.

The decision components for past profit and future crop prices are based on a partial budgeting approach that compares land use alternatives. Under this budgeting approach, farmer agents take into account added and reduced income, as well as added and reduced costs from changing an acre of land from crop production to conservation (Tigner, 2006). The result from performing this budget indicates the net gain or loss in income that a farmer agent may incur if they make the land conversion. It is advised that farmers take into account long term crop price projections when deciding on land use decision.

Table 4.2. Variables in farmer agent equations.

Farmer Agent Variables	Description	Unit
$C_{t-1:t-X}$	Mean total amount of land allocated to conservation during the previous X years	Hectares
D_{t-1}	Previous year's conservation land decision	Hectares
$\delta C_{futures:Y}$	Conservation decision based on crop price projections for Y years into the future	Hectares
$\delta C_{profit:X}$	Conservation decision based on mean past profit of previous X years	Hectares
δC_{cons}	Conservation decision based on conservation goal	Hectares
$C_{neighbor}$	Weighted mean conservation land of the farmer agent's neighbors	Hectares
$Profit_{diff}$	Differences in profit between an acre of crop and an acre of conservation land	($/Hectare)
$Hectares_{tot}$	Total land owned by farmer agent	Hectares
$Profit_{crop:t}$	Profit derived from an acre of crop land in year t	($/Hectare)
$Profit_{cons:t}$	Profit derived from an acre of conservation land in year t	($/Hectare)
$CropPrice_t$	Crop price for year t	($/MT)
$Yield_t$	Average farm yield per hectare for year t	(MT/Hectare)
$ProdCost_t$	Production cost per hectare for year t	($/Hectare)
$FedSub_t$	Federal subsidy per hectare for year t	($/Hectare)
$CropIns_t$	Crop insurance per hectare for year t	($/Hectare)
$ConsSubsidy_t$	Conservation subsidy rate per hectare for year t	($/Hectare)
$Cost_{prairie:t}$	Cost of establishing and maintaining native prairie for year t	($/Hectare)
P_{upper}	Upper percentile of historical profit differences	($)
P_{middle}	Middle percentile of historical profit differences	($)
P_{lower}	Lower percentile of historical profit differences	($)
maxChange	Conservation change as a fraction of $Cons_{max}$	Dimensionless
ConnStrength	Connection strength between two farmer agents	Dimensionless

The past profits decision is solely based on outcomes that have been fully realized for the previous X years. In this decision, the land allocated to conservation is based on the net

amount of money that could have been earned per hectare of conservation land versus crop land and is calculated as:

$$\delta C_{profit:X} = \left[A \cdot Profit_{diff}{}^2 + B \cdot Profit_{diff} + C\right] \cdot Cons_{max} \cdot Hectares_{tot} \quad (4.8)$$

where $Profit_{diff}$ is the difference in profit between a hectare of cropland and a hectare of conservation land (Table 4.2), $Cons_{max}$ is the farmer agent's maximum conservation parameter, $Hectacres_{tot}$ is the area of the agent's land, and A, B, C are equation coefficients discussed later.

$Profit_{diff}$ is calculated as:

$$Profit_{diff} = \frac{1}{n}\sum_{t=t-1}^{t=t-X} Profit_{crop:t} - Profit_{cons:t} \quad (4.9)$$

where,

$$Profit_{crop:t} = (CropPrice_t \cdot Yield_t) - ProdCost_t + FedSub_t + CropIns_t \quad (4.10)$$

and,

$$Profit_{cons:t} = ConsSubsidy_t - Cost_{prairie:t} \quad (4.11)$$

$Profit_{crop:t}$ is the profit received for cropland in year t (Table 4.2), $CropPrice_t$ is the realized crop price for year t, $Yield_t$ is the farmer's realized mean yield (per hectare) for year t, $ProdCost_t$ is the crop production cost for year t, $FedSub_t$ is the amount of federal subsidies the farmer received in year t, $CropIns_t$ is the total amount of crop insurance received in year t, $Profit_{cons:t}$ is the profit received for conservation land in year t, $ConsSubsidy_t$ is the conservation subsidy established in year t, and $Cost_{prairie:t}$ is the cost associated with establishing and maintaining conservation land in year t (Chapter 2, Section 3.7).

The future crop prices decision is based on a combination of past performance information and projected future crop prices. Equations (4.8) and (4.11) are used to calculate the

land allocated to conservation based on future crop price, $\delta C_{futures}$, with equation (4.9) and (4.10) being replaced with the following:

$$Profit_{diff} = Profit_{crop:t-1} - Profit_{cons:t-1} \quad (4.12)$$

$$Profit_{crop} = (CropPrice_{t:t+Y} \cdot Yield_{t-1}) - ProdCost_{t-1} + FedSub_{t-1} + CropIns_{t-1} \quad (4.13)$$

where $Profit_{crop:t-1}$ and $Profit_{cons:t-1}$ are the profits received for cropland and conservation land in year $t-1$, and $CropPrice_{t:t+Y}$ is the projected crop price for the upcoming Y years (Table 4.2, section 4.2.8). The first term in equation (4.8) is a second-degree polynomial of form $Ax^2 + Bx + C = y$, therefore three equations need to be simultaneously solved to determine coefficients A, B, C.

δC_{profit} and $\delta C_{futures}$ can take on values between -100% to 100% depending upon whether the farmer agent observes a positive or negative $Profit_{diff}$. If the farmer agent observes a positive $Profit_{diff}$, the agent uses all historical positive $Profit_{diff}$ values from the start of the simulation through $t-1$ to solve for the coefficients using the following system of equations:

$$\begin{aligned} A(P_{upper})^2 + B(P_{upper}) + C &= -maxChange \\ A(P_{middle})^2 + B(P_{middle}) + C &= -0.5maxChange \\ A(P_{lower})^2 + B(P_{lower}) + C &= 0 \end{aligned} \quad (4.14)$$

where P_{upper}, P_{middle}, and P_{lower} are upper, middle, and lower percentiles of the historical positive $Profit_{diff}$ values (Table 4.2), respectively, and $maxChange$ is the maximum allowed change in conservation land in any given year, which is equal to 1.0 (up to 100% change possible). When $Profit_{diff}$ is positive (i.e. greater profit was earned from crop production than conservation land), the farmer agent will potentially decrease the amount of land in conservation. A similar process occurs when the farmer observes a negative $Profit_{diff}$ (i.e.

greater profit was earned from conservation land than crop production), however $+maxChange$ is associated with the equation containing P_{lower}. In this case, the farmer agent will potentially increase the amount of land in conservation.

P_{lower}, P_{upper}, and P_{middle} are a function of the farmer agent's risk aversion weight:

$$P_{lower} = 25 \cdot W_{risk-averse}$$

$$P_{upper} = 50 \cdot W_{risk-averse} + 50 \tag{4.15}$$

$$P_{middle} = 20 \cdot W_{risk-averse} + (mid - 10)$$

where,

$$mid = \frac{P_{upper} - P_{lower}}{2} + P_{lower} \tag{4.16}$$

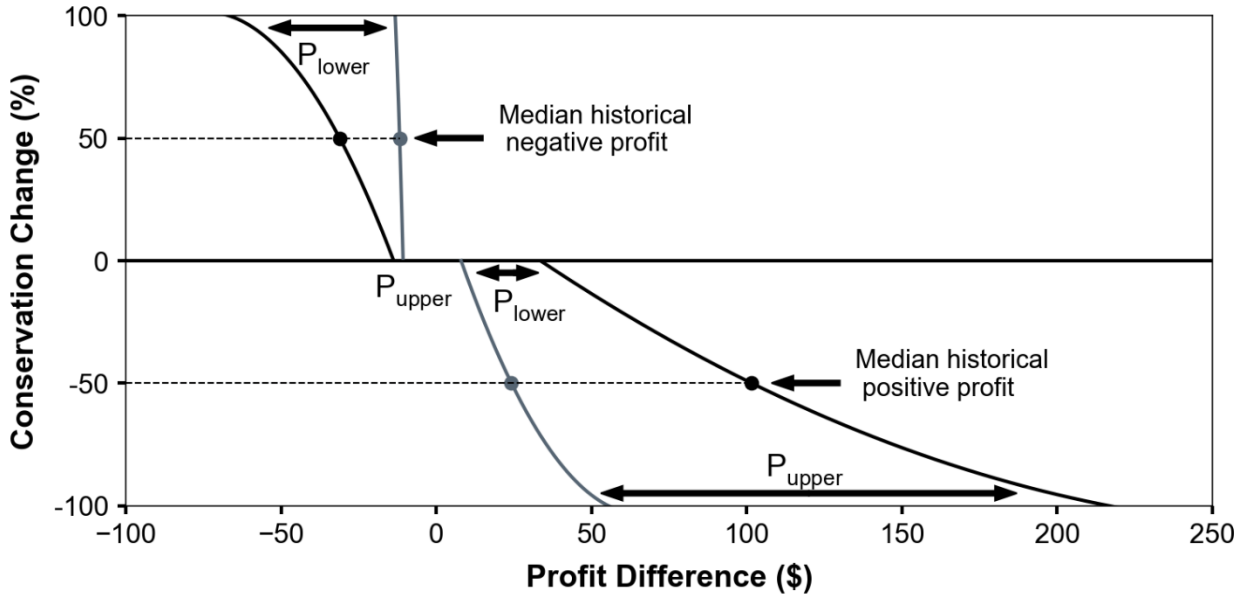

Figure 4.3. Example of percent conservation change for δC_{profit} and $\delta C_{futures}$. Gray curves indicate a farmer agent with a risk aversion weight of 0 (non-risk averse), and black curves indicate a farmer agent with a risk aversion weight of 1 (very risk averse).

The system in equation 4.14 is illustrated in Figure 4.3. Half of the maximum allowable percent increase in conservation land ($+0.5maxChange$) is assumed to correspond to the P_{middle} percentile of negative $Profit_{diff}$, whereas half of the maximum allowable percent

decrease in conservation land ($-0.5maxChange$) corresponds to the P_{middle} percentile of historical positive $Profit_{diff}$ (Figure 4.3). P_{lower}, P_{upper}, and P_{middle} change as a farmer is assigned a higher risk-aversion weight. When $W_{risk-averse}$ = 0.0, a farmer will begin to decrease his/her conservation land starting at the minimum $Profit_{diff}$ value in their positive $Profit_{diff}$ history. This farmer will decrease conservation land by 100% at the 50th percentile of positive $Profit_{diff}$ history. When $W_{risk-averse}$ = 1.0, a farmer will begin to decrease his/her conservation land at the 25th percentile of positive $Profit_{diff}$ history and will decrease by 100% at the maximum positive $Profit_{diff}$ value in their history. A similar procedure occurs when $Profit_{diff}$ is negative, except that conservation land is increased.

4.2.6.4 Conservation Decision Variable

The total amount of agricultural land that a farmer converts to conservation in any given year is defined by the Bernoulli distribution:

$$P(n) = p^n(1-p)^{1-n} \qquad n \in \{0,1\} \tag{4.17}$$

Here, p indicates the probability of fully implementing conservation land and $1-p$ indicates the probability of not implementing any conservation land. The variable n is simply the support of the distribution that labels a success of full implementation as 1 and a failure of full implementation as 0. The probability p of fully implementing conservation land is a function of the agent's $Cons_{max}$ parameter and is computed by:

$$p = 10 \cdot Cons_{max} \tag{4.18}$$

The probability p scales from 0 at a $Cons_{max}$ of 0, to 1 at a $Cons_{max}$ of 0.1. Therefore, farmer agents with a $Cons_{max}$ of 0.05 and 0.1 will have a 50% and 100% probability of fully

implementing (10% of total agricultural land) conservation land in any given year based on their conservation decision variable.

4.2.7 City Agent Module

At the end of each year, the city agent calculates flood damage based on the maximum discharge event for the year. Flood damages are calculated using a flood damage function defined by Tesfatsion et al. (2017):

$$FDam = \frac{FDmax}{1 + \exp[-(\text{discharge} - \text{Q50})/dQ)]} \tag{4.19}$$

where $FDam$ is the total flood damage in dollars ($) (Table 4.3), $FDmax$ is the maximum flood damage that can be incurred in dollars ($), Q50 is the flow at which damage is 50% of the maximum, and dQ is the width of the transition of the flood damage curve. $Q50$ is defined as:

$$Q50 = \frac{Q_{min} + Q_{max}}{2.0} \tag{4.20}$$

where Q_{min} is the flow at which damage is 1% of the maximum damage and Q_{max} is the flow at which damage is 99% of the maximum damage. Q_{min} is set to 229.45 m^3/s and Q_{max} is set to 501.43 m^3/s based on the 10 year flood stage and 100 year flood stage calculated from simulated discharge (section 4.4) created using historically observed precipitation as input and current land use conditions for the study site. Maximum damage is set to $50 000 000 based on estimates of flood damage during the 2010 Ames, IA flood. dQ specifies how rapidly flood damages accrue from minor flood stage to maximum flood stage (Tesfatsion et al., 2017):

$$dQ = \frac{Q_{max} - Q_{min}}{9.2} \tag{4.21}$$

The flood damage for the previous year $t - 1$ is used to compute the conservation goal of the city agent for the current year t.

Each year, the city agent calculates a new conservation goal based on flood damage that occurs during the previous year. The conservation goal of the city agent is calculated as:

$$G_t = G_{t-1} + (A_{tot} - C_{tot}) \cdot P \tag{4.22}$$

$$P = P_{new} \cdot FDam \tag{4.23}$$

$$P_{new} = \frac{ConsGoal}{FDmax} \tag{4.24}$$

where G_t is the conservation goal for the new year t, G_{t-1} is the unfulfilled hectares in conservation from the previous conservation goal for year $t-1$, A_{tot} is the total land area in the catchment, C_{tot} is the total number of hectares currently in conservation, P is the percentage of new production land added into conservation, P_{new} indicates how much land to add into conservation based on the flood damage $FDam$ for year $t-1$, and $ConsGoal$ is a function that indicates the new percentage of conservation land to be added if maximum flood damage occurs. It is assumed that the city agent's conservation goal at maximum flood damage fluctuates based on cash rental rates. When cash rental rates are low (25th percentile of inflation-adjusted cash rental rates), the city agent's conservation goal is assumed to be high due to cheap land prices. On the other hand, when cash rental rates are high (75th percentile of inflation-adjusted cash rental rates), the city agent's conservation goal is assumed to be low due to expensive land. The change in conservation goal varies between parameters $ConsGoal_{lower}$ and $ConsGoal_{upper}$ (Table 4.1).

The city agent's conservation goal at maximum flood damage during year t is then represented by a linear function of the current year's cash rental rate:

$$ConsGoal = m(CashRent_t) + b \tag{4.25}$$

where m represents the rate of change of conservation goal per unit change in inflation-adjusted historical cash rent (i.e. cash rental rates from the start of the simulation to year $t-1$, adjusted for inflation to the current year t):

$$m = \frac{ConsGoal_{upper} - ConsGoal_{lower}}{CashRent_{IA_{lower}} - CashRent_{IA_{upper}}} \tag{4.26}$$

And the intercept b is represented by:

$$b = ConsGoal_{lower} - \frac{ConsGoal_{upper} - ConsGoal_{lower}}{CashRent_{IA_{lower}} - CashRent_{IA_{upper}}} \cdot CashRent_{IA_{upper}} \tag{4.27}$$

$CashRent\_IA_{lower}$ is the 25th percentile of inflation-adjusted cash rents, $CashRent\_IA_{upper}$ is the 75th percentile of inflation-adjusted cash rent, and $CashRent_t$ is the cash rent of the current year t (Table 4.3). Adjusting historical cash rental rates for inflation to the current year t is performed using the Bureau of Labor Statistics Consumer Price Index. As an example, cash rental rates for year $t-10$ are adjusted using the equation:

$$CashRent_{IA_{t-10}} = CashRent_{t-10} \cdot \frac{CPI_t}{CPI_{t-10}} \tag{4.28}$$

Table 4.3. Variables in city agent equations.

City Agent Variables	Description	Unit
FDam	Current year's flood damage	($)
FDmax	Maximum attainable flood damage	($)
Q50	Discharge at with flood damage if 50% of maximum	(m^3/s)
Q_{min}	Discharge at with flood damage if 1% of maximum	(m^3/s)
Q_{max}	Discharge at with flood damage if 99% of maximum	(m^3/s)
dQ	Width of transition of flood damage curve	(m^3/s)
G_t	Government agent conservation goal for the current year t	Hectares
G_{t-1}	Unfullfilled conservation land from the previous year's t-1 conservation goal	Hectares
A_{tot}	Total land in watershed	Hectares
C_{tot}	Total land currently in conservation	Hectares
P	Total conservation land to be added to the goal as a percentage of production land	Dimensionless
P_{new}	Variable describing change in conservation goal with flood damage	(1/$)
ConsGoal	Conservation goal at maximum flood damage	Dimensionless
$CashRent_t$	Cash rent during the current year t	($/Ha)
$CashRent\_IA_{lower}$	25th percentile of inflation-adjusted cash rents	($/Ha)
$CashRent\_IA_{upper}$	75th percentile of inflation-adjusted cash rent	($/Ha)
CPI_t	Consumer price index for year t	Dimensionless

4.2.8 Market Agent Module

The primary purpose of the market agent is to provide forecasts of crop prices at the start (February) of each year and realized crop prices at the end (October) of each year when farmer agents harvest their crop. Each farmer agent receives yearly forecasts of future crop prices that predict crop prices for 10 years into the future (i.e. year t to year $t + 10$). The market agent formulates a forecast based on historical crop prices and error estimates of U.S Department of Agriculture (USDA) crop price forecasts.

Twelve years of USDA crop price forecasts for 2001-2012 were analyzed against realized crop prices to form error functions for use by the Market agent. For each 10-year forecast, errors were calculated between the historical crop prices and the forecasted crop prices. As an example, the 2005 forecast predicted crop prices for the 2004/2005 – 2014/2015 marketing years. Actual crop prices from each year in the 2005-2015 range were used to calculate an error for each year in the 2005 forecast. Through marketing year 2009/2010, errors were generally in the -$1/Bu to -$2/Bu range (-$39.3/MT to -$78.7/MT) with errors reaching a peak of -$4.44/Bu (-$174.5/MT) for 2012/2013 when crop prices were high. A multiple linear regression was performed between crop price magnitude, time from forecast year, and error to see if any variables could explain the pattern in errors found. In general, crop price magnitude explained most of the error pattern seen for each forecast, with error showing little correspondence with time from forecast year. When the starting crop price was low prior to 2007 (i.e. crop price at the beginning of the forecast), the USDA forecasts underestimated crop prices by as much as 50-60% when crop prices were high several years later (Figure 4.4). However, when starting crop prices were higher after 2007, the USDA forecasts underestimated

high crop prices by 20-40%. From $2/Bu – $7/Bu ($78.7/MT – $275.1/MT), errors change from approximately +30% to -40%. The error for each forecast was modeled as:

$$Error_{CropPrice} = A \cdot Price^2 + B \cdot Price + C \tag{4.29}$$

where A, B, C are coefficients from the regression. For each year from 2001-2011, the Pearson's r value was 0.9 or higher except for 2012, which had a Pearson's r of 0.71. This is indicative of a strong relationship between price and error. In the market agent, each of the 12 error equations for the 12 price forecasts are used (Figure 4.4).

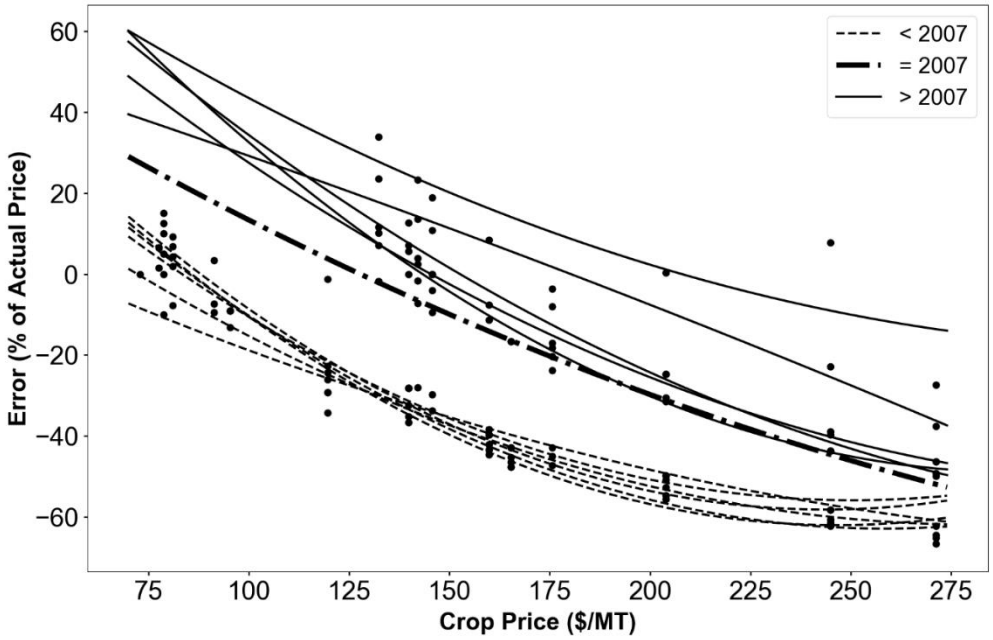

Figure 4.4. Relationships between crop price and error used in the Market Agent module. Fine dotted curves indicate errors for forecasts prior to 2007, while solid curves indicate errors for forecasts after 2007.

The error equation with a starting crop price closest to the current year's crop price is used by the market agent to formulate a 10-year forecast based on historical crop prices. The 10-year forecast is developed using the following equation:

$$CropPriceForecast_{t+n} = CropPrice_{t+n} + \left(\frac{Error_{CropPrice}}{100} \cdot CropPrice_{t+n}\right) \tag{4.30}$$

where $CropPriceForecast_{t+n}$ is the forecasted crop price for year $t+n$ (t is the current year), $CropPrice_{t+n}$ is the historical crop price for year $t+n$, and $Error_{CropPrice}$ is the error based on $CropPrice_{t+n}$.

4.2.9 Model Stochasticity

Adjustments and stochastic variability are added to select agricultural variables, which include crop yields, production costs, cash rent values, and opportunity costs associated with conservation land to account for economic and environmental randomness within the system. Random factors for these variables are drawn from uniform continuous distributions that are based on field data of crop yields, empirical survey data, and estimates published by Iowa State University Extension and Outreach. Changes in these distributions are also accounted for, depending on crop price levels. See chapter 3, section 3.7, for a more detailed description of these adjustments.

4.2.10 Model Initialization

4.2.10.1 Study Site and Hydrology Model Initialization

The study site is modeled after the Squaw Creek watershed located in Central Iowa, USA. The Squaw Creek watershed is located within the Des Moines lobe, which is characterized by relatively flat and hummocky topography as well as poorly drained soils with high silt and clay content (30-40% silt and clay) (Prior, 1991; USDA-Natural Resources Conservation Service (USDA-NRCS), 2015). One dominating feature which defines this region is the numerous prairie pothole depressions that periodically flood, particularly during heavier rainfall during the month of May and June (Miller et al., 2009). Approximately 70% of the watershed is in row crop agriculture, with one major urban center (Ames, IA) at the outlet of the watershed, and several small communities upstream. The watershed is represented through 14

subbasins in the hydrology module, and hydrologic parameters for the runoff and routing functions are taken from Schmeig et al. (2011).

4.2.10.2 Agent Model Initialization

At the start of each model simulation, the number of agents, and the location and landscape characteristics of each agent are initialized. A total of 100 farmer agents are implemented in the model. Based on 14 subbasins total, approximately 7 farmer agents are allocated to each subbasin. Each farmer agent manages approximately 121.4 hectares of agricultural land. It is assumed that the location of the city agent is at the outlet of the watershed (i.e. the most downstream subbasin). After the location is defined, each farmer agent's agricultural land is randomly assigned up to 8 different soil types common to Central Iowa. The percentage of each soil type is chosen from a uniform distribution, with the constraint that each soil type must encompass at least 0.1 Ha. This constraint was placed so that certain soil types don't encompass unusually small areas of land.

After defining each farmer agent's agricultural land, the farmer agent decision-making parameters are chosen based on a series of distributions defining these characteristics. First, each farmer agent's $Cons_{max}$ parameter, which defines the "conservation-mindedness" of that farmer agent, is randomly chosen from the Gaussian distribution $\mathcal{N}(0.06,\ \mathcal{U}(0.005, 0.015))$. The mean was determined through model calibration as described in section 4.3. Currently, the standard deviation of $Cons_{max}$ is unknown. Thus, a random value is chosen from the uniform distribution $\mathcal{U}(0.005, 0.015)$ to represent the standard deviation. All farmer agents in a simulation have their $Cons_{max}$ parameter initialized using the same standard deviation. If specific survey data of farmers is available, these parameters can be changed within the model input file.

Second, the farmer agent decision weights and parameters X and Y are initialized. The farmer decision weights are initialized from the Gaussian distribution $\mathcal{N}(\mathcal{U}(x_1,\ x_2),\ \mathcal{U}(0.005, 0.015))$. Currently, data is not available to characterize the possible mean value of each decision weight. Through model calibration (section 4.3), the possible upper and lower bound of each decision weight was determined and assigned to $(x_1,\ x_2)$. As before, the standard deviation is represented by a uniform distribution with arbitrarily chosen bounds to capture a range of possible decision weights. For each simulation, a random set of mean decision weights is generated from $\mathcal{U}(x_1,\ x_2)$ such that the decision weights sum to 1. In addition, a standard deviation is chosen from $\mathcal{U}(0.005, 0.015)$ to represent the possible spread of each weight. Each farmer agent then has his/her decision weights initialized based on the set of mean decision weights and the standard deviation. If data is available, mean and standard deviation values can be input into the model input file. The parameters X and Y are initialized from uniform distributions $\mathcal{U}(1, 5)$ and $\mathcal{U}(5, 10)$, respectively. It is assumed that farmer agents may consider up to the last 5 years of past profit information. Since future crop price forecasts are 10 years in length, it is assumed that farmers may consider the forecast out to between 5 and 10 years.

Lastly, each farmer agent's decision curves for the past profit and future price variables are established. As discussed in section 4.2.6.3, the lower and upper percentiles defining the decision curves are dependent on the risk aversion weight of each farmer agent. Once these lower and upper percentiles are established based on equation 4.15, stochasticity is added to these percentiles to obtain the final percentiles that will characterize each farmer agent's decision-making space for the profit variables. The stochastic variability is drawn from the

uniform distribution $\mathcal{U}(-0.1, 0.1)$, which represents a possible change of ±10% for the lower and upper percentiles.

4.2.10.3 Pothole Initialization

Each farmer agent's land is randomly characterized by up to 10% pothole land. Thus, a farmer agent can have a maximum of 15 TYPE3 or up to 60 TYPE1 pothole depressions within the landscape. The total hectares allocated to pothole land is randomly chosen from the uniform distribution $\mathcal{U}(0\ Ha, 12.14\ Ha)$. The upper value 12.14 Ha is based on each farmer agent having a total of 121.4 Ha of agricultural land. A random number of TYPE1, TYPE2, andTYPE3 potholes may characterize the total pothole acreage. Thus, one farmer agent may have just 2 TYPE1 potholes whereas another farmer may have 10 TYPE1 potholes even though both farmer agent have the same number of pothole acres.

4.2.11 Model Input

4.2.11.1 Economic Data

The agent-based model requires economic inputs of historical crop prices ($/MT), crop production costs ($/Ha), cash rental rates ($/Ha), and federal government subsidy estimates ($/Ha). Historical economic data from the years 1970-2016 is used to drive the agent-based model. Federal crop subsidies are based on 16 years of historical estimates (2000-2016) (Hofstrand, 2018). Crop subsidies from 1970-2000 are based off crop subsidies during 2000-2005 and are assumed to have existed during the entire simulation time period. All economic data was obtained from Iowa State University Agricultural Extension and Illinois FarmDoc.

4.2.11.2 Climate Data

Climate simulations of precipitation and temperature from the North American Coordinated Regional Climate Downscaling Experiment (NA-CORDEX) are used to simulate the model into the future (Mearns et al., 2013). Data was obtained through the National Center for Atmospheric Research climate data gateway and the Earth System Grid Foundation. Precipitation is on an hourly timestep and is used to drive the hydrology and the crop modules. Mean daily temperature is on a daily time step and is used in the crop module. Functions in the model automatically compute the monthly mean temperatures and monthly precipitation for crop yield estimates.

Table 4.4. Climate simulations used for driving the coupled modeling system.

Global Climate Model (GCM)	Regional Climate Model (RCM)	Spatial Resolution	Scenario	Abbreviation
CanESM2	CanRCM4	0.44°	rcp4.5	CanESM2.44.rcp4.5
CanESM2	CanRCM4	0.44°	rcp8.5	CanESM2.44.rcp8.5
HadGEM2-ES	WRF	0.22°	rcp8.5	HadGEM2.22.rcp8.5
MPI-ESM-LR	RegCM4	0.22°	rcp8.5	MPI.22.rcp8.5
MPI-ESM-LR	RegCM4	0.44°	rcp8.5	MPI.44.rcp8.5

Five climate simulations are used, with varying combinations of global and regional models, as well as grid spacing and scenarios (Table 4.4). One climate simulation (CanESM2.CanRCM4) was available for the RCP4.5 scenario, while four climate simulations were available for the RCP8.5 scenario (van Vuuren et al., 2011). Each climate simulation was bias corrected using KDDM (kernel density distribution mapping) (Mcginnis et al., 2015). The KDDM technique calculates the probability distribution function (PDF) for each dataset, then uses trapezoidal integration to convert the PDFs to the corresponding cumulative distribution functions (CDF). With this technique, the historical climate simulations (1950-2005) are bias corrected using historical data. That correction is then applied to the future climate simulations

(2006-2100). Hourly simulations of precipitation were bias corrected using hourly stage IV precipitation data (2002-2016). Temperature simulations were bias corrected using daily mean temperatures (2000-2015). Daily mean temperatures were computed using hourly temperature data obtained from the Ames, Iowa Automated Surface Observing System (ASOS). Each climate simulation is abbreviated as shown is table 4.4.

4.3 Calibration

An indirect calibration approach was taken for model development and determining an appropriate range of model parameters (Windrum et al., 2007). Since the subsidy program offered by the city agent is similar to the federal Conservation Reserve Program (CRP), the model was developed and calibrated to reproduce the range and variability of conservation land seen in the CRP program. CRP data from 1986-2016 for Central Iowa Agricultural District was used in the calibration process and two main objectives functions were used:

$$MAE = \frac{\sum_{i=1}^{n} |y_i - x_i|}{n} \tag{4.31}$$

$$Pearson's\ r = \frac{\sum_{i=1}^{n}(x_i - \bar{x})(y_i - \bar{y})}{\sqrt{\sum_{i=1}^{n}(x_i - \bar{x})^2}\sqrt{\sum_{i=1}^{n}(y_i - \bar{y})^2}} \tag{4.32}$$

In the first step of calibration, 360 simulations using 20 random sets of farmer agent decision weights were used to determine the appropriate mean $ConsMax$ of the farmer agent population. In this step, the focus was on matching the magnitude of CRP land seen for Central Iowa using the MAE function. The mean $ConsMax$ of the farmer population was incrementally shifted by 0.01 from 0.01-0.09, with 2 simulations for each of the 20 random set of farmer weights performed for each $ConsMax$ level. Output from the first calibration step was filtered using a criteria of $r > 0.6$ and $MAE < 25\%$ of total observed conservation land, and the

$ConsMax$ of the filtered simulations was analyzed. $ConsMax$ was reduced to the 0.05-0.07 range after the first calibration step.

In the second calibration step, $ConsMax$ was incremented by 0.001, and 20 simulations were performed for each increment with decision weights stochastically drawn from the uniform distribution $\mathcal{U}(0.05, 0.95)$ using a pseudo-random number generator such that the decision weights summed to 1. Output from the second step was filtered using a criteria of $r >$ 0.7 and $MAE < 25\%$ of total observed conservation land. The range of decision weights was reduced based on the min and max values of the decision weights in the filtered output.

The third and final calibration step involved 400 simulations with stochastic sampling from the reduced range of decision weights a filtering using a criteria of $r > 0.75$ and $MAE <$ 15%.

4.4 Scenario Analysis

Scenarios using future simulations of temperature and precipitation with historical economic variables are compared against simulations of historical climate. Eight sets of simulations are conducted for each climate simulation. In the first set of two simulations, farmer decision-making is turned on, but the conservation land for each farmer agent is constrained by their $ConsMax$ parameter. These simulations (abbreviated as "constrained") utilize 1970-2016 historical economic data but are based on temperature and precipitation for the 2018-2065 and the 2050-2097 periods, respectively. In the second set of simulations (abbreviated as "unconstrained"), the $ConsMax$ parameter of each farmer agent is allowed to change through time if $D_{t-1} > Cons_{max} \cdot Hectares_{tot}$ (i.e. the conservation decision is greater than the current maximum fraction of land a farmer is willing to put into conservation). In the third set of simulations (abbreviated as "constant"), farmer decision-making is turned off. Conservation

land is kept at the mean observed conservation land for the 2006-2016 period. In the last set of simulations (abbreviated as "constrained - nonpothole"), farmer decision-making is turned on, but pothole flooding is turned off to determine the effect of on-farm flooding on farmer decision-making. All sets of simulations utilize the same economic and environmental data as the first two simulations.

4.5 Results

4.5.1 Calibration

The optimal mean $ConsMax$ value was determined to be 0.06 and the final optimal decision weight ranges were determined to be: $W_{risk-averse} = (0.1, 0.43)$, $W_{futures} = (0.07, 0.24)$, $W_{profit} = (0.07, 0.34)$, $W_{cons} = (0.18, 0.37)$, $W_{neighbor} = (0.05, 0.35)$. The median r and MAE values of the simulations after filtering with the criteria in step three ($r > 0.75, MAE < 15\%$) were 0.79 and 11% respectively. Sixty-six simulations matched these criteria in step three, whereas only seven matched these criteria in step one and 26 matched these criteria in step two. A sample of four model simulations are plotted against observed conservation land in figure 4.5. The model simulated conservation land generally aligns with trends in the observed conservation land (Figure 4.5). Simulated conservation land is not maintained following a rise in crop prices in the mid-1990s and from 2006-2013, which is similar to the observed data (red). The drop in conservation land during these time periods occurs because the subsidy rate is not modified rapidly enough in comparison to market forces to incentivize the farmer (Newton, 2017). In 2008 and 2011, corn prices rose to a record high values, and farmer in the Midwest U.S. (e.g., Iowa, Minnesota) were converting significant portions of CRP land back into crop production (Marcotty, 2011; Secchi and Babcock, 2007). It is estimated that when corn prices rise by $1.00, 10-15% of CRP land in Iowa is converted back

to production (Secchi and Babcock, 2007). The model does capture the smaller decrease in conservation land between 2007-2014, even though crop prices rose more dramatically than in the mid-1990s. Simulated conservation land also decreases and then rises at a similar rate around the time that the CRP program was implemented (1985).

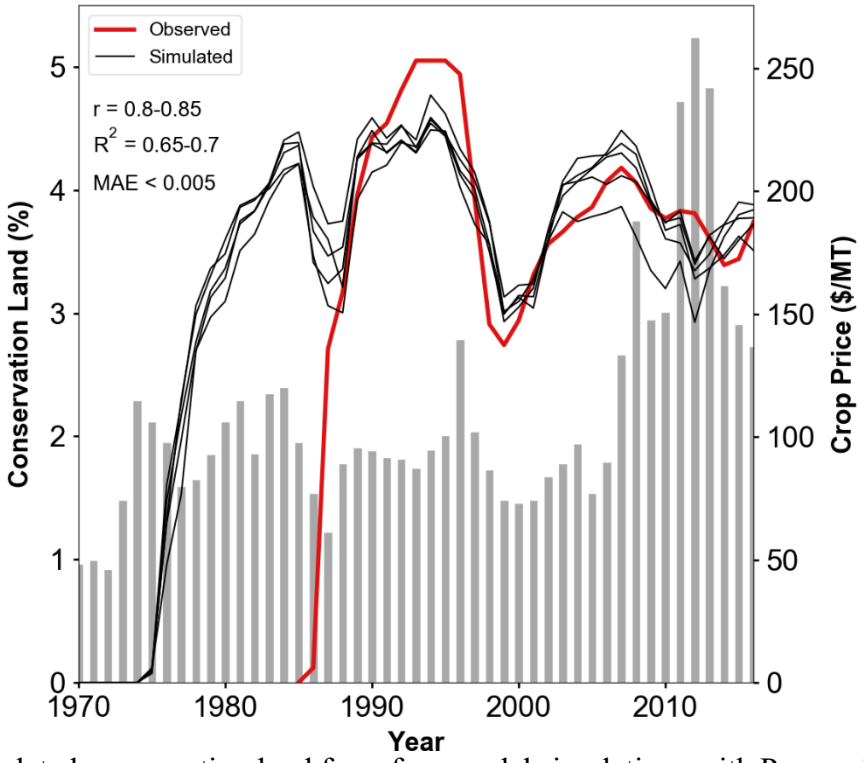

Figure 4.5. Simulated conservation land from four model simulations with Pearson's r > 0.8 and MAE < 0.005 in comparison to observed conservation land.

4.5.2 Peak Discharge Analysis

When farmer agents are allowed to modify their land but are constrained by their $ConsMax$ parameter (constrained scenario), mean 95th percentile discharge decreases on average by 6.5% relative to the constant scenario (conservation land is kept at the 2006-2016 mean) (Figure 4.6, red). This 6.5% decrease from the constant scenario corresponds to the approximately 40-50% increase in conservation land from the historical mean (Figure 4.7). Under almost all climate simulations, particularly during 2050-2097, farmer agents are

implementing the maximum conservation land that their $ConsMax$ parameter allows (6% of total agricultural land in the watershed). The historical mean 2006-2016 conservation land was 3.7%, or approximately 450 Ha in terms of the total agricultural land in the model (12000 Ha). Farmer agents implement approximately 700 Ha under the constrained scenario, which equates to 5.8% of total agricultural land.

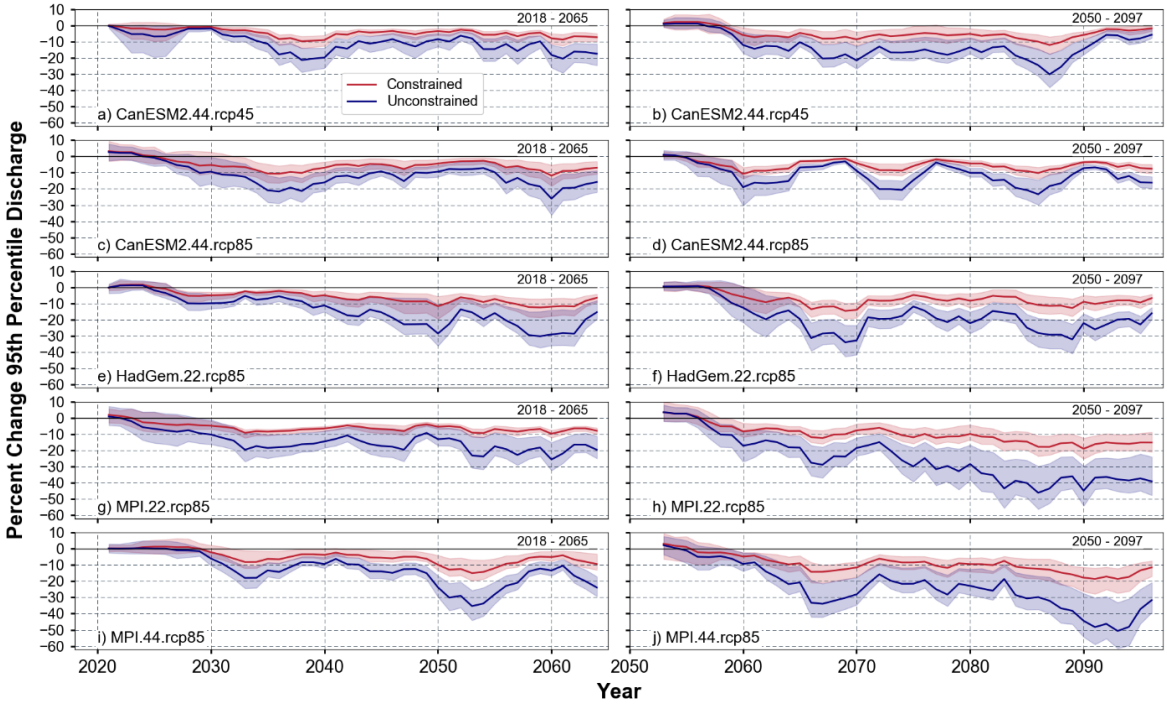

Figure 4.6. Percent change in 95th percentile discharge for the constrained (red) and unconstrained (blue) scenarios relative to the constant scenario for 2018-2065 (column 1) and 2050-2097 (column 2).

In general, a large difference between the RCP4.5 and RCP8.5 is not realized under the constrained scenario. The CanESM2.44.rcp45 simulation displays at most a 10% decrease in the peak discharge between the constrained and constant scenarios (Figure 4.6 a,b). This percent change is similar to CanESM2 simulations under the RCP8.5 trajectory. Farmer agents implement a similar amount of total conservation land under RCP4.5 and RCP8.5 for the CanESM2 simulations (Figure 4.7a-d). The only model simulations that differ more significantly from the RCP4.5 trajectory are the MPI.22.rcp85 and MPI.44.rcp85 simulations

(Figure 4.6g-j). These simulations show up to a 20% decrease from the constant scenario during the later half of the century (2050 - 2097). This change in peak discharge is a result of a more consistent 40-60% increase in conservation land implemented by farmer agents (Figure 4.7h, j).

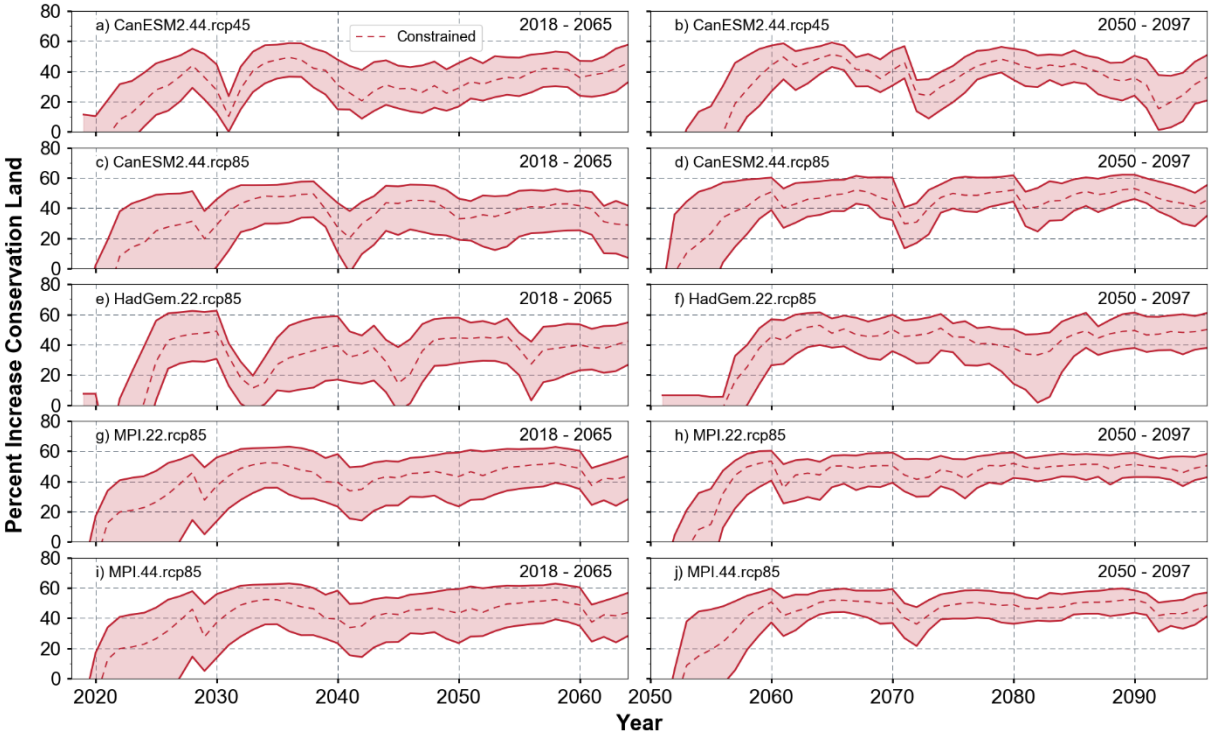

Figure 4.7. Percent increase in conservation land for the constrained scenario relative to the constant scenario for 2018-2065 (column 1) and 2050-2097 (column 2).

In terms of changes between the 2018-2065 and 2050-2097 periods, only a slightly larger decrease in the mean 95th percentile discharge is evident during 2050-2097 for the constrained scenario, particularly for the MPI simulations (Figure 4.6h,j). Model simulations for 2018-2065 do show more variability in conservation land. This variability is generally in line with changes in crop prices. During the second half of the century, variability in conservation land does occur, but changes are not as well pronounced. A good example of this result occurs under the HadGem simulation. Farmer agents decrease conservation land during the 2030-2035 period from 50% to 10%, but the same decrease is not present around 2062 even though the

economics (i.e. crop prices, production costs, etc.) are identical (Section 4.4) for those years (Figure 4.7e,f). The decrease in variability does result in minor differences, with HadGem showing a 5-10% decrease in peak discharge for 2060-2070 versus a 0-5% decrease for 2030-2040 (Figure 4.6e,f).

When farmer agents are allowed to modify their land, but are not constrained by their $ConsMax$ parameter (unconstrained scenario), mean 95th percentile discharge decreases by 16% on average relative to the constant scenario (Figure 4.6, blue). Under this scenario, farmers increase conservation land by 80-120% relative to the 2000-2016 mean (Figure 4.8, blue). Farmer agents transition from a mean $ConsMax$ parameter of 0.06 to a mean $ConsMax$ parameter of 0.067-0.09. Thus, these farmers would never actually reach the upper limit of the $ConsMax$ parameter (0.1).

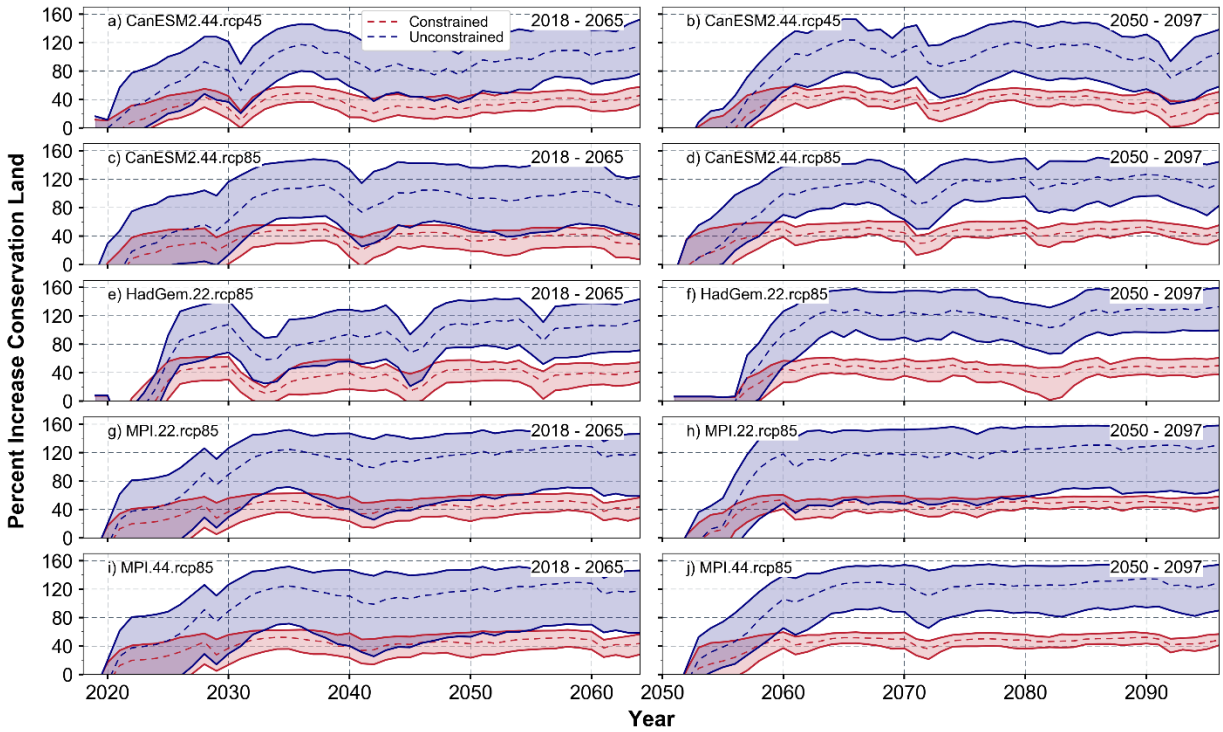

Figure 4.8. Percent change in conservation land for the constrained (red) and unconstrained (blue) scenarios relative to the constant scenario for 2018-2065 (column 1) and 2050-2097 (column 2).

Under the RCP8.5 trajectory, the unconstrained scenario indicates a greater decrease in peak discharge relative to the RCP4.5 trajectory. The CanESM2 simulations suggest that mean peak discharge would decrease by approximately 20% relative to the constant scenario, regardless of the climate trajectory (4.5 or 8.5). However, when comparing the HadGem or MPI simulations against CanESM2.44.rcp4.5, particularly for the 2050-2097 period, mean 95th percentile discharge decreases by 10-30% more than under RCP4.5 (Figure 4.6f, h, j). Overall, more variability in conservation land is present under RCP4.5, with conservation land decreasing to 80% during certain periods (i.e. 2072 and 2092) (Figure 4.8b). This variability is not as pronounced under RCP 8.5. (Figure 4.8, f, h, j).

4.5.3 Climate and Human Impact Analysis

Comparing changes in the mean 95th percentile discharge for the constant and unconstrained scenarios against the historical (1970-2016), mean 95th percentile discharge reveals that the watershed transitions to an overall wetter flow regime starting around 2050 (Figure 4.9), particularly under the RCP8.5 trajectory. If conservation land is kept constant at the historical mean, mean 95th percentile discharge increases by 18% and 30% under the RCP4.5 and RCP8.5 trajectories for 2018-2065, respectively. During the 2050-2097 period, the mean peak discharge is indicated to increase by 30% and 75% under the RCP 4.5 and RCP 8.5 trajectories, respectively.

The RCP4.5 trajectory displays the smallest changes in mean peak discharge, while more significant increases are realized under RCP8.5. The CanESM2 model under RCP4.5 shows most changes remaining between ±50% for both periods (Figure 4.9a, b). The same model does show that flow will become more variable in the second half of the century (2050-2097) under the RCP8.5 trajectory. Peak discharge is shown to be 25-50% lower than the

historical mean during two periods (2065-2070, 2075-2078), which would indicate dry overall conditions. However, the 2080-2090 period under the same simulation shows a 200% increase relative to historical flow (Figure 4.9d).

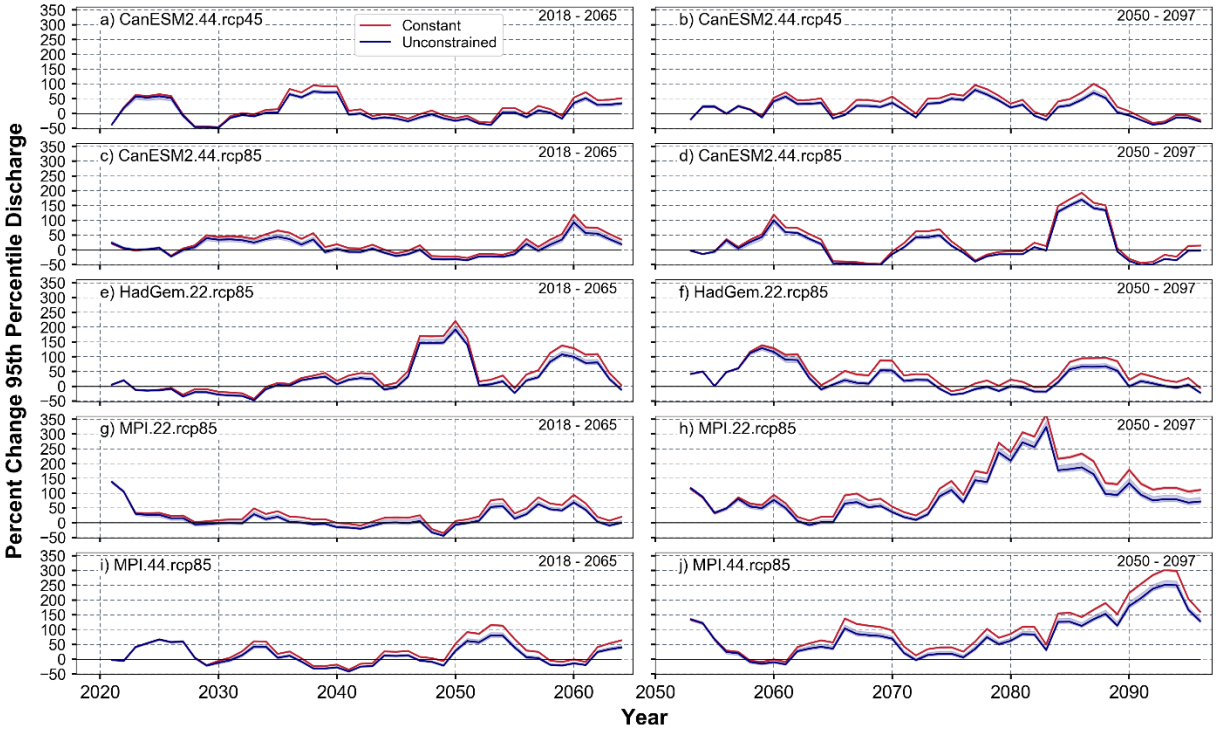

Figure 4.9. Percent change in 95th percentile discharge for the constant (red) and unconstrained (blue) scenarios against the 1970-2016 mean 95th percentile discharge. Column 1 depicts change for 2018-2065 and column 2 depicts change for 2050-2097.

The MPI simulations (RCP8.5), in particular, show flow transitioning from relatively minor changes to significantly wetter conditions beyond 2070. Under the MPI.22.rcp85 simulation, mean peak flow increases by 93% for the 2050-2097 period relative to the 2018-2065 period for the constant scenario (Figure 4.9g, h). The MPI.44.rcp85 simulation shows a more modest change of 80% between these two time periods (Figure 4.9i, j). This increase in flow corresponds to the trends in precipitation that the MPI simulations depict (Figure 4.10g-j). Total summer precipitation (April-August) is projected to increase by 160% under both MPI simulations by 2100 relative to the historical observed total precipitation. However, overall

results are more unclear for the later half of the century since the HadGEM model does not agree with the results from the MPI simulations. In fact, under the HadGEM simulation, flow is increased from 2045-2065, but from 2065-2085, peak flow is not significantly changed from the mean historical peak flow (Figure 4.9e, f). The HadGEM model does suggest that total summer precipitation will increase by 130% beyond 2040, but this does not translate to consistent increased peak flow (Figure 4.10e). The MPI simulations, particularly the MPI.22.rcp85 simulation, do show a transition to more intense 1-day precipitation beyond 2070, which combined with the increase in total summer precipitation, may be the cause for the > 200% increase in mean 95th percentile flow (Figure 4.9 h, j; Figure 4.10h, j).

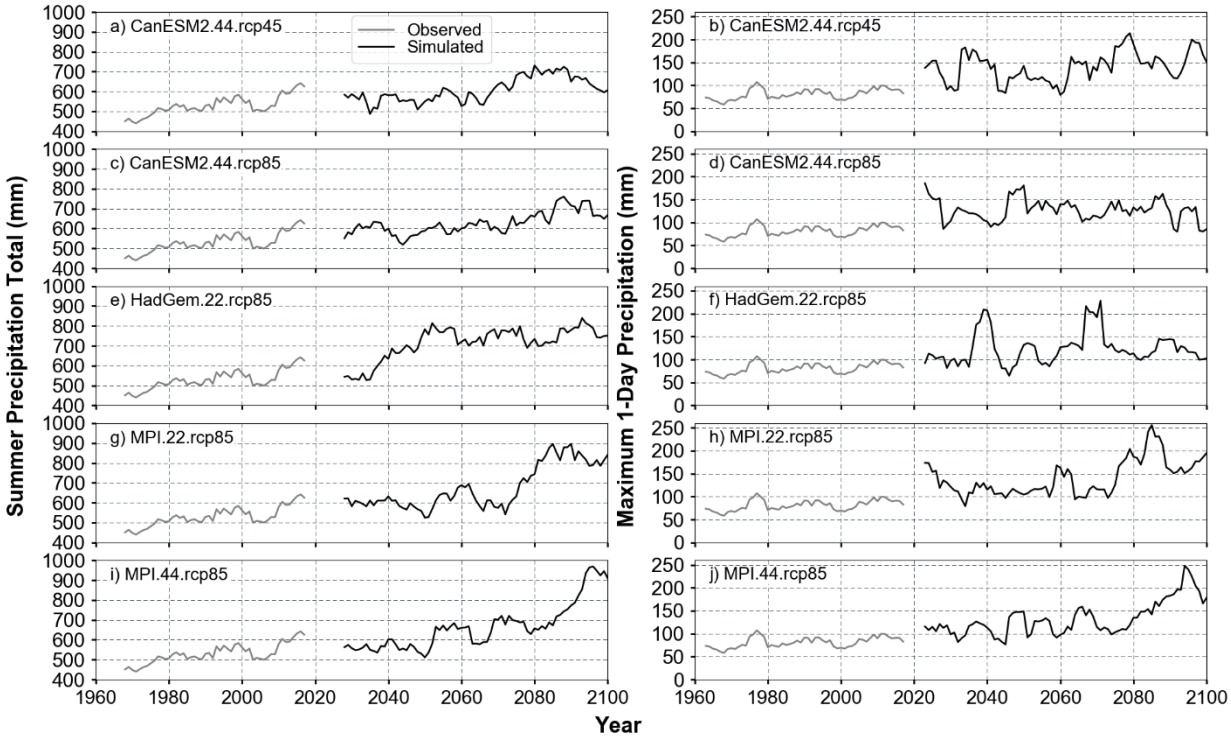

Figure 4.10. Trends in total precipitation and maximum 1-day precipitation for the summer months of April-August for the observed time series (gray) and climate simulations (black).

Based on the changes to peak flow relative to the historical flow conditions, the climate system drives most of the change seen in simulated peak discharge. However, the effect from conversion of agricultural land to conservation land (i.e. human impact) is not negligible under

future climate. Under the RCP8.5 trajectory, the unconstrained scenario shows a 16% increase in mean 95th percentile flow versus the 29% increase under the constant scenario for the 2018-2065 period. A similar results is obtained for the 2050-2097 period, with a 55% increase shown under the unconstrained scenario in comparison to the 75% increase under the constant scenario.

To accurately capture the effects of human activities in contrast to climate on mean peak discharge, the percent contribution (impact) to change in mean 95th percentile discharge from both components was computed. The climate impact was computed from the constant scenario, while the human impact was computed from change in 95th percentile discharge between the unconstrained and constant scenarios. All climate simulations point to a more dominant climate impact during the 2050-2097 period versus the 2018-2065 period, particularly the CanESM2.44.rcp45 simulation and both MPI simulations (Figure 4.11). Approximately 60-90% of the change in mean 95th percentile discharge can be attributed to climate under the MPI scenarios during the later half of the century, while only ~20% impact comes from the human system (Figure 4.11h, j). Likewise, the climate impact under the CanESM2.44.rcp45 simulation is 60-80% (Figure 4.11b). During the 2018-2065 period, the human system has a greater influence on peak discharge. The human system under the CanESM2 simulations, as well as the MPI simulations, has up to an 80% impact on flow during certain periods, particularly when mean peak discharge is not significantly changed from the historical peak discharge (i.e. 2040-2060) (Figure 4.11a, c, g, i). The HadGEM model is the only simulation that deviates from the other models in the study, with a dominant climate impact from 2045-2065, but a more prominent human impact later in the century (Figure 4.11e, f).

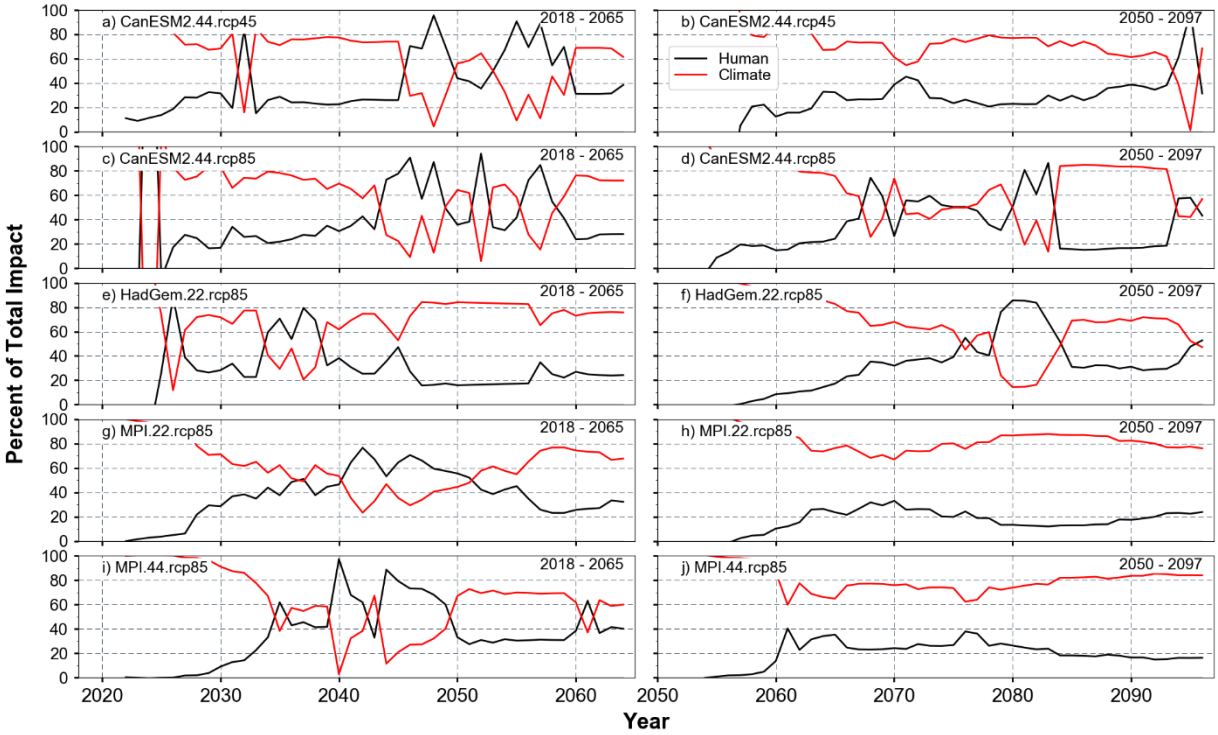

Figure 4.11. Percent of total impact on 95th percentile discharge from the human system (black) and the climate system (red) (column 2).

4.5.4 Flood Frequency Analysis

All climate simulations point to an increased risk of flooding in the watershed under future precipitation outcomes (Figure 4.12). Under historical climate, the hydrology model indicates 7 years containing an event with a return period of > 10 years (0.14 frequency value). This corresponds well with the actual observed frequency of 0.12 (6 years) calculated from observed discharge data for the Squaw Creek watershed. Under future climate scenarios, this flood frequency increases to 0.3-0.5 for the 2018-2065 period, and further increases to 0.5-0.7 under some simulations for the 2050-2097 period. The constant scenario results in the greatest increase in flooding under the RCP4.5 and 8.5 trajectories for both periods, while the unconstrained scenario results in the lowest increase due to greater implementation of conservation land. The frequency of flooding, however, is similar between RCP4.5 and 8.5. The CanESM2.44.rcp45 simulation produces approximately 30-33 years with a flood event of return

period >10 years, while the MPI simulations under RCP8.5 produce similar frequency outcomes. Overall, the impact of increased conservation land is not enough to substantially reduce the frequency of flooding under future climate. Under the MPI simulations, the human system reduces the number of years with flooding by 4-5. However, this reduction is small in comparison to the increase of flooding from 7 years (historical period) to over 24 years during the 2050-2097 period.

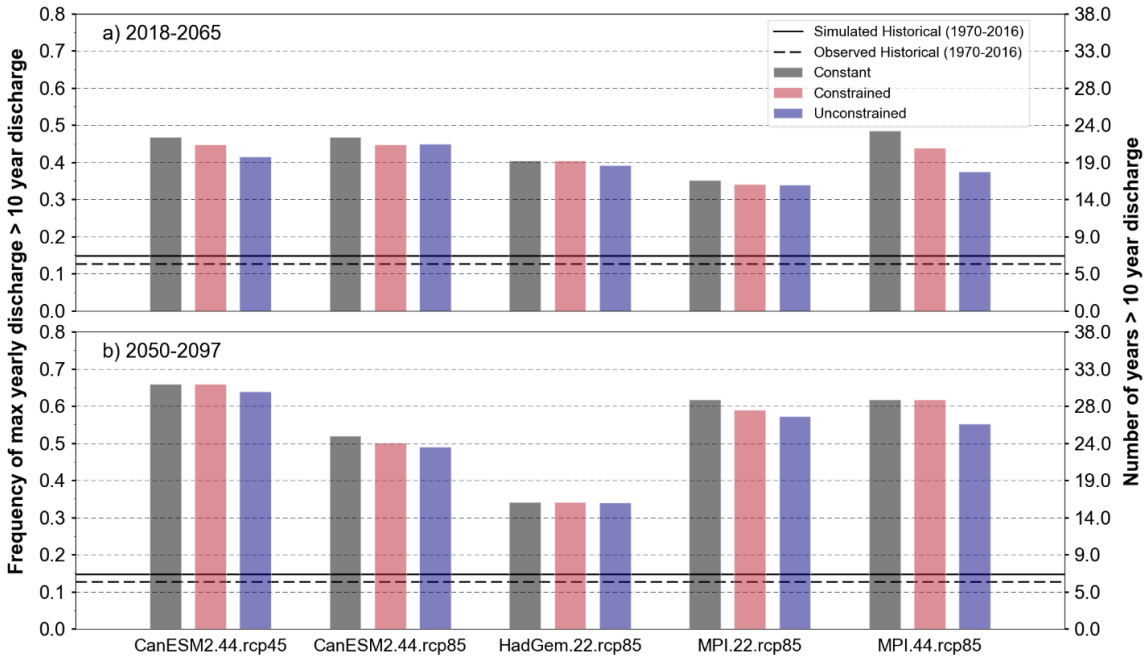

Figure 4.12. Frequency of maximum annual discharge exceeding the 10 year event discharge over the entire 47 year simulation period for 2018-2065 and 2050-2097.

4.5.5 Pothole Flooding Analysis

Lastly, it is worth noting the impact of prairie pothole flooding on farmer agent decision-making. Overall, conservation land between the scenario were farmer agents have pothole land versus the scenario where pothole land is absent only results in <10% difference in conservation land (Figure 4.13). It would be expected that if farmer agents have more land that floods, thereby reducing mean crop yield for the entire farm, they would be inclined to

implement more conservation land. Under historical climate (1970-2016), the farmer agents consistently implement 7% more conservation land on average (range of 2-11% more conservation land) during the entire simulation period if potholes are present. However, this result is not clear under future climate scenarios. On the one hand, the MPI.44.rcp85 simulation for 2050-2097 shows a greater downward spread in the percent change in conservation land when potholes are not present (Figure 4.13j), but on the other hand, the HadGEM.22.rcp85 simulation for 2018-2065 suggest that more conservation land is implemented under the nonpothole scenario.

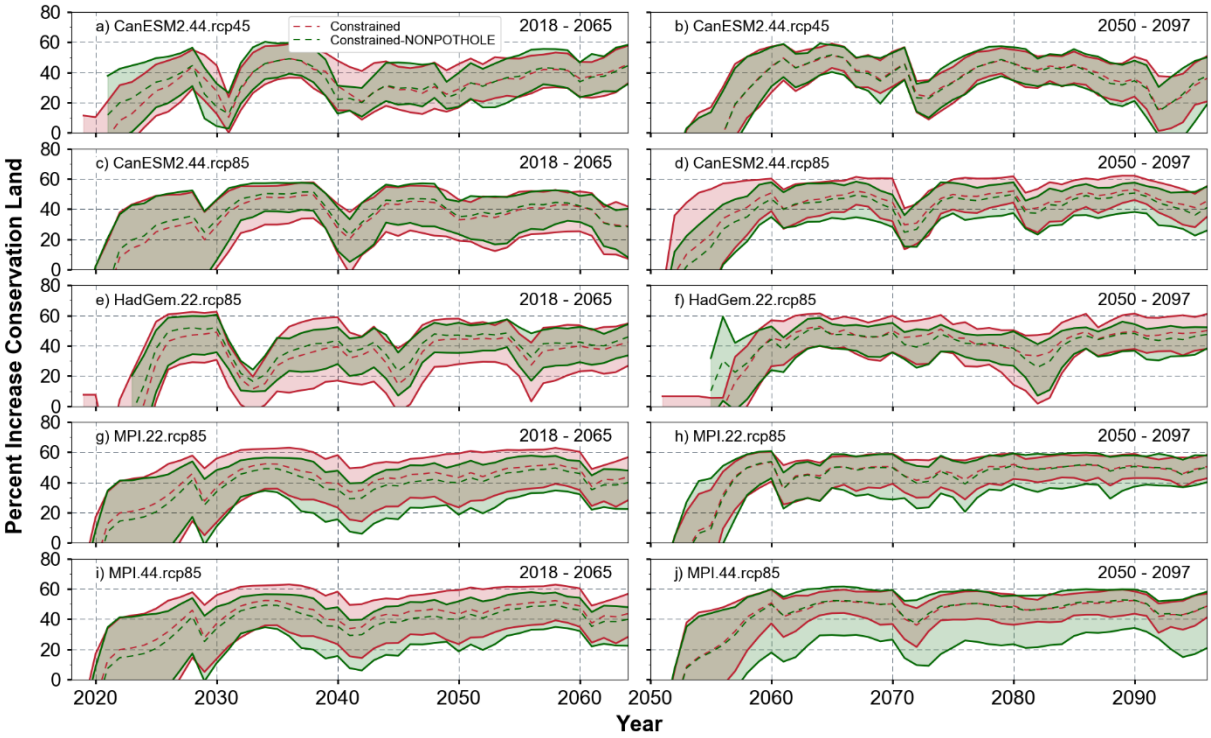

Figure 4.13. Percent change in conservation land for the constrained (red) and constrained-nonpothole (green) scenarios relative to the constant scenario for 2018-2065 (column 1) and 2050-2097 (column 2).

Figure 4.14 displays the fraction of flooded area for pothole TYPE1 under the climate simulations in comparison to the historical climate. Pothole flooding generally does not deviate significantly from the historical simulated flooded with the exception of short 3-5 year periods

(Figure 4.14). The MPI simulations are the only simulations to show a more significant deviation from the historical period, with most change seen after year 2070. In contrast, the CanESM2 simulations are the only simulations to show several dry periods beyond 2050.

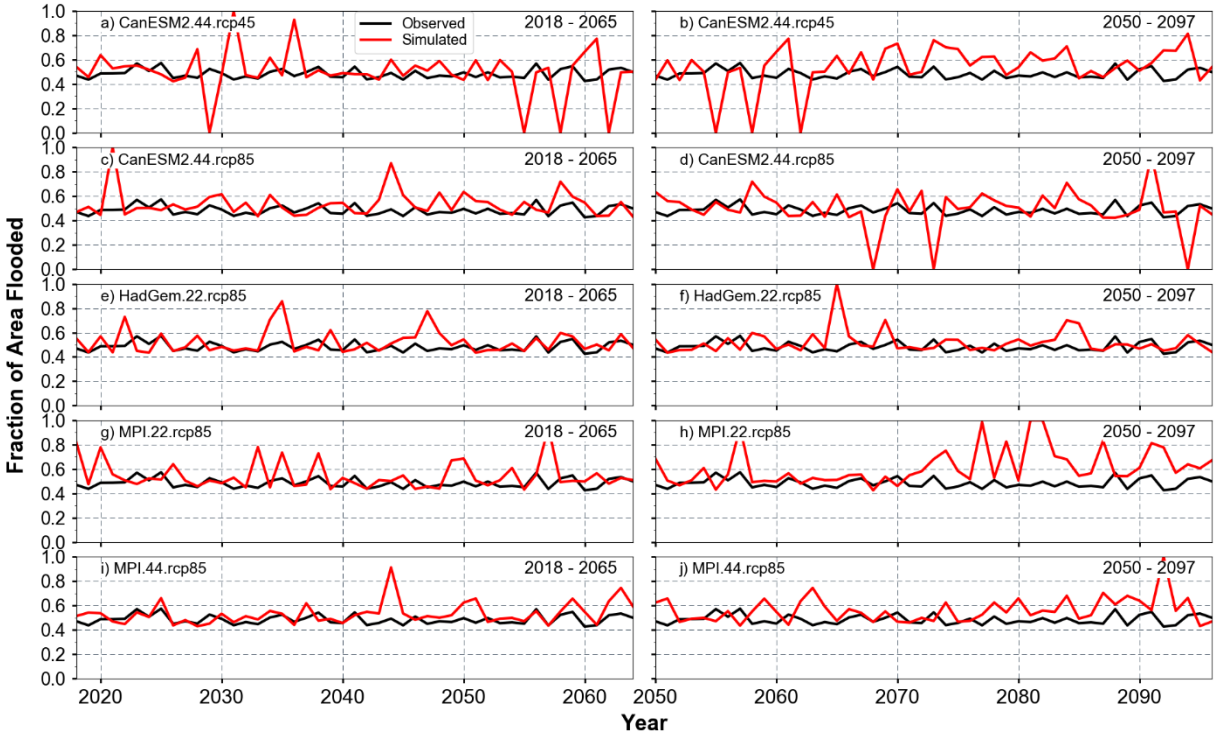

Figure 4.14. Fraction of area flooded for pothole TYPE1.

4.6 Discussion

Simulations of conservation land under all climate scenarios suggest that farmer agents would be more likely to implement conservation land in the future. One of the primary causes of this increase in conservation may be due to the poor yields predicted by the crop regression model. Analyzing the yield output from the regression model reveals that yields are lower by 25% and 30% under the RCP4.5 scenario during the 2018-2065 and 2050-2097 periods compared to historical yields. This decrease in yield is even more substantial under the RCP8.5 scenario, with a 27% and 42% decrease during the first and second half of the century, respectively. These numbers are, however, supported by a number of recent studies (Hatfield et al., 2011; Rosenzweig

et al., 2014; Schlenker and Roberts, 2009; Xu et al., 2016). A study by Xu *et al.*, (2016), which used the Agro-IBIS model driven by CMIP5 climate output, found yield to decrease by 13-42% under RCP4.5 and 17-50% under RCP8.5 for Iowa. Similarly, crop yields are shown to decrease by 30-46% by the end of the century in a study conducted by Schlenker and Roberts (2009). Many of these studies conclude that increasing temperatures in the North Central U.S will cause increasing crop loss in the future. Farmers may need to find alternative sources of revenue under future climate if crop prices are not modified in response to yield declines in this region. In the case of this ABM, the farmers revert to implementing more conservation land. However, even in the unconstrained scenario, the farmer population mean $ConsMax$ never exceeds the maximum $ConsMax$ possible (0.1), which would indicate that some profitability from crops remains.

Climate projections for the North Central U.S show that precipitation frequency and intensity are expected to increase (Janssen et al., 2014; Wuebbles et al., 2014). Under analysis conducted by Wuebbles *et al.* (2014) of CMIP5 model output, the Extreme Precipitation Index (Kunkel et al., 1999) rises from about 0.4 and 0.6 for the 2016-2025 period to 0.6 and 1.9 for the end of the century under the RCP4.5 and RCP8.5 trajectories, respectively. The model output analyzed in their study suggests that the 20 year return period annual maximum daily precipitation will increase by 20-25% or more for the Midwest under the RCP8.5 scenario. Prein *et al.* (2017) drew similar conclusions about precipitation trends for the North Central U.S, with extreme precipitation increasing during the winter and summer months, and moderate precipitation decreasing during the summer. These results support the precipitation output obtained in this study, which suggests that the intensity of 1-day maximum precipitation may increase by 50-100% during certain periods (e.g. MPI.44.rcp85 – 2080-2100). Analysis by month indicates that precipitation intensity increases mostly during the months of May-July. On the contrary, August

actually sees precipitation intensity lower than the historical mean during many time periods, suggesting drier conditions later in the summer. The projected changes in precipitation (i.e. increasing intensity) are broadly consistent with studies of historical precipitation trends (Kunkel et al., 1999; Villarini et al., 2013).

The increasing precipitation intensity may be driving increases in peak discharge across the Midwest. In this study, peak discharge decreases under more conservation land in all cases when compared to the constant scenario, with a 30-50% decrease suggested in some simulations. However, these results are overshowed by the dominant climate impact on the system, with mean 95th percentile discharge expected to increase by 33% in the unconstrained scenario under the RCP8.5 projection. Results from a number of recent studies that have investigated the effects of climate on hydrologic outcomes support the findings in this study (Cherkauer and Sinha, 2010; Frans et al., 2013; Naz et al., 2016; Teshager et al., 2016a). Using CMPI5 data to simulate the VIC model for HUC8 basins through 2050, Naz *et al.* (2016) found that runoff from most subbasins in the Midwest will increase by 6-30% during the March-May period. However, total runoff for Iowa specifically shows little change for the period later in the summer (June-August). Additionally, their study shows that 95th percentile discharge increases by at least 5% for all subbasins in the region, with many subbasins showing an increase of 15-20% or more. Simulations in this study do show higher increases in discharge than Naz *et al.* (2016) however, with a 29% increase for the 2018-2050 under the constant scenario, and a 16% increase under the unconstrained scenario. A study by Cherkauer and Sinha (2010), which used the VIC model to simulate watersheds in Illinois and Wisconsin, similarly found that seasonal average peak flows increase by approximately 10-20% for spring and summer under three climate scenario, with some watersheds showing a 20-30% increase.

However, not every study indicates that discharge will increase for the Midwest Corn belt region. For instance, Milly *et al.*, (2002) found that what is considered to be the current 100 yr return period flood becomes a 5-10 year flood over the Great Lakes region, 40-80 year flood over the Ohio valley, but does not change significantly for the upper Misssissippi river basin. Chien *et al.* (2013) found that annual discharge will decrease by 45% for several watersheds in Illinois under future climate, with most decrease occurring during the summer months. Therefore, there is some degree of uncertainty as to whether future climate will actually increase discharge in the Midwest.

Recent studies of observed data do suggest that the potential for flooding across the Midwest is increasing, and that much of that change is a result of changing precipitation patterns rather than land use changes (Frans et al., 2013; Gupta et al., 2015; Mallakpour and Villarini, 2015; Ryberg et al., 2014; Tomer and Schilling, 2009). Tomer and Schilling (2009) for instance, found that climate has been the primary driver in changing discharge since the 1970s for four watersheds in Iowa and Illinois as opposed to the period prior to 1970. Frans *et al.* (2013) and Gupta *et al.* (2015) come to slightly different conclusions, showing that changes in precipitation have largely dominated changes in streamflow for watersheds in Iowa and Minnesota over the entire last century. Results from this study indicate a dominant climate impact on the system, particularly during the latter half of the 21st century. Some model simulations, particularly MPI, suggest an 80% impact from climate by the end of the century under the RCP8.5 scenario. Even under the RCP4.5 scenario, findings indicate a 60-80% impact from climate, with a relatively small impact from the human system.

4.7 Conclusions

In this study, four farmer agent decision-making scenarios were simulated using temperature and precipitation projected under RCP4.5 and RCP8.5 climate trajectories. Five climate simulations representing these trajectories were bias-corrected using the Kernel Density Distribution Method to extract a time series of precipitation (hourly) and temperature (daily) (Mcginnis et al., 2015). In the first scenario, farmer agents were allowed to modify their conservation land through time, but their decision was constrained by their $ConsMax$ parameter (i.e. maximum amount of land that the farmer is willing to put into conservation). In the second scenario, farmer agents were allowed to modify their "conservation-mindedness" (i.e. $ConsMax$ parameter) through time if their decision was greater than the limit imposed by their $ConsMax$ parameter. In the third scenario, conservation land was kept at the mean historical 2006-2016 level to isolate the impact from climate. Lastly, on-farm pothole flooding was turned off to determine the effect of on-farm flooding to conservation decision-making.

The primary findings of this study are:

- The climate simulations indicate mean 95th percentile discharge increasing by 75% under the RCP 8.5 trajectory for the 2050-2097 period relative to the historical 1970-2016 period if conservation land is kept at the historical mean (constant scenario). The RCP4.5 simulation (CanESM2) indicates a smaller increase of 30% for the 2050-2097 period under the constant scenario.

- Under the unconstrained scenario, mean 95th percentile discharge increases by 55% under the RCP 8.5 trajectory for the 2050-2097 period relative to the historical 1970-2016 period. Thus, the increase in mean peak discharge is 20% less than under the constant scenario.

- Under the unconstrained scenario, the farmer population transitions from a mean $ConsMax$ of 0.6 to a $ConsMax$ of 0.7-0.8 by the end of the 2018-2065 period. When precipitation and temperature for the 2050-2097 period were considered, the farmer population transitions to a $ConsMax$ of 0.8-0.9. Thus, the population never reaches the maximum value of $ConsMax$ possible.

- During the 2018-2065 period, the human system and climate system compete in terms of impact on mean 95th percentile discharge. However, during the 2050-2097 period, the impact from the climate system becomes dominant. The MPI simulations under the RCP8.5 trajectory indicate the climate system being responsible for up to 80% of the change in mean 95th percentile discharge.

- Despite the unconstrained scenario showing a 20% lower increase in mean 95th percentile discharge as compared to the constant scenario, frequency of flooding exceeding the 10 year event increases from 0.14 to 0.3-0.6. This equates to an increase from 7 years with a 10 year flood to 20-30 years with a 10 year flood.

- The effect of on-farm flooding of pothole depressions was relatively minor, with only one model (MPI-ESM-LR) indicating less conservation land implemented under the nonpothole scenario for both 2018-2065 and 2050-2097.

Results from this study indicate that future climate change will increase flooding across the Midwest Corn Belt, and by the second half of the century, the climate system will become the primary determinant of streamflow outcomes in this region. These results align with conclusions from recent studies for the North Central U.S, which point to increasing flood frequency under observed conditions mainly due to changes in precipitation patterns (i.e. Tomer and Schilling,

2009; Frans *et al.*, 2013; Ryberg *et al.*, 2014; Gupta *et al.*, 2015; Mallakpour and Villarini, 2015), and further increases in flooding concerns under future climate scenarios (Naz et al., 2016) due to changing precipitation frequency or intensity (Janssen et al., 2014; Prein et al., 2017). However, Rogger *et al.* (2017) points out that many studies of land use and climate impacts on streamflow at the larger scale indicate climate to be the major driver in changing streamflow, whereas studies at the smaller field scale clearly show a large impact from land use change. Uncertainty exists as to how land use change effects scale up to the size of a larger watershed, and thus this topic is a point of ongoing research (Rogger et al., 2017).

Future work can be done to further improve the reliability of this assessment. One area of concern that was not addressed in this study is how economic variables such as crop prices, production costs, land rental prices may vary under future climate. Good growing conditions in the corn belt can result in a high crop yield, which creates a larger grain supply and lower crop prices (Irwin et al., 2017). Production costs and land rental values do show correlation with crop prices based on the historical economic data used in this study. Thus, developing future scenarios of crop prices through statistical methods may create more realistic simulations of future land use changes.

Another important area of consideration is future agricultural land use changes due to other market forces such as biofuel production. It is estimated that by 2030, 37 million Ha of land will be converted to biofuel crop production (Howells et al., 2013), which could have important implications on various hydrologic processes such as infiltration and runoff, particularly if a large percentage of land is converted to growing perennial crop types (Cibin et al., 2016; Zaibon et al., 2017). Updating the agricultural decision making in the ABM to include

multiple land use choices (i.e. conservation, biofuels, corn-soybean production) may allow for further scenario testing under changing climate and market conditions.

Lastly, it may be beneficial to conduct the same analysis as in this study, but using other empirical downscaling approaches to derive detailed precipitation and temperature time series data (Chen et al., 2013). Chen *et al.* (2013) found that uncertainty associated with the choice of downscaling approach (i.e. bias correction or scaling) is just as great as that associated with the actual regional climate model, with each approach having its own advantages and disadvantages. Thus, deriving the forcing data using other approaches may allow for a more complete hydrologic uncertainty assessment.

4.8 Acknowledgments

Funding for this project was provided by an Iowa State University College of Liberal Arts and Sciences seed grant. We would like to thank all other seed grant participants, including Jean Goodwin, Chris R. Rehmann, William W. Simpkins, Leigh Tesfatsion, Dara Wald, and Alan Wanamaker.

4.9 References

Ahn, K. H. and Merwade, V.: Quantifying the relative impact of climate and human activities on streamflow, J. Hydrol., 515, 257–266, doi:10.1016/j.jhydrol.2014.04.062, 2014.

Arbuckle, J. G.: Farmer Attitudes toward Proactive Targeting of Agricultural Conservation Programs, Soc. Nat. Resour., 26(6), doi:10.1080/08941920.2012.671450, 2013.

Arbuckle, J. G.: Iowa Farm and Rural Life Poll 2016 Summary Report, Ames, IA., 2017.

Arbuckle, J. G., Prokopy, L. S., Haigh, T., Hobbs, J., Knoot, T., Knutson, C., Loy, A., Mase, A. S., McGuire, J., Morton, L. W., Tyndall, J. and Widhalm, M.: Climate change beliefs, concerns, and attitudes toward adaptation and mitigation among farmers in the Midwestern United States, Clim. Change, 117(4), 943–950, doi:10.1007/s10584-013-0707-6, 2013.

Arnell, N. W. and Gosling, S. N.: The impacts of climate change on river flood risk at the global scale, Clim. Change, 134(3), 387–401, doi:10.1007/s10584-014-1084-5, 2016.

Bao, Z., Zhang, J., Wang, G., Fu, G., He, R., Yan, X., Jin, J., Liu, Y. and Zhang, A.: Attribution for decreasing streamflow of the Haihe River basin, northern China: Climate variability or human activities?, J. Hydrol., 460-461, 117–129, doi:10.1016/j.jhydrol.2012.06.054, 2012.

Burton, R. J. F.: The influence of farmer demographic characteristics on environmental behaviour: A review, J. Environ. Manage., 135, 19–26, doi:10.1016/j.jenvman.2013.12.005, 2014.

Carpenter, S. R., Cole, J., Pace, M. L., Batt, R., Brock, W. A. and Cline, T.: Early Warnings of Regime Shifts, Science (80-.)., 332(6033), 1076–1079, doi:10.1126/science.1203672, 2011.

Chelsea Nagy, R., Graeme Lockaby, B., Kalin, L. and Anderson, C.: Effects of urbanization on stream hydrology and water quality: The Florida Gulf Coast, Hydrol. Process., 26(13), 2019–2030, doi:10.1002/hyp.8336, 2012.

Chen, J., Brissette, F. P., Chaumont, D. and Braun, M.: Performance and uncertainty evaluation of empirical downscaling methods in quantifying the climate change impacts on hydrology over two North American river basins, J. Hydrol., 479, 200–214, doi:10.1016/j.jhydrol.2012.11.062, 2013.

Cherkauer, K. a. and Sinha, T.: Hydrologic impacts of projected future climate change in the Lake Michigan region, J. Great Lakes Res., 36(SUPPL. 2), 33–50, doi:10.1016/j.jglr.2009.11.012, 2010.

Chien, H., Yeh, P. J. F. and Knouft, J. H.: Modeling the potential impacts of climate change on streamflow in agricultural watersheds of the Midwestern United States, J. Hydrol., 491(1), 73–88, doi:10.1016/j.jhydrol.2013.03.026, 2013.

Christensen, N. S., Wood, A. W., Voisin, N., Lettenmaier, D. P. and Palmer, R. N.: The effects of climate change on the hydrology and water resources of the Colorado River basin, Clim. Change, 62(1-3), 337–363, doi:10.1023/B:CLIM.0000013684.13621.1f, 2004.

Cibin, R., Trybula, E., Chaubey, I., Brouder, S. M. and Volenec, J. J.: Watershed-scale impacts of bioenergy crops on hydrology and water quality using improved SWAT model, GCB Bioenergy, 8(4), 837–848, doi:10.1111/gcbb.12307, 2016.

Cruise, J. F., Laymon, C. a. and Al-Hamdan, O. Z.: Impact of 20 Years of Land-Cover Change on the Hydrology of Streams in the Southeastern United States, J. Am. Water Resour. Assoc., 46(6), 1159–1170, doi:10.1111/j.1752-1688.2010.00483.x, 2010.

Davis, C. G. and Gillespie, J. M.: Factors affecting the selection of business arrangements by U.S. hog farmers, Rev. Agric. Econ., 29(2), 331–348, doi:10.1111/j.1467-9353.2007.00346.x, 2007.

Dziubanski, D. J., Franz, K. J. and Helmers, M. J.: Effects of Spatial Distribution of Prairie Vegetation in an Agricultural Landscape on Curve Number Values, JAWRA J. Am. Water Resour. Assoc., 53(2), 365–381, doi:10.1111/1752-1688.12510, 2017.

Edmonds, P.: A comparison of conventional annual and alternative perennial cropping systems under contemporary and future precipitation scenarios in the US Prairie Pothole Region, Grad. Theses Diss. 15298, doi:https://lib.dr.iastate.edu/etd/15298, 2017.

Frans, C., Istanbulluoglu, E., Mishra, V., Munoz-Arriola, F. and Lettenmaier, D. P.: Are climatic or land cover changes the dominant cause of runoff trends in the Upper Mississippi River Basin?, Geophys. Res. Lett., 40(6), 1104–1110, doi:10.1002/grl.50262, 2013.

Granovetter, M.: The Strength of Weak Ties, Am. J. Sociol., 78(6), 1360–1380, 1973.

Groisman, P. Y., Knight, R. W. and Karl, T. R.: Changes in Intense Precipitation over the Central United States, J. Hydrometeorol., 13(1), 47–66, doi:10.1175/JHM-D-11-039.1, 2012.

Guo, Y. and Shen, Y.: Quantifying water and energy budgets and the impacts of climatic and human factors in the Haihe River Basin, China: 2. Trends and implications to water resources, J. Hydrol., 527, 251–261, doi:10.1016/j.jhydrol.2015.04.071, 2015.

Gupta, S. C., Kessler, A. C., Brown, M. K. and Zvomuya, F.: Climate and agricultural land use change impacts on streamflow in the upper midwestern United States, Water Resour. Res., 51(7), 5301–5317, doi:10.1002/2015WR017323, 2015.

Gutowski, W. J., Takle, E. S., Kozak, K. a., Patton, J. C., Arritt, R. W. and Christensen, J. H.: A Possible Constraint on Regional Precipitation Intensity Changes under Global Warming, J. Hydrometeorol., 8(6), 1382–1396, doi:10.1175/2007JHM817.1, 2007.

Hatfield, J. L., Boote, K. J., Kimball, B. a., Ziska, L. H., Izaurralde, R. C., Ort, D., Thomson, a. M. and Wolfe, D.: Climate impacts on agriculture: Implications for crop production, Agron. J., 103(2), 351–370, doi:10.2134/agronj2010.0303, 2011.

Helmers, M. J., Zhou, X., Asbjornsen, H., Kolka, R., Tomer, M. D. and Cruse, R. M.: Sediment Removal by Prairie Filter Strips in Row-Cropped Ephemeral Watersheds, J. Environ. Qual., 41(5), 1531, doi:10.2134/jeq2011.0473, 2012.

Hernandez-Santana, V., Zhou, X., Helmers, M. J., Asbjornsen, H., Kolka, R. and Tomer, M.: Native prairie filter strips reduce runoff from hillslopes under annual row-crop systems in Iowa, USA, J. Hydrol., 477, 94–103, doi:10.1016/j.jhydrol.2012.11.013, 2013.

Hoag, D., Luloff, A. E. and Osmond, D.: How Farmers and Ranchers Make Decisions on Conservation Practices, Raleigh, NC., 2012.

Hofstrand, D.: Tracking the Profitability of Corn Production, Ames, IA., 2018.

Howells, M., Hermann, S., Welsch, M., Bazilian, M., Segerström, R., Alfstad, T., Gielen, D., Rogner, H., Fischer, G., Van Velthuizen, H., Wiberg, D., Young, C., Alexander Roehrl, R., Mueller, A., Steduto, P. and Ramma, I.: Integrated analysis of climate change, land-use, energy and water strategies, Nat. Clim. Chang., 3(7), 621–626, doi:10.1038/nclimate1789, 2013.

Huang, S., Young, C., Feng, M., Heidemann, K., Cushing, M., Mushet, D. M. and Liu, S.: Demonstration of a conceptual model for using LiDAR to improve the estimation of floodwater mitigation potential of Prairie Pothole Region wetlands, J. Hydrol., 405(3-4), 417–426, doi:10.1016/j.jhydrol.2011.05.040, 2011.

Irwin, S., Good, D. and Hubbs, T.: The Role of Weather in the Pattern of Corn Prices over Time. [online] Available from: https://farmdocdaily.illinois.edu/2017/06/role-of-weather-in-the-corn-price-pattern-over-time.html, 2017.

Janssen, E., Wuebbles, D. and Kunkel, K.: Observational and Model based Trends and Projections of Extreme Precipitation over the Contiguous United States, Earth's Futur., 1–15, doi:10.1002/2013EF000185.Received, 2014.

Karl, T. R., Melillo, J. M. and Peterson, T. C.: Global Climate Change Impacts in the United States, Cambridge University Press. [online] Available from: www.globalchange.gov/usimpacts, 2009.

Karmalkar, A. V. and Bradley, R. S.: Consequences of global warming of 1.5 °c and 2 °c for regional temperature and precipitation changes in the contiguous United States, PLoS One, 12(1), 1–17, doi:10.1371/journal.pone.0168697, 2017.

Kunkel, K. E., Andsager, K. and Easterling, D. D. R.: Long-Term Trends in Extreme Precipitation Events over the Conterminous United States and Canada, J. Clim., 12(1998), 2515–2527, doi:http://dx.doi.org/10.1175/1520-0442(1999)012<2515:LTTIEP>2.0.CO;2, 1999.

Larry W. Mays: Water Resources Engineering, 2nd ed., John Wiler & Songs, Inc., Hoboken, NJ., 2011.

Mallakpour, I. and Villarini, G.: The changing nature of flooding across the central United States, Nat. Clim. Chang., 5(3), 250–254, doi:10.1038/nclimate2516, 2015.

Marcotty, J.: High crop prices a threat to nature?, StarTribune, 11th November [online] Available from: http://www.startribune.com/high-crop-prices-threat-to-nature/134566683/, 2011.

Mcdeid, S. M.: Morphologic characterization of upland depressional wetlands on the Des Moines Lobe of Iowa, Ames, IA., 2017.

Mcginnis, S., Nychka, D. and Mearns, L. O.: A New Distribution Mapping Technique for Climate Model Bias Correction, in Machine Learning and Data Mining Approaches to Climate Science, pp. 91–99, Springer International Publishing Switzerland., 2015.

McGuire, J., Morton, L. W. and Cast, A. D.: Reconstructing the good farmer identity: Shifts in farmer identities and farm management practices to improve water quality, Agric. Human Values, 30(1), 57–69, doi:10.1007/s10460-012-9381-y, 2013.

Miller, B. A., Crumpton, W. G. and van der Valk, A. G.: Spatial Distribution of Historical Wetland Classes on the Des Moines Lobe, Iowa, Wetlands, 29(4), 1146–1152, doi:10.1672/08-158.1, 2009.

Milly, A. P. C. D., Betancourt, J., Falkenmark, M., Hirsch, R. M., Zbigniew, W., Lettenmaier, D. P., Stouffer, R. J. and Milly, P. C. D.: Stationarity Is Dead : Stationarity Whither Water Management ?, Science (80-.)., 319(5863), 573–574, doi:10.1126/science.1151915, 2008.

Milly, P. C. D., Wetherald, R. T., Dunne, K. a. and Delworth, T. L.: Increasing risk of great floods in a changing climate, Nature, 415(6871), 514–517, doi:10.1038/415514a, 2002.

Montanari, a., Young, G., Savenije, H. H. G., Hughes, D., Wagener, T., Ren, L. L., Koutsoyiannis, D., Cudennec, C., Toth, E., Grimaldi, S., Blöschl, G., Sivapalan, M., Beven, K., Gupta, H., Hipsey, M., Schaefli, B., Arheimer, B., Boegh, E., Schymanski, S. J., Di Baldassarre, G., Yu, B., Hubert, P., Huang, Y., Schumann, a., Post, D. a., Srinivasan, V., Harman, C., Thompson, S., Rogger, M., Viglione, a., McMillan, H., Characklis, G., Pang, Z. and Belyaev, V.: "Panta Rhei—Everything Flows": Change in hydrology and society—The IAHS Scientific Decade 2013–2022, Hydrol. Sci. J., 58(6), 1256–1275, doi:10.1080/02626667.2013.809088, 2013.

Naik, P. K. and Jay, D. a.: Distinguishing human and climate influences on the Columbia River: Changes in mean flow and sediment transport, J. Hydrol., 404(3-4), 259–277, doi:10.1016/j.jhydrol.2011.04.035, 2011.

Naz, B. S., Kao, S. C., Ashfaq, M., Rastogi, D., Mei, R. and Bowling, L. C.: Regional hydrologic response to climate change in the conterminous United States using high-resolution hydroclimate simulations, Glob. Planet. Change, 143, 100–117, doi:10.1016/j.gloplacha.2016.06.003, 2016.

Newman, M. E. J., Watts, D. . J. and Strogatz, S. H.: Random graph models of social networks, Pnas, 99(suppl. 1), 2566–72, doi:10.1073/pnas.012582999, 2002.

Newton, J.: Change on the Horizon for the Conservation Reserve Program?, [online] Available from: https://www.fb.org/market-intel/change-on-the-horizon-for-the-conservation-reserve-program (Accessed 15 January 2018), 2017.

Nowak, P.: Why farmers adopt production technology, Soil Water Conserv., 47(1), 14–16, 1992.

Pfrimmer, J., Gigliotti, L., Stafford, J. and Schumann, D.: Motivations for Enrollment Into the Conservation Reserve Enhancement Program in the James River Basin of South Dakota, Hum. Dimens. Wildl., 22(4), 1–8, doi:10.1080/10871209.2017.1324069, 2017.

Prein, A. F., Rasmussen, R. M., Ikeda, K., Liu, C., Clark, M. P. and Holland, G. J.: The future intensification of hourly precipitation extremes, Nat. Clim. Chang., 7(1), 48–52, doi:10.1038/nclimate3168, 2017.

Prior, J.: Landforms of Iowa, 1st ed., University of Iowa Press, Iowa City, Iowa., 1991.

Rogger, M., Agnoletti, M., Alaoui, a, Bathurst, J. C., Bodner, G., Borga, M., Chaplot, V., Gallart, F., Glatzel, G., Hall, J., Holden, J., Holko, L., Horn, R., Kiss, a, Quinton, J. N., Leitinger, G., Lennartz, B., Parajka, J., Peth, S., Robinson, M., Salinas, J. L., Santoro, a, Szolgay, J., Tron, S. and Viglione, a: Land use change impacts on floods at the catchment scale: Challenges and opportunities for future research, Water Resouces Res., 53(June 2013), 5209–5219, doi:10.1002/2017WR020723.Received, 2017.

Rosenzweig, C., Elliott, J., Deryng, D., Ruane, A. C., Müller, C., Arneth, A., Boote, K. J., Folberth, C., Glotter, M., Khabarov, N., Neumann, K., Piontek, F., Pugh, T. a. M., Schmid, E., Stehfest, E., Yang, H. and Jones, J. W.: Assessing agricultural risks of climate change in the 21st century in a global gridded crop model intercomparison, Proc. Natl. Acad. Sci., 111(9), 3268–3273, doi:10.1073/pnas.1222463110, 2014.

Ryberg, K., Lin, W. and Vecchia, A.: Impact of Climate Variability on Runoff in the North_central United States, J. Hydrol. Eng., 19(1), 148–158, doi:10.1061/(ASCE)HE.1943-5584, 2014.

Saltiel, J., Bauder, J. W. and Palakovich, S.: Adoption of Sustainable Agricultural Practices: Diffusion, Farm Structure, and Profitability, Rural Sociol., 59(2), 333–349, 1994.

Scharffenberg, W. A.: Hydrologic Modeling System User's Manual, United State Army Corps Eng. [online] Available from: http://www.hec.usace.army.mil/software/hec-hms/documentation/HEC-HMS_Users_Manual_4.0.pdf, 2013.

Schilling, K. E., Chan, K. S., Liu, H. and Zhang, Y. K.: Quantifying the effect of land use land cover change on increasing discharge in the Upper Mississippi River, J. Hydrol., 387(3-4), 343–345, doi:10.1016/j.jhydrol.2010.04.019, 2010.

Schlenker, W. and Roberts, M. J.: Nonlinear temperature effects indicate severe damages to U.S. crop yields under climate change, Proc. Natl. Acad. Sci., 106(37), 15594–15598, doi:10.1073/pnas.0906865106, 2009.

Secchi, S. and Babcock, B. A.: Impact of High Corn Prices on Conservation Reserve Program Acreage., Iowa Ag Rev., 13(2), 4–7 [online] Available from: http://search.ebscohost.com/login.aspx?direct=true&db=eih&AN=25148415&site=ehost-live DP - EBSCOhost DB - eih, 2007.

Sivapalan, M., Savenije, H. H. G. and Blöschl, G.: Socio-hydrology: A new science of people and water, Hydrol. Process., 26(8), 1270–1276, doi:10.1002/hyp.8426, 2012.

Steffens, K. J. and Franz, K. J.: Late 20th-century trends in Iowa watersheds: An investigation of observed and modelled hydrologic storages and fluxes in heavily managed landscapes, Int. J. Climatol., 32(9), 1373–1391, doi:10.1002/joc.2361, 2012.

Tannura, M. A., Irwin, S. H. and Good, D. L.: Weather, Technology, and Corn and Soybean Yields in the U.S. Corn Belt. [online] Available from: http://www.farmdoc.uiuc.edu/marketing/reports, 2008.

Tesfatsion, L., Rehmann, C. R., Cardoso, D. S., Jie, Y. and Gutowski, W. J.: An agent-based platform for the study of watersheds as coupled natural and human systems, Environ. Model. Softw., 89, 40–60, doi:10.1016/j.envsoft.2016.11.021, 2017.

Teshager, A. D., Gassman, P. W., Schoof, J. T. and Secchi, S.: Assessment of impacts of agricultural and climate change scenarios on watershed water quantity and quality, and crop production, Hydrol. Earth Syst. Sci., 20(8), 3325–3342, doi:10.5194/hess-20-3325-2016, 2016.

Tigner, R.: Partial Budgeting: A Tool to Analyze Farm Business Changes, Ames, IA., 2006.

Tomer, M. D. and Schilling, K. E.: A simple approach to distinguish land-use and climate-change effects on watershed hydrology, J. Hydrol., 376(1-2), 24–33, doi:10.1016/j.jhydrol.2009.07.029, 2009.

Turner, R. E. and Rabalais, N. N.: Linking landscape and water quality in the Mississippi river basin for 200 years, Bioscience, 53(6), 563–572, doi:10.1641/0006-3568(2003)053[0563:llawqi]2.0.co;2, 2003.

Upadhyay, P., Pruski, L. O. S., Kaleita, a. L. and Soupir, M. L.: Evaluation of AnnAGNPS for simulating the inundation of drained and farmed potholes in the Prairie Pothole Region of Iowa, Agric. Water Manag., 204(April), 38–46, doi:10.1016/j.agwat.2018.03.037, 2018.

USDA-Natural Resources Conservation Service (USDA-NRCS): National Engineering Handbook, Part 630, Washington, DC., 2004.

USDA-Natural Resources Conservation Service (USDA-NRCS): Field Office Technical Guide, [online] Available from: http://www.nrcs.usda.gov/wps/portal/nrcs/main/national/technical/fotg/ (Accessed 9 April 2016), 2015.

Villarini, G., Smith, J. a. and Vecchi, G. a.: Changing frequency of heavy rainfall over the central United States, J. Clim., 26(1), 351–357, doi:10.1175/JCLI-D-12-00043.1, 2013.

Van Vuuren, D. P., Edmonds, J., Kainuma, M., Riahi, K., Thomson, A., Hibbard, K., Hurtt, G. C., Kram, T., Krey, V., Lamarque, J. F., Masui, T., Meinshausen, M., Nakicenovic, N., Smith, S. J. and Rose, S. K.: The representative concentration pathways: An overview, Clim. Change, 109(1), 5–31, doi:10.1007/s10584-011-0148-z, 2011.

Wang, D. and Cai, X.: Comparative study of climate and human impacts on seasonal baseflow in urban and agricultural watersheds, Geophys. Res. Lett., 37(6), 1–6, doi:10.1029/2009GL041879, 2010.

Wang, D. and Hejazi, M.: Quantifying the relative contribution of the climate and direct human impacts on mean annual streamflow in the contiguous United States, Water Resour. Res., 47(9), doi:10.1029/2010WR010283, 2011.

Windrum, P., Fagiolo, G. and Moneta, A.: Empirical Validation of Agent-Based Models: Alternatives and Prospects, J. Artif. Soc. Soc. Simul., 10(2), 2007.

Wu, Q. and Lane, C. R.: Delineation and Quantification of Wetland Depressions in the Prairie Pothole Region of North Dakota, Wetlands, 36(2), 215–227, doi:10.1007/s13157-015-0731-6, 2016.

Wuebbles, D., Meehl, G., Hayhoe, K., Karl, T. R., Kunkel, K., Santer, B., Wehner, M., Colle, B., Fischer, E. M., Fu, R., Goodman, A., Janssen, E., Kharin, V., Lee, H., Li, W., Long, L. N., Olsen, S. C., Pan, Z., Seth, A., Sheffield, J. and Sun, L.: CMIP5 climate model analyses: Climate extremes in the United States, Bull. Am. Meteorol. Soc., 95(4), 571–583, doi:10.1175/BAMS-D-12-00172.1, 2014.

Xu, H., Twine, T. E. and Girvetz, E.: Climate Change and Maize Yield in Iowa, PLoS One, 11(5), 1–20, doi:10.1371/journal.pone.0156083, 2016.

Ye, X., Zhang, Q., Liu, J., Li, X. and Xu, C. Y.: Distinguishing the relative impacts of climate change and human activities on variation of streamflow in the poyang lake catchment, china, J. Hydrol., 494, 83–95, doi:10.1016/j.jhydrol.2013.04.036, 2013.

Zaibon, S., Anderson, S. H., Thompson, A. L., Kitchen, N. R., Gantzer, C. J. and Haruna, S. I.: Soil water infiltration affected by topsoil thickness in row crop and switchgrass production systems, Geoderma, 286, 46–53, doi:10.1016/j.geoderma.2016.10.016, 2017.

Zhang, A., Zhang, C., Fu, G., Wang, B., Bao, Z. and Zheng, H.: Assessments of Impacts of Climate Change and Human Activities on Runoff with SWAT for the Huifa River Basin, Northeast China, Water Resour. Manag., 26(8), 2199–2217, doi:10.1007/s11269-012-0010-8, 2012.

Zhang, X., Wan, H., Zwiers, F. W., Hegerl, G. C. and Min, S. K.: Attributing intensification of precipitation extremes to human influence, Geophys. Res. Lett., 40(19), 5252–5257, doi:10.1002/grl.51010, 2013.

Zhou, X., Helmers, M. J., Asbjornsen, H., Kolka, R. and Tomer, M. D.: Perennial Filter Strips Reduce Nitrate Levels in Soil and Shallow Groundwater after Grassland-to-Cropland Conversion, J. Environ. Qual., 39(6), 2006, doi:10.2134/jeq2010.0151, 2010.

Zhou, X., Helmers, M. J., Asbjornsen, H., Kolka, R., Tomer, M. D. and Cruse, R. M.: Nutrient removal by prairie filter strips in agricultural landscapes, J. Soil Water Conserv., 69, 54–64, doi:10.2489/jswc.69.1.54, 2014.

CHAPTER 5

GENERAL CONCLUSIONS

The overarching goal of this research was to improve understanding of hydrologic uncertainty through use of a novel modeling approach, Agent-Based Modeling, which allows for explicit dynamic connections between the hydrologic system and various components of the human system (economic, social, market, etc.). Connections were made between unrelated variables and hydrologic response. The primary findings of the objectives are as follow:

Objective #1

- Crop prices had the largest impact on mean peak discharge, with a 47% larger reduction in mean peak discharge under low crop prices in comparison to high crop prices. Changes in subsidy rates and crop yields did not have as significant of an impact on peak discharge as crop prices.
- Farmer agents were more inclined to eliminate conservation land – a 5-6% increase in mean peak discharge was indicated under high crop prices, while only a 2-3% decrease in mean peak discharge was indicated under low crop prices, in comparison to the historical baseline simulation (i.e. historical yield scenario).
- Heavily weighing a farmer agent's future price or past profit decision variables produces the largest difference in mean peak discharge between scenarios. For instance, under these weighting scenarios, a 7% difference in mean peak discharge was seen between high and low crop prices as opposed to a 0-2% difference under the risk averse or conservation weighting schemes.

Objective #2

- The climate simulations indicated mean 95th percentile discharge increasing by 75% under the RCP 8.5 trajectory for the 2050-2097 period relative to the historical 1970-2016 period if conservation land is kept at the historical mean (constant scenario). However, under the unconstrained scenario, mean 95th percentile discharge increased by 55% under the RCP 8.5 trajectory for the 2050-2097 period. Thus, the increase in mean peak discharge is 20% less than under the constant scenario.

- Secondly, during the 2018-2065 period, the human system and climate system compete in terms of impact on mean 95th percentile discharge. However, during the 2050-2097 period, the impact from the climate system becomes dominant. The MPI simulations under the RCP8.5 trajectory indicated the climate system being responsible for up to 80% of the change in mean 95th percentile discharge.

5.1 Future work potential

The current model design contains several limitations that could be addressed in future studies. These model limitations include the handling of land cover and hydrology as well as agent decisions and interaction.

One of the primary limitations of the hydrologic model is the representation of the conservation land in each subbasin. Curve Number values taken from Dziubanski et al., (2017) were used to represent the native prairie strips implemented by each farmer agent. However, these CN values were derived for agricultural plots of approximately 0.5-3 Ha in size. The question remains whether these CN values can be scaled up to the size of a several hundred acre farm plot and produce reasonable discharge results (i.e. does the CN value of a 2 Ha plot with

10% native prairie vegetation equate to the CN value of a 100 Ha plot with 10% native prairie vegetation). Simanton et al., (1996) did show CNs decreasing as drainage size increases; however, their study was conducted in the semi-arid region of Arizona. According to Hawkins et al., (2009), the NRCS does not provide any guidance as to the drainage size limitations for use of the CN method. In fact, the original CN tables were derived for sites varying from 0.1 Ha to 18000 Ha. Thus, it is not clear exactly how the CN may vary with scale. This limitation can be overcome by incorporating a more advanced hydrologic model. A model that includes better spatial distribution and explicit vegetation processes would allow for more robust assessment of land use impacts, hydrology and crop production.

Aside from the hydrologic modeling, the agent-based model has limitations regarding the specific decision-making implemented as well as the information and characteristics used by the agents. Numerous studies have indicated that there are many other factors to consider when examining farmer decision-making regarding conservation practices. These studies have identified variables such as farm size, type of farm, age of farmer, off farm income, land tenure agreement, education from local experts, among others, to be significant in determining adoption of conservation practices (Daloğlu et al., 2014; Lambert et al., 2007; Ryan et al., 2003; Saltiel et al., 1994; Schaible et al., 2015). Introducing some of these farmer characteristics may be necessary to obtain more realistic simulations under future climate.

5.2 Implications on hydrologic studies

Hydrologic modeling studies need to explicitly represent human decision-making within the landscape to accurately assess hydrologic outcomes under future climate and provide reliable information for water management decisions (Montanari et al., 2013; Sivapalan et al., 2012). The findings of this study displayed a particular advantage of using Agent-Based

Modeling as a tool to study hydrologic uncertainty: the ability to explicitly quantify hydrologic changes based on perturbations in seemingly unrelated variables such as land rental prices or market forces. A different way to incorporate the impact of human activities is through scenario-based approaches, where accurate scenarios can be formed based on statistical or modeling approaches. However, the scenario-based approach is limited. It would be difficult to quantify the effect of, for example, a social network, on hydrologic outcomes, particularity since a social network may be based on randomness (probabilistic) within the system. The agent-based modeling approach can allow hydrologist to incorporate many variables of uncertainty in the human system to gain a better picture of the range of outcomes possible. However, much caution and consideration must be used when deciding on using the agent-based modeling approach. One must consider several key questions from the agent-based modeling standpoint: what exactly is it that I want to model, what connections do I explicitly want to represent between the social and hydrologic systems, is the data available to characterize the agents, and is there macro and micro level data available that can be used to calibrate the agent-based model. From the hydrologic modeling standpoint, one must consider these key questions: what are the key hydrologic processes that need to be modeled, how complex is the model that I want to use, is data available to calibrate and drive the model, how many inputs are required, and what are the explicit hydrologic connections that I want to represent between the system (as above). Agent-based modeling can prove to be a useful tool for hydrologists, but there are many variables to consider. Above all, when using the ABM approach, the model needs to be developed such that it is simple, yet accurately represent critical decision-making within the landscape.

5.3 References

Daloğlu, I., J.I. Nassauer, R.L. Riolo, and D. Scavia, 2014. Development of a Farmer Typology of Agricultural Conservation Behavior in the American Corn Belt. Agricultural Systems 129:93–102.

Dziubanski, D.J., K.J. Franz, and M.J. Helmers, 2017. Effects of Spatial Distribution of Prairie Vegetation in an Agricultural Landscape on Curve Number Values. JAWRA Journal of the American Water Resources Association 53:365–381.

Hawkins, R.H., T. Ward, D.E. Woodward, and J. Van Mullem, 2009. Curve Number Hydrology: State of the Practice. American Society of Civil Engineers, Reston, VA.

Lambert, D.M., P. Sullivan, R. Claassen, and L. Foreman, 2007. Profiles of US Farm Households Adopting Conservation-Compatible Practices. Land Use Policy 24:72–88.

Montanari, a., G. Young, H.H.G. Savenije, D. Hughes, T. Wagener, L.L. Ren, D. Koutsoyiannis, C. Cudennec, E. Toth, S. Grimaldi, G. Blöschl, M. Sivapalan, K. Beven, H. Gupta, M. Hipsey, B. Schaefli, B. Arheimer, E. Boegh, S.J. Schymanski, G. Di Baldassarre, B. Yu, P. Hubert, Y. Huang, a. Schumann, D. a. Post, V. Srinivasan, C. Harman, S. Thompson, M. Rogger, a. Viglione, H. McMillan, G. Characklis, Z. Pang, and V. Belyaev, 2013. "Panta Rhei—Everything Flows": Change in Hydrology and Society—The IAHS Scientific Decade 2013–2022. Hydrological Sciences Journal 58:1256–1275.

Ryan, R.L., D.L. Erickson, and R. De Young, 2003. Farmers' Motivation for Adopting Conservation Practices along Riparian Zones in a Mid-Western Agricultural Watershed. Journal of Environmental Planning and Management 46:19–37.

Saltiel, J., J.W. Bauder, and S. Palakovich, 1994. Adoption of Sustainable Agricultural Practices: Diffusion, Farm Structure, and Profitability. Rural Sociology 59:333–349.

Schaible, G.D., A.K. Mishra, D.M. Lambert, and G. Panterov, 2015. Factors Influencing Environmental Stewardship in U.S. Agriculture: Conservation Program Participants vs. Non-Participants. Land Use Policy 46:125–141.

Simanton, J.R., R.H. Hawkins, M. Mohseni-Saravi, and K.G. Renard, 1996. Runoff Curve Number Variation with Drainage Area, Walnut Gulch, Arizona. Transactions of the ASAE 39:1391–1394.

Sivapalan, M., H.H.G. Savenije, and G. Blöschl, 2012. Socio-Hydrology: A New Science of People and Water. Hydrological Processes 26:1270–1276.